MONASH University

Investigating neurodegenerative disease mechanisms using the zebrafish, *Danio rerio*

Rita Joana Soares Serrano

BSc. (Biology), MSc. (Molecular Genetics and Biomedicine)

A thesis submitted for the degree of Doctor of Philosophy

at Monash University

School of Biological Sciences, June 2019

Copyright notice

Abstract

Cerebellar ataxia and epileptic encephalopathies are two devastating disorders associated with the central nervous system. Cerebellar ataxia is characterized by loss of cerebellar neuronal cells, leading to impaired motor control, and epileptic encephalopathies by recurrent seizures, behavioural abnormalities, and impaired brain development, leading to motor and cognitive retardation. Although several genes have been associated with these disorders, many cases lack a genetic diagnosis and most subtypes still lack a mechanistic understanding of the molecular pathways that result in the disease pathology, hampering the development of therapeutics.

Mutations in transmembrane protein 33 (*TMEM33*) and plexinB3 (*PLXNB3*) were identified by collaborators of the Bryson-Richardson lab as candidate genes for cerebellar ataxia. Moreover, previous authors identified mutations in ubiquitin-like activating enzyme 5 (*UBA5*) in patients diagnosed with cerebellar ataxia or epileptic encephalopathy. The goals of this dissertation were to evaluate these genes as candidates for cerebellar ataxia and to better understand the pathophysiology associated with mutations in *UBA5*.

In the first part of this thesis, I describe the characterisation of *tmem33* and *plxnb3* zebrafish loss of function models and show that *plxnb3* and *tmem33* mutants do not demonstrate disease-related phenotypes. In the second part of this thesis, I describe the establishment of zebrafish *uba5* loss of function models using the CRISPR technology for genome editing. I confirmed that *uba5* mutant alleles resulted in reduced ubiquitin-like fold modifier 1 (Ufm1) protein levels, suggesting that the Ufm1 pathways is compromised. Examination of *uba5* mutants further identified motor dysfunction, reduced growth rate, and reduced lifespan, as observed in patients. Moreover, there are signs of neurodegeneration and abnormal mitochondria in the central and peripheral nervous systems (CNS & PNS) under electron microscopy. I then showed that the *uba5* phenotype is accompanied by decreased glutamine concentration, potentially due to impaired glutamine synthetase activity. These findings can explain many of the symptoms observed in the disease, significantly increase our knowledge of the affected molecular pathways in *UBA5*-related disease, and may lead towards successful treatments of these diseases.

Declaration

This thesis is an original work of my research and contains no material which has been accepted for the award of any other degree or diploma at any university or equivalent institution and that, to the best of my knowledge and belief, this thesis contains no material previously published or written by another person, except where due reference is made in the text of the thesis.

Print Name: Rita Joana Soares Serrano

Date: 13th June 2019

Acknowledgements

Firstly, I would like to thank to my supervisor Assoc. Prof. Robert Bryson-Richardson for his guidance during the last 4 years. Rob, I can't thank you enough for always being around to answer my questions, for always pushing me forward, and helped me develop into a better researcher.

Thanks also to my associate supervisor Assoc. Prof. Coral Warr, and my advisory panel, Dr. Jan Kaslin, Dr. Brent Neumann, and Dr. Richard Burke for all their valuable feedback throughout my PhD.

Secondly, to all the members of the Bryson-Richardson lab, past and present, for providing a great environment to do science. In particular, I would like to thank Dr. Tamar Sztal for her willing to share her expertise with me, and for all the discussions about science and life. To Clara Lee, for her assistance with my projects and for all the laughs we shared. To Emily Baxter and Callum Dark, for being my PhD buddies and making this journey smoother. To Mo Zhao, for being supportive and keep me focused in writing my thesis.

Finally, a few personal acknowledgements. Mel, thanks for all the motivational chats and encouragement throughout the writing process. Pedro, thanks so much for always being there for me and make me smile. To my mum, for always believing in me.

"Success may be defined by the moments when everything is going right, but it's largely determined by what we do in the moments when everything is going wrong." (quote by Jen Heemstra).

Table of Contents

List of Tables

List of Figures

Chapter 1. Introduction

Chapter 2. Materials & Methods

Chapter 3. Characterization of *tmem33* mutant zebrafish to investigate the potential role of *TMEM33* in cerebellar ataxia.

Chapter 4. Characterization of *plxnb3* mutant zebrafish to investigate the potential role of *PLXNB3* in cerebellar ataxia.

Chapter 5. Characterization of zebrafish *uba5* loss of function mutants

List of abbreviations

ADCA - Autosomal dominant cerebellar ataxia

ALS – amyotrophic lateral sclerosis

ASC1 – activating signal co-integrator 1

ARCA – Autosomal recessive cerebellar ataxia

CNS – central nervous system

ER – endoplasmic reticulum

EEG – electroencephalography

EM – electron microscopy

FXTAS – fragile X-associated tremor ataxia syndrome

GAP – GTPase activating protein

GFAP – glial fibrillary acidic protein

GnRH – gonadotropin-releasing hormone

GS – glutamine synthetase

NCAM – neural cell adhesion molecule

PLXNB3 – plexin B3

PNS – peripheral nervous system

ROS – reactive oxygen species

SCA – spinocerebellar ataxia

Sema – semaphorin

sgRNA – single guide RNA

TCA – tricarboxylic acid

TMEM – transmembrane protein

TMEM33 – transmembrane protein 33

UBA5 – ubiquitin-like activating enzyme 5

Ubl – ubiquitin-like

UFC1 – ubiquitin-fold modifier conjugating enzyme 1

UFBP1 – ufm1-binding protein 1

UFL1 – ufm1-protein ligase 1

UFM1 – ubiquitin-fold modifier 1

Chapter 1. Introduction

Neurodegenerative diseases are a leading-cause of disability and mortality (Feigin et al., 2017), and estimated to affect one in six individuals worldwide (WHO, 2006). They are characterized by loss of subsets of neuronal cells, leading to central and/or peripheral nervous system dysfunction. Accordingly, these disorders are often diverse in their pathophysiology, and may result in motor, sensory and/or cognitive deficiencies.

Neurodegenerative diseases are still one of the greatest challenges in medicine and scientific research. This is largely due to the fact that, while genetic causes have been identified, the pathomechanism underlying the clinical phenotype remains to be elucidated for the majority of neurodegenerative diseases. Additionally, many patients are negative for mutations in known genes, suggesting that other genes associated with disease have yet to be identified. Identifying novel genes associated with disease may consequently lead to improved clinical diagnosis. Once novel genes are found to segregate with disease, it is critical to investigate whether the mutations in these genes share pathomechanisms with previously described mutations, or if the mechanisms of neurodegeneration are unique to them. Elucidating these answers may reveal molecular mechanisms that are currently unknown to play a role in disease and assist the development of targeted therapies.

Work conducted by collaborators of the Bryson-Richardson lab has identified novel candidate genes associated with neurodegenerative disease. The novel genes were identified in patients pre-screened for known disease genes using whole exome sequencing, linkage analysis and/or homozygosity mapping. The novel genes are: *ubiquitin-like modifier activating enzyme 5* (*UBA5*), which homozygous recessive variants were associated with a severe neonatal-onset demyelinating disorder in three individuals of a single family; *plexinB3* (*PLXNB3*), which homozygous/hemizygous deletion was associated with X-linked cerebellar ataxia in two individuals of the same family; and, *transmembrane protein 33* (*TMEM33*), which homozygous recessive variants were associated with autosomal recessive cerebellar ataxia identified in two siblings (Nowak, K., Laing, N. et al., personal communication). Since the start of my PhD several authors have further published case reports of compound heterozygous mutations in *UBA5* associated with a severe infantile-onset epileptic encephalopathy and childhood-onset cerebellar ataxia. These case reports increased the number of individuals with *UBA5* mutations to 18, widening the phenotypic spectrum (Arnadottir et al., 2017; Colin et al., 2016; Daida et al., 2018; Low et al., 2018; Mignon-Ravix et al., 2018; Muona et al., 2016).

Early-onset epileptic encephalopathies and cerebellar ataxias are among the most debilitating neurodegenerative diseases, and the mechanism of pathogenesis remains poorly understood and no effective treatments are available. The main objective of this work was to confirm the association of

the identified mutations with the disease through validation in an animal model and to explore the underlying mechanism of disease.

1.1 Early-onset Epileptic Encephalopathies

Early-onset epileptic encephalopathies comprise approximately 40% of cases of epilepsy starting prior to 3 years of age (Eltze et al., 2013). Early-onset epileptic encephalopathies are mainly characterized by pharmaco-resistant seizures, abnormal electroencephalographic (EEG) findings, and progressive brain dysfunction. These disorders arise during early infancy, affecting the developing brain, and resulting in significant neurodevelopmental deficits (Berg et al., 2010). Consequently, patients characteristically exhibit cognitive, sensory, and/or motor dysfunction, and a poor prognosis. The International League Against Epilepsy (ILAE) describes encephalopathy as a disorder in which the epileptic activity itself contributes to the neurodevelopmental impairment (Berg et al., 2010). However, it is not presently understood whether the abnormal brain activity leads to the neurodevelopmental deficits, the neurodevelopmental defects cause the seizure phenotype, or there are independent pathophysiological pathways that contribute to both neurodevelopmental impairment and epilepsy (Berg et al., 2010; Hamdan et al., 2017; Helbig and Tayoun, 2016; Nabbout et al., 2013).

Early-onset epileptic encephalopathies are diagnosed based on age of onset, type of seizures, EEG findings, and developmental status, being classified into 8 major syndromes: early myoclonic encephalopathy, Ohtahara syndrome, West syndrome, Dravet syndrome, epilepsy of infancy with migrating focal seizures, Lennox-Gastaut syndrome, Landau-Kleffner syndrome, and epilepsy with continuous spike-waves during slow-wave sleep (Auvin et al., 2016; Nieh and Sherr, 2014). Nevertheless, an increasing number of patients do not meet the criteria of the defined early-onset epileptic encephalopathy syndromes. Novel syndromes are currently emerging with mild to severe epileptic activity, brain abnormalities, movement disorders, and delayed growth, increasing the phenotypic range of epileptic encephalopathies (Scheffer et al., 2017; Smigiel et al., 2018).

1.1.1 Infancy onset epileptic encephalopathies

Infancy-onset epileptic encephalopathies include the early myoclonic encephalopathy, Ohtahara syndrome, West syndrome, epilepsy of infancy with migrating focal seizures, and Dravet syndrome. The Ohtahara syndrome manifests within 3 months of birth, and is characterized by generalized or lateralized spasms. The EEG typically presents a suppression burst pattern, consisting of cycles of low-amplitude cerebral activity interrupted by periodic bursts of higher frequency activity, during

the day and night cycles. The patients show severe motor developmental delay and intellectual disability (Beal et al., 2012). Similar to the Ohtahara syndrome, early myoclonic encephalopathy arises in the first 3 months and is characterized by EEG with suppression burst pattern that occurs mainly during sleep. The patients exhibit focal myoclonus (involuntary shock-like movements), tonic spasms, motor and cognitive impairment, and may persist in a vegetative state (Beal et al., 2012). In contrast, epilepsy of infancy with migrating focal seizures starts within the first 6 months of age. The disorder is recognized by the occurrence of abnormal activity in one region of the brain (i.e. focal seizures), and the patients frequently show neurodevelopmental regression, and microcephaly (Coppola, 2013). The Dravet syndrome differs from other epileptic encephalopathy syndromes by the manifestation of prolonged and frequent febrile seizures that occur in the first year of life. The patients often exhibit motor and cognitive decline in early childhood, and develop autistic traits (Wolff et al., 2006). Instead, West syndrome affects children within two years of life. It is defined by an EEG pattern of hypsarrhythmia, a random pattern of high amplitude slow waves and spikes, and the patients typically present infantile spasms and developmental regression (D'Alonzo et al., 2018).

1.1.2. Childhood onset epileptic encephalopathies

Childhood-onset epileptic encephalopathies comprise the Landau-Kleffner syndrome, Lennox-Gastaut syndrome and epilepsy with continuous spike-waves during slow-wave sleep. The Landau-Kleffner syndrome occurs within 3 and 7 years of age and is characterized by verbal agnosia, which is the inability to understand and use language, and EEG with continuous spike waves during sleep (Hughes, 2011). In contrast, Lennox-Gastaut syndrome affects children prior 5 years of age, revealing an EEG with fast activity and generalized wave discharges. The patients show multiple types of seizures, mental retardation or regression, loss of the ability to control behavior, and, occasionally, dementia (Mastrangelo, 2017). Lastly, epileptic encephalopathy with continuous spike and wave during sleep arises in children of 4-5 years of age, who exhibit sleep-induced epileptic activity. These are frequently preceded by motor and cognitive dysfunction, hypotonia, or ataxia (Singhal and Sullivan, 2014).

1.1.3. Molecular pathways in epileptic encephalopathies

Epileptic encephalopathies can result from brain injury, metabolic deficiencies, or genetic defects (Holland and Hallinan, 2010; Prasad and Hoffmann, 2010). Genes causing epileptic encephalopathies are mainly expressed in the nervous system, and have a role in major neurological

functions or in neuronal development. The 3 main pathophysiological pathways identified in epileptic encephalopathies include dysregulation of influx and outflow of ions at the neuronal plasma membrane due to mutations in ion-channels encoding genes, impaired synaptic diffusion of neurotransmitters, and impaired development of GABAergic interneurons (i.e. inhibitory neurons) (Helbig et al., 2017).

Mutations in ion-channel encoding genes is the primary genetic etiology associated with epileptic encephalopathies (Gursoy and Ercal, 2016). Defects in *SCN1A,* encoding the alpha-1 subunit of the neuronal voltage-gated sodium channel, is the most frequent cause. SCN1A controls the influx of Na^+ and initiation and propagation of action potentials in the nervous system, and is mainly detected in inhibitory neuronal cells. Accordingly, *SCN1A* mutations are associated with deficient Na^+ signaling in GABAergic cerebellar Purkinje cells (Ogiwara et al., 2007; Yu et al., 2006), and result in reduced number of GABAergic interneurons in the forebrain (Han et al., 2012). Other ion-channel encoding genes linked with epileptic encephalopathy include *KCNQ2,* encoding the potassium voltage-gated channel subunit Kv7.2, and *HCN1,* encoding the hyperpolarization activated cyclic nucleotide gated channel 1 (Allen et al., 2014; Nava et al., 2014). KCNQ2 regulates outward K^+ currents and the response of neurons to synaptic input, restricting neuronal excitability (Peters et al., 2005), while HCN1 is required to stabilize the neuronal membrane potential against excitatory or inhibitory inputs (Kase and Imoto, 2012). Ion channel-related epileptic encephalopathy patients typically show epileptic activity, which is accompanied by developmental deficits, movement disorders, ataxia and/or involuntary muscle contractions, and rigidity (Depienne et al., 2009b; Nakamura et al., 2013). Dysfunction of the membrane action potential, which is required to balance excitation and inhibition in the nervous system, is a common cause of epilepsy and can explain the epileptic behavior in these patients (Helbig and Tayoun, 2016; Scharfman, 2007). However, the pathophysiological mechanism that results in the remaining features of the disease has not yet been identified.

Defects in synaptic proteins related with neurotransmitter release and uptake, and synaptic vesicle trafficking are also commonly associated with epileptic encephalopathy. These are the consequence of mutations in, for example, *syntaxin binding protein 1* (*STXBP1*), which is involved in regulation of glutamate (excitatory neurotransmitter) and GABA (inhibitory neurotransmitter) synaptic release, *dynamin-1* (*DNM1*) that is required for synaptic vesicle trafficking during increased levels of neuronal activity (Dhindsa et al., 2015; Nakashima et al., 2016), and the solute carrier family 25 member 22 (*SLC25A22*), a mitochondrial glutamate carrier expressed in astrocytes (Molinari et al., 2009). Moreover, mutations in NMDA receptor subunits genes have been shown to cause a number of epileptic encephalopathy syndromes, including early-onset epileptic encephalopathy, Landau-Kleffner syndrome and epileptic encephalopathy with continuous spike-wave in sleep (Burmashev

and Szepetowski, 2015; Dong et al., 2016; Lesca et al., 2013; Ohba et al., 2015; Venkateswaran et al., 2014). Similar to the channelopathies, dysfunction of synaptic transmission can result in seizures by disrupting the balance between excitatory and inhibitory signals in neurons (Scharfman, 2007).

Mutations in genes involved in intracellular signal transduction, and genes encoding neurotransmitters receptors and intracellular transporters, and genes encoding proteins involved in metabolic pathways, revealed that additional pathways are implicated in epileptic encephalopathies (Gursoy and Ercal, 2016; Mastrangelo, 2015). These include, for example, mutation in the *aristaless-related homeobox gene* (*ARX*), a transcription factor involved in the patterning of GABAergic interneurons (Kato et al., 2007), *protocadherin 19* (*PCDH19*) which is a calcium dependent cell adhesion protein associated with synaptogenesis (Depienne et al., 2009a), *solute carrier family 2 member 1* (SLC2A1) involved in glucose transport (Suls et al., 2009), and *pyridoxamine 5'-phosphate oxidase* (*PNPO*) implicated in vitamin B6 metabolism (Mills et al., 2014).

Current treatments for epileptic encephalopathies are mainly focused on the control of seizures, with minimal contribution to prevention of the loss of neurologic function and inevitable poor prognosis. The available treatments have been shown to improve the epileptic activity in a subset of patients, but are not effective for all type of seizures or all epileptic encephalopathy syndromes (Jain et al., 2013; Nariai et al., 2018). Hence, there is a lack of effective treatments for many epileptic encephalopathy syndromes, and the outcome of the treatments differs based on the etiology associated with the clinical phenotype. The first-line of therapy in epileptic encephalopathies typically comprises conventional antiepileptic drugs, such as valproic acid and lamotrigine (Arzimanoglou et al., 2009; Doege et al., 2013; Lemmon and Kossoff, 2013), felbamate (Zupanc et al., 2010), rufinamide (Glauser et al., 2008), potassium bromide (Lotte et al., 2012), or benzodiazepines (Trivisano et al., 2011). These antiepileptic drugs promote transitory seizure control in a small percentage of patients, but epilepsy is refractory to antiepileptic drugs in most patients. Treatment with adrenocortitropic hormone (ACTH) and/or corticosteroids is also utilized, which is reported to result in more long-lasting effects compared to antiepileptic drugs (Buzatu et al., 2009; Pellock et al., 2010). Yet, there only a few published trials describing the efficacy of these drugs, and the outcome depends on course and duration of the epileptic syndrome prior to treatment (Buzatu et al., 2009; Mackay et al., 2004). The benefits of the available treatments are consequently limited. This reveals a need for development of targeted treatments not only for the epileptic behavior but also neurological dysfunction. The development of these therapies is, however, presently restricted due to the lack of understanding of the molecular mechanisms underlying the phenotype in the patients and the heterogeneity of phenotypes associated with the disorder.

1.2. Cerebellar Ataxias

Cerebellar ataxias are disorders characterized by gait abnormalities and poor balance, often accompanied by poor coordination of eye and hand movements and impaired speech. Cerebellar ataxias are mainly associated with atrophy of the cerebellum, due to Purkinje cells loss, and neurodegeneration within the spinal cord. Along with ataxia and atrophy of the cerebellum, spasticity (continuous contraction of muscle), difficulty in swallowing, delayed motor development, peripheral sensory loss, motor neuron disease, tremor, epilepsy, or cognitive impairment may also occur; still, these clinical symptoms are observed in different cerebellar ataxia subtypes (Sandford and Burmeister, 2014).

Cerebellar ataxias can be autosomal recessive, autosomal dominant or X-linked inherited (Jayadev and Bird, 2013; Paulson, 2009; Sandford and Burmeister, 2014). To date, more than 50 genes have been identified to cause cerebellar ataxia, but for approximately 40% of subtypes the associated gene remains unidentified. Among the mutations associated with cerebellar ataxia the majority are nucleotide repeat expansions, which result in protein aggregation. Aggregated proteins are toxic to the cell and their accumulation is a common pathogenic event in many human disorders, including neurodegenerative diseases (Soto, 2003). Other common cerebellar ataxia subtypes are the consequence of mutations in genes that influence synaptic transmission via calcium, glutamate, or GABA signaling (Carlson et al., 2009; Duenas et al., 2006)

Two new genes associated with cerebellar ataxia are *PLXNB3* and *TMEM33* (Novak et al., personal communication). Mutations in these genes were identified to segregate in the affected individuals, respectively, as X-linked and autosomal recessive variants.

1.2.1. Autosomal dominant cerebellar ataxias

Autosomal dominant cerebellar ataxias (ADCAs) are progressive disorders that affect individuals from 30 years of age. ADCAs are mainly classified in 3 subtypes: type 1, with optic atrophy, basal ganglia impairment and muscular atrophy; type 2, with retinal degeneration, and type 3, with symptoms mainly associated with the cerebellum (Klockgether, 2008). The most common ADCA subtypes result from CAG repeat expansions (SCA1-3, 6, 7, 17 and DRPLA) that generate poly-glutamine repeats in the translated proteins. The repeat expansions result in accumulation of protein aggregates in affected regions of the brain (Sullivan et al., 2019). It is hypothesized that the aggregated proteins are toxic to the cell and contribute to disruption of cellular homeostasis and subsequent neuronal dysfunction (Shao and Diamond, 2007). These CAG expansion subtypes are typically more severe than ADCAs caused by other types of mutation, and the prognosis is poor.

Other identified repeat expansions subtypes are associated with repeat expansions in intronic or untranslated regions of the genes (SCA10, 12 and 31) (Holmes et al., 2003; Matsuura et al., 2000; Sato et al., 2009). These repeat expansions interfere with regulation of transcription of the gene, altering transcription levels, or produce toxic RNA transcripts, but the mechanism that leads to ataxia is still unknown. Additionally, ADCA subtypes can further result from mutation in ion-channel encoding genes (e.g. mutations in the calcium channel gene *CACNA1A,* or potassium channel gene *KCNA1*)(D'Adamo et al., 2015; Kim et al., 2006), genes involved in glutamate transmission (*SPTBN2*) (Mizuno et al., 2019), or mitochondrial activity (*AFG3L2*) (Di Bella et al., 2010).

1.2.2. Autosomal recessive cerebellar ataxias

Autosomal recessive cerebellar ataxias (ARCAs) occur more frequently than ADCAs and mainly affect individuals before 25 years of age. These disorders differ from ADCAs as they often are associated with peripheral neuropathy and the patients exhibit symptoms outside of the nervous system (Fogel and Perlman, 2007). For example, ataxia telangiectasia is associated with cancer susceptibility (Alsbeih, 2011), while oculomotor apraxia 1 is characterized by high cholesterol levels (Moreira et al., 2001).

The most common ARCA subtype is the Friedreich ataxia, caused by GAA repeat expansions in the first intron of the *frataxin* (*FXN*) gene. The GAA expansions result in decreased mRNA transcription, and reduced levels of frataxin that leads to iron accumulation in mitochondria and increased oxidative stress (Wilson, 2006). Besides GAA repeats, ARCAs can also be caused by mutations in genes involved in DNA repair mechanisms (*MRE11A*) (Alsbeih, 2011), cell cycle control and cell growth (*PIK3R5*) (Al Tassan et al., 2012), exocytosis regulation (*SYT14, synaptotagmin 14*) (Doi et al., 2011), lipoprotein assembly (*ATTP, alpha-tocopherol transfer protein gene*) (Usuki and Maruyama, 2000), coenzyme Q10 metabolism (*ADCK3*) (Lagier-Tourenne et al., 2008) and chaperone function (*SIL1*) (Senderek et al., 2006).

1.2.3. X-linked ataxias

X-linked cerebellar ataxias are rare compared to autosomal dominant and autosomal recessive cerebellar ataxias, and consequently there is a lack of knowledge on the phenotypic presentation and genetic causes. The best-studied X-linked cerebellar ataxia is the fragile X-associated tremor ataxia syndrome (FXTAS), caused by a CGG repeat expansion in the 5' untranslated region of the

FMR1 gene. FXTAS is associated with mental retardation and abnormal facial features (Robertson et al., 2016; Todd et al., 2013).

The literature indicates that cerebellar ataxias result from a wide range of underlying genetic causes, and different pathways are potentially involved in the neurodegenerative processes of specific subtypes. Similar to epileptic encephalopathies, most cerebellar ataxia subtypes remain poorly characterized. As a result, there is insufficient understanding of the molecular mechanisms triggered by mutation in the affected genes, and there are limited treatments for these disorders. Current therapeutics are aimed at alleviating ataxia and tremor in the patients through modulation of neurotransmitters, which are believed to play a role in cerebellar and motor dysfunction (Ogawa, 2004; Perlman, 2000; Sarva and Shanker, 2014), and are not focused in preventing the progressive neurodegeneration. These include pharmacological treatments that modulate dopamine, serotonin, acetylcholine, glutamate, or GABA signaling (Manto, 2005; Ogawa, 2004; Sarva and Shanker, 2014), but the effectiveness of these treatments remains inconclusive. Drugs, such as 5-hydroxytryptophan, buspirone, and physostigmine, have been shown to improve tremor and ataxia in small samples of patients, but the outcomes were not reproducible in larger trials, and occasionally resulted in worsening of the clinical presentation (Manto, 2005; Ogawa, 2004; Sarva and Shanker, 2014). As in epileptic encephalopathies, the development of targeted therapies is needed, which may be facilitated by identification of the molecular pathways that are disrupted in each cerebellar ataxia subtype.

1.3. Zebrafish models of epileptic encephalopathy and cerebellar ataxia

Our current understanding about the biology of neurodegenerative diseases has arisen from investigating the physiological function of genes associated with disease using animal models (Auluck et al., 2002; Hua et al., 2010; Yamamoto et al., 2000). Zebrafish is a well-established model organism to investigate human disease, sharing 70% orthologues with the human genes. Zebrafish embryos develop externally facilitating genetic manipulation, drug treatments and analysis of phenotypic alterations (Meyers, 2018). Additionally, zebrafish models have been used to study human neurological disease due to the highly similar neuronal structures and functions with the human brain (Kalueff et al., 2014; McCammon and Sive, 2015; Mueller and Wullimann, 2003). In particular, zebrafish models have been useful in validating disease-causative mutations and providing insights into the pathophysiology of neurological disease, including epileptic encephalopathies and cerebellar ataxias.

Using electro-graphical recordings, Suls et al. (2013) demonstrated that *ch2* knockdown in zebrafish caused epileptic discharges associated with whirlpool-like movement, and whole-body trembling,

validating the involvement of mutations in *CH2* in Dravet syndrome. Knockout of *vars* (*valyl-tRNA synthetase*), discovered to cause a developmental encephalopathy with microcephaly and early-onset epilepsy in ten patients, was shown to result in microcephaly and epileptic behavior in zebrafish (Siekierska et al., 2019). Additionally, Grone et al. (2016) revealed that *stxbp1a* mutant zebrafish have spontaneous seizures and reduced motor function, accompanied by deficient glycolysis and mitochondrial oxidative phosphorylation. This study allowed the confirmation that mutations in *STXBP1*, one of the genetic causes of epileptic encephalopathy, results in impaired glucose and mitochondrial metabolism. Zebrafish were further used to demonstrate that *snc1ab* mutation causes convulsive behavior that can be ameliorated using clemizole, providing a potential therapeutic avenue for Dravet syndrome patients (Baraban et al., 2013). Moreover, Grone et al. (2017) revealed that *scn1lab* mutant zebrafish have increased locomotor activity at night and anxiety-related behavior, associated with sleep abnormalities observed in the patients, which are suppressed by both clemizole and diazepam.

Besides epileptic encephalopathy, zebrafish models have recapitulated key neurological traits of cerebellar ataxias. *K*nockdown of *ca8*, a gene associated with ataxia and quadrupedal gait, demonstrated decreased cerebellar size, and increased neuronal apoptosis and abnormal motor activity in zebrafish (Aspatwar et al., 2013). *kcnj10* morphant zebrafish were shown to recapitulate the phenotype of patients with EAST syndrome, which includes seizures, ataxia, sensorineural deafness and renal tubular defects. Morphant zebrafish presented abnormal brain morphology, seizures, abnormal upright posture and unidirectional bursts of speed (Mahmood et al., 2013). Burns et al. (2014) additionally used zebrafish to show that *cwf19l1* knockdown results in abnormal movement pattern and reduced number of cerebellar purkinje cells, confirming that *CWF19L1* mutation causes non-progressive congenital ataxia with mental retardation. Margolin et al. (2013) utilized zebrafish to validate mutations in *RNF216* and *OTUD4* as cause of cerebellar ataxia, dementia, and hypogonadotropic hypogonadism. This study confirmed that knockout of either each gene or both genes simultaneously results in the disease phenotype (Margolin et al., 2013). Studies by Yanicostas et al. (2012) also demonstrated the requirement of *atxn7,* known to cause spinocerebellar ataxia type 7, for differentiation of retina photoreceptors and cerebellar granule cells in zebrafish. In addition, *snx14* knockdown in zebrafish revealed that reduction in purkinje cell numbers is associated with impaired autophagic degradation, suggesting a potential mechanism that leads to disease (Akizu et al., 2015). Taken together, these studies demonstrate that zebrafish are useful to model behavioral and neurophysiological symptoms of epileptic encephalopathies and cerebellar ataxias.

1.4. The transmembrane proteins family (TMEMs) and disease

A *TMEM33* mutation was identified by our collaborators as a potential cause of SCA. Transmembrane proteins comprise approximately 30% of all proteins of the human proteome (Wallin and von Heijne, 1998). TMEMs allow the diffusion of small molecules including nutrients, electrolytes, and metabolic factors across the membrane of mitochondria, endoplasmic reticulum (ER), lysosomes, or Golgi apparatus, and can be part of signaling pathways through the binding of ligands (Wallin and von Heijne, 1998). The function of the majority of the TMEMs is unknown, however several studies have reported that many TMEMs may be implicated in neurological disease.

TMEM proteins encoding genes have been proposed as potential neurological disease modifiers. Variants in *TMEM39A* were identified in association with multiple sclerosis, an autoimmune disease of the central nervous system, showing a significant correlation in a genome-wide association study (GWAS) performed in a Spanish cohort (Varade et al., 2012). Another GWAS identified a significant association between multiple SNPs within *TMEM106B* and a higher risk of developing frontotemporal lobar degeneration and TDP-43 positive neuronal inclusions (Van Deerlin et al., 2010). Moreover, studies have suggested that *TMEM106B* variants may act as genetic modifiers in frontotemporal lobar degeneration, and possibly are associated with an earlier disease onset (Cruchaga et al., 2011; van der Zee et al., 2011). Additionally, *TMEM106B* variants were associated with increased risk of developing cognitive impairment in ALS patients (Vass et al., 2011), and hippocampal sclerosis in Alzheimer's patients (Rutherford et al., 2012). In support of the second study, Satoh et al. (2014) indicated that *TMEM106B* expression is decreased in the brain of Alzheimer patients, and is possibly a risk factor for Alzheimer's disease.

TMEM encoding genes have been also investigated as potential candidates for panic disorder. Erhardt et al. (2010) identified variants within *TMEM132D* correlated with panic disorder through a genome-wide case–control association analysis in German patients. The *TMEM132D* variants were associated with severe anxiety within patients with major depression (Erhardt et al., 2010). Furthermore, Gregersen et al. (2014) revealed that variants in *TMEM132E* are similarly correlated with panic disorder in the Danish population, suggesting that *TMEM132E* may contribute to the risk of developing panic disorder. Also, *TMEM132D* variants were previously implicated in bipolar disorder (Sklar et al., 2008).

Notably, mutations in *TMEM* proteins encoding genes were recently identified as cause of nervous system disorders. Mutations in *TMEM230* were identified as cause of autosomal dominant familial Parkinson disease (Deng et al., 2016). *TMEM230* mutations result in impaired trafficking and recycling of synaptic vesicles, causing the pathogenesis associated with Parkinson disease.

TMEM260 mutations were further identified in patients with pediatric neurodevelopmental, cardiac, renal, and axial skeletal syndrome (Ta-Shma et al., 2017). The authors validated *TMEM260* as the gene associated with disease using zebrafish *tmem260* mutants, which recapitulated key features of the disorder (Ta-Shma et al., 2017). Additionally, hypomyelinating leukodystrophy, a disorder characterized by ataxia, spasticity, and lack of myelination in the brain, was revealed to be caused by a dominant mutation (*c.754 G > A*, *p. Asp252Asn*) in the *TMEM106B* gene (Simons et al., 2017). The dominant mutation was shown to result in decreased levels of cathepsin L, a lysosomal enzyme, leading to lysosomal dysfunction (Ito et al., 2018). These studies indicate that *TMEM* protein encoding genes are strong candidates for neurological disease.

1.5. Plexin / Semaphorin interaction and implication in neurological disease

Another gene investigated in this study is plexinB3 (*PLXNB3*), a gene which encodes a transmembrane receptor for semaphorins. Semaphorins are secreted or membrane-bound proteins initially identified as axon guidance cues in the PNS and CNS (Mann et al., 2007; Pasterkamp and Giger, 2009). Axon guidance is a process required for the correct development of the neuronal network, ensuring the projection of axonal tracts to their appropriate targets. This is accomplished by interaction of guidance proteins, such as semaphorins, and semaphorin-receptors localized at the surface of neurons (Mann et al., 2007; Pasterkamp and Giger, 2009).

In neurons, the main receptors for semaphorins are plexins. Plexins are grouped into four subfamilies in vertebrates based on amino acid sequence homology (PlexinA1-4, PlexinB1-3, PlexinC1 and PlexinD1) (Tamagnone et al., 1999) , and are structurally composed of an extracellular domain implicated in semaphorin binding (SEMA domain), and an intracellular GTPase Activating Protein (GAP) domain that is necessary for downstream signaling (Kong et al., 2016). The GAP domain facilitates the regulation of the activity of small GTPase, such as Ras and Rac1, which induces reorganization of the cytoskeleton to effect projection of the axon to its targets (Burridge and Wennerberg, 2004).

Semaphorins directly bind to the extracellular SEMA domain of plexins to transduce signals across the neuronal membrane. Yet, a subset of semaphorins (class III) was identified to primarily bind to neuropilins (Pasterkamp and Kolodkin, 2003; Tamagnone et al., 1999). Neuropilins, a class of semaphorin-receptors, have short intracellular domains and are consequently unable to transduce the signal of semaphorins. Instead, neuropilins form complexes with plexins, specifically of the plexin-A subfamily, to mediate intracellular signaling (Pasterkamp and Kolodkin, 2003; Tamagnone et al., 1999). As an example, semaphorin 3F (Sema3F) preferentially binds neuropilin-1 in the PNS,

and neuropilin-1 subsequently forms a complex with plexinA4 to activate the downstream signaling (Yaron et al., 2005).

Specific interactions between semaphorins, neuropilins and plexins have been reported, including the interaction between Sema5A and PlexinB3 (Alto and Terman, 2017; Artigiani et al., 2004; Yazdani and Terman, 2006). Interaction of plexin-neuropilin-semaphorin complexes are known to be implicated in regulation of axonal repulsion and attraction, neuronal migration, axonal pruning (i.e. removal of axonal branches), and synaptic formation during nervous system development and maintenance (Mann et al., 2007; Shim et al., 2012; Waimey and Cheng, 2006).

An increasing number of studies have reported an association between changes in expression levels of plexins/semaphorins with psychiatric disorders and neurodegenerative disease. A study by Suda et al. (2011) has revealed that *PLXNA4* mRNA level is significantly reduced in the anterior cingulate cortex (ACC) of autistic patients compared to control brain samples. Considering that previous neuroimaging studies demonstrated that the ACC in autistic patients presents white matter abnormalities (Barnea-Goraly et al., 2010), and disruption of *PLXNA4* in mice is associated with abnormal white matter development (Suto et al., 2005), it is hypothesized that dysfunctional PLXNA4 signaling may contribute to the pathophysiology of autism spectrum disorder. A microarray analysis of 7,700 genes revealed that *SEM5A* expression is downregulated in patients with familial autism spectrum disorder (Melin et al., 2006). Furthermore, a genome-wide association study discovered a significant correlation of variants within *SEMA4D*, *SEMA5A, SEMA6A,* and *PLXNC1*, with autism spectrum disorder (Hussman et al., 2011).

Besides autism spectrum disorder, semaphorin-plexin signaling was also implicated in schizophrenic disorder (Mah et al., 2006), Alzheimer's disease (Good et al., 2004; Jun et al., 2014; Korner et al., 2016), Multiple Sclerosis (Qureshi et al., 2017; Williams et al., 2007), and Kallmann disease (Hanchate et al., 2012; Kansakoski et al., 2014). Specifically, Mah et al. (2006) identified a significant association of a SNP within *PLXNA2* and schizophrenia. Although the mechanism underlying schizophrenia remains elusive, *Plxna2* is known to be expressed in the neocortex (Murakami et al., 2001), a region of the brain shown to be affected in patients (Frumin et al., 2002).

Good et al. (2004) revealed that semaphorin3A accumulates in hippocampal neurons, co-localizing with CMRP2 and phosphorylated tau, which is known to form the neurofibrillary tangles, in individuals diagnosed with Alzheimer's disease. In line with this study, GWAS conducted to investigate risk factors for Alzheimer's disease identified a significant association of a variant in *PLXNA4,* the receptor for Sema3A, with dementia and formation of plaques in the brain (Jun et al., 2014). These studies suggest that disruption of Semaphorin3A-PlexinA4 signaling may contribute to

neurodegeneration in Alzheimer's disease. Additionally, *Sem3A* expression was also revealed to be increased in the motor cortex and spinal cord tissue of ALS patients (Korner et al., 2016).

Variants in *SEMA3A* were further associated with Kallmann syndrome, a disorder characterized by gonadotropin-releasing hormone (GnRH) deficiency and inability to smell due to deficient migration of GnRH neurons. Comparative genomic hybridization studies identified a deletion of 231kb within *SEMA3A* that segregates in patients with Kallmann syndrome (Hanchate et al., 2012). Heterozygous variants in both *SEMA3A* and *SEMA7A* were subsequently identified in Kallmann syndrome patients (Kansakoski et al., 2014). Sem3A was previously associated with the development of GnRH neurons and the olfactory bulb in mice (Cariboni et al., 2011; Taniguchi et al., 2003). Therefore, it is hypothesized that Sema3A dysfunction may contribute to the phenotype in Kallmann syndrome patients.

Semaphorin-plexin signaling may likewise be involved in multiple sclerosis, a disorder characterized by demyelinated plaques in the CNS that fail to remyelinate. Work by Williams et al. (2007) demonstrated that Sema3A and Sema3F, known to mediate oligodendrocyte precursor cells guidance, are mainly expressed in demyelinated areas of the brain in multiple sclerosis patients. Considering that remyelination requires the migration of oligodendrocyte precursor cells, the authors hypothesized that dysfunctional semaphorin signaling may interfere with remyelination in multiple sclerosis patients (Williams et al., 2007). In line with this hypothesis, a variant in *PLXNA3*, which can bind to Sema3A or Sema3F, was recently associated with disease severity and disability in multiple sclerosis patients (Qureshi et al., 2017).

Overall, these studies suggest that semaphorins and plexins are potential therapeutic targets for neurological disease.

1.6. UBA5 and the ubiquitin-fold modifier 1 (UFM1) pathway

A new gene associated with epileptic encephalopathy and cerebellar ataxia is ubiquitin-like activating enzyme 5, *UBA5*. UBA5 is the activating enzyme of the ubiquitin-fold modifier 1 (UFM1) pathway, a recently identified protein modification system (Komatsu et al., 2004).

One of the best-characterized post-translational modifications is ubiquitination. Protein ubiquitination is facilitated through an ATP-dependent process catalyzed by E1 activating, E2 conjugating, and E3 ligase enzymes (Komander and Rape, 2012). Prior to conjugation to target proteins, ubiquitin monomers are released from translated poly-ubiquitin chains by the action of de-ubiquitinating enzymes, which allow the exposure of a di-glycine (GG) C-terminal tail. The exposure of the C-terminal tail is required for activation of ubiquitin by the E1 enzyme, and subsequent

attachment to target proteins. E1-mediated activation of ubiquitin is ATP-dependent, resulting in the formation of a thioester E1-ubiquitin intermediate (Komander and Rape, 2012). An E2 enzyme subsequently binds to the E1-ubiquitin thioester bond, in a reaction known as transthiolation reaction, and ubiquitin is transferred to the target protein by the coordinated action of the E2 conjugating enzyme and E3 ligase. The E3 enzyme assists in the selective binding of ubiquitin with the target proteins (Komander and Rape, 2012).

Protein ubiquitination is involved in a number of cellular functions, including membrane protein endocytosis (Mukhopadhyay and Riezman, 2007), DNA transcription through transcription factor or histone ubiquitination (Muratani and Tansey, 2003), sub-cellular protein translocation, and protein degradation of abnormally expressed or misfolded proteins through the ubiquitin-proteasome system (Hochstrasser, 1996). Consequently, dysfunction or mutation of components of the ubiquitination pathway have been associated with many diseases, including neurodegenerative disorders (Jiang and L Beaudet, 2004). For example, mutations in *parkin*, encoding a ubiquitin E3 protein ligase, is a common cause of Parkinson's disease (Dawson and Dawson, 2010).

Ubiquitin-like (Ubl) proteins with structural similarities with ubiquitin have been identified. The majority of these Ubl proteins are conjugated to target proteins in a manner similar to ubiquitination through a process mediated by specific E1, E2 and E3 enzymes (Table 1.1), and also lead to altered protein function or location (Cappadocia and Lima, 2018).

UFM1 is a recently identified small Ubl (Komatsu et al., 2004). UFM1 is translated as a precursor form that is cleaved by UFM1-specific proteases (UfSP1 or UfSP2) and converted in a mature form (Daniel and Liebau, 2014). The mature form of UFM1 is exclusively activated by UBA5, an E1 enzyme, forming a bond with the active cysteine site in UBA5. Subsequently, UFM1 is transferred to the ubiquitin-fold modifier conjugating enzyme 1 (UFC1), the E2 enzyme (Komatsu et al., 2004). Recent studies demonstrated that UBA5 acts as a dimer and activates UFM1 in a trans-binding manner. One UBA5 monomer interacts with UFM1 and UFC1 C-terminal regions, while the second UBA5 monomer activates UFM1 by adenylation (Oweis et al., 2016). Once UFM1 is transferred to the E2 enzyme, UFM1-UFC1 intermediates will interact with UFM1-protein ligase 1 (UFL1), resulting in the transfer of UFM1 onto an acceptor lysine residue on the target protein (Tatsumi et al., 2010) (Figure 1.1).

Table 1.1. Ubiquitin-like proteins and their respective E1, E2 and E3 enzymes

Ubiquitin-like	E1	E2	E3
SUMO1, SUMO2, SUMO3	SAE1/UBA2	UBC9	Siz/PIAS
NEDD8	NAE1/ UBA3	UBC12, UBE2F	IAP
URM1	UBA4	unknown	unknown
UFM1	**UBA5**	**UFC1**	**UFL1**
FAT10	UBA6	USE1	unknown
ISG15	UBA7	UBC8	Herc5/Epf1
ATG12	ATG7	ATG10	ATG5-ATG12
LC3	ATG7	ATG3	ATG5-ATG12

Based on Cappadocia and Lima (2018)

One of the identified targets of UFM1 is the UFM1-binding protein 1 (UFBP1). UFBP1 localizes to the cytosolic side of the endoplasmic reticulum (ER) membrane and forms a complex with Cdk5rap3, another identified target of the UFM1 pathway (Lemaire et al., 2011; Tatsumi et al., 2010). Knockdown of UFBP1 was demonstrated to result in ER stress and increased cell death in mice (Cai et al., 2015). The link between the UFM1 pathway and ER stress is well documented. Upregulation of the UFM1 pathway was shown to reduce ER stress-induced apoptosis in pancreatic and ischemic heart cells (Azfer et al., 2006; Lemaire et al., 2011). Knockdown of the UFM1 pathway was additionally described to result in ER stress-induced apoptosis in fetal liver cells (Tatsumi et al., 2011). In agreement with a role of the UFM1 pathway in the ER stress response, UFM1 was reported as a target of XBP-1, a transcription factor activated under ER stress (Zhang et al., 2012).

Aside from maintaining ER homeostasis, the UFM1 pathway has been implicated in cell differentiation and cellular growth. Cdk5rap3 was shown to be recruited by UFL1 (i.e. the E3 enzyme) to a protein complex at the ER plasma membrane, where it is protected from proteasomal degradation (Wu et al., 2010). Cdk5rap3 is known to inhibit NF-kB (Gusarova et al., 2007), a transcription factor that regulates cell proliferation and apoptosis (Xiao and Fu, 2010), suggesting a potential role of the UFM1 pathway in these processes. Additionally, loss of function of the UFM1

pathway has been directly associated with defective development of erythroid and megakaryocyte progenitors in mice (Tatsumi et al., 2011). This study revealed, however, that rescue of UBA5 in the erythroid lineage reverts anaemia, but is not sufficient to impede the mice death at later stages, indicating that UFM1 has additional cellular functions (Tatsumi et al., 2011).

The involvement of the UFM1 pathway in disease has been as well described. Yoo et al. (2014) identified activating signal co-integrator 1 (ASC1) as one of the targets of the UFM1 pathway. Poly-ufmylation of ASC1, a transcriptional co-activator of estrogen receptor-α, was shown to result in development of breast cancer cells through the recruitment of key transcription factors to ERα target genes such as cyclin D (Yoo et al., 2014). Additionally, a UfSP2 (i.e. UFM1-specific protease) mutation was identified in individuals with Beukes familial hip dysplasia, who have degenerative osteoarthritis of the hip joint (Watson et al., 2015). Rubio et al. (2013) also revealed that patients with Schizophrenia have decreased expression of UFL1. Furthermore, components of the UFM1 pathway were identified in the mitochondria of *Leishmania donovani*, a pathogen that causes Leishmaniosis. In *L. donovani*, the UFM1 pathway targets the mitochondrial trifunctional protein (MTP) regulating acetyl-CoA production, and downregulation of the UFM1 pathway leads to impaired growth and death of the pathogens (Gannavaram et al., 2011).

Despite the progress made in recent years, the exact role of the UFM1 pathway in ER homeostasis, cellular differentiation, and mitochondria is not yet known, and additional investigation is necessary to identify the targets of the UFM1 pathway.

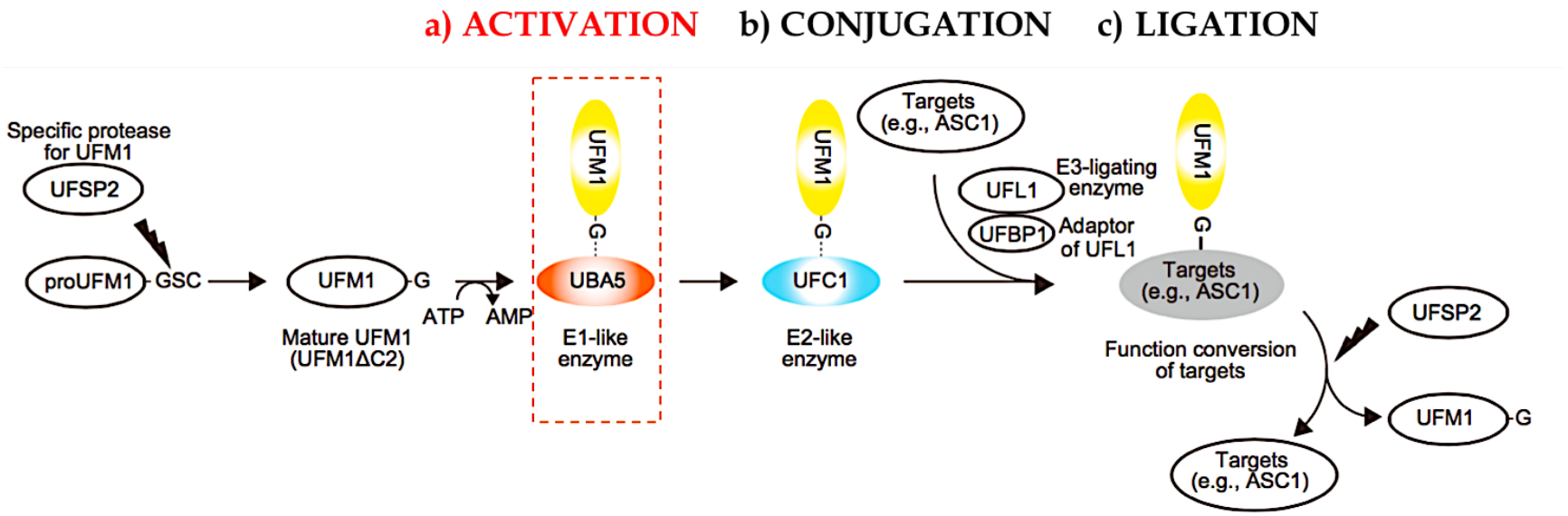

Figure 1.1. The UFM1 pathway. The process of attaching UFM1 to its target proteins requires three steps performed by an E1 activating enzyme (UBA5), E2 conjugating enzymes (UFC1), and an E3 ligase (UFL1). UFM1 is activated in an ATP-dependent manner by UBA5, and then transferred to the active cysteine of UFC1. Thereafter, UFL1 assists the bond between UFM1 and the target protein.
Adapted from (Muona et al., 2016). Reprinted from American Journal of Human Genetics, Vol.99 /issue number 3, Muona et al., Biallelic variants in UBA5 link dysfunctional UFM1 Ubiquitin-like Modifier Pathway to severe infantile-onset encephalopathy, Pages No 683-694., Copyright (2016), with permission from Elsevier

1.7. Aims of the thesis

A great number of genes have been associated with epileptic encephalopathies and cerebellar ataxias, which have provided insight into the mechanisms associated with these two disorders. However, additional research is required to understand how mutation in many of these genes affects the nervous system and the underlying molecular pathways involved in disease.

This thesis focuses on the functional characterisation of the novel genes identified by collaborators of the Bryson-Richardson lab. We aimed to evaluate the new candidate genes, *plxnb3* and *tmem33*, by investigating the functional consequences of loss of function of these genes using ENU mutant and CRISPR mutant zebrafish models, respectively. Moreover, we aimed to generate a CRISPR mutant zebrafish model to investigate the molecular alterations triggered by mutation in *uba5.* The specific aims addressed in this thesis were as follows:

I. Investigate if mutations in *plxnb3* and *tmem33* result in cerebellar ataxia, by characterizing the locomotor function and cerebellar morphology (chapter 3 and 4).

II. Investigate how mutations in *uba5* result in epileptic encephalopathy and cerebellar ataxia (chapter 5).

Chapter 2. Materials & Methods

2.1. Zebrafish husbandry and strains

Zebrafish strains used in this study were maintained in the Fish Core facility at Monash University and handled according to standard operating procedures approved by the Monash Animal Services Animal Ethics Committee (MARP/2015/004/BC). For breeding purposes, adult males and females were placed in breeding tanks on the previous day. Embryos were maintained in E3 embryo medium at 28°C. The following strains were used in this study: wild type fish of TU background were used for CRISPR genome editing; the *plexin b3*^{sa10506} strain was ordered from the Zebrafish International Resource Centre (ZIRC). The strain carries a point mutation (T>A) that results in a premature stop (*p.1119**); the *Tg* (*olig2*: *EGFP*) ^{zf532} (Yeo and Chitnis, 2007) and *Tg* (*huc*: *EGFP*) ^{knu3} (Park et al., 2000) strains were kindly provided by Dr. Jan Kaslin (Australian Regenerative Medicine Institute).

2.2. Microinjection of embryos

Embryos were collected from pairs of male and female zebrafish in breeding boxes, approximately 20 minutes after dividers were removed and placed in E3 embryo medium. A 4% low-melting agarose block with grooves was used to line up embryos for microinjection. Microinjections were performed using a Femtojet microinjection system (Eppendorf) and a M-152 Narishige micromanipulator, under a Leica M80 dissecting microscope.

2.3. sgRNA synthesis

Target sites for CRISPR/Cas9 mutagenesis were identified using CHOPCHOP online software (Montague et al., 2014). Oligonucleotides were ordered from Sigma. Synthesis of sgRNAs was performed following the protocol outlined by Gagnon et al. (2014) using the High Scribe T7 High Yield RNA Synthesis Kit (NEB). sgRNAs (150 ng/µl) were co-injected with Cas9 protein (800 ng/µl; PNA Bio) and a stop cassette (GTCATGGCGTTTAAACCTTAATTAAGCTGTTGTAG) with 20-bp homology arms into one-cell stage embryos (Figure 2.1). Oligonucleotides used in this study were for *uba5* exon 1 5′- CAGCTTGAGTTCCTCAACGG – 3′; *uba5* exon 3 5′ – GTGGTGGGAGTCGGTG GGGT – 3′; and *tmem33* exon 4 5′ – GAGTAGAGCCTTCCTGGCCC – 3′. The stop cassettes used were for *uba5* exon 1 5′- AGAGAAGAACATGGCCAccgGTCATGGCGTTTAAACCTTAATTAAG CTGTTGTAGttgaggaactcaagctgCGA – 3′; *uba5* exon 3 5′ –TGTGGCGGTGGTGGGAGTCGgtcatggc gtttaaaccttaattaagctgttgtagGTGGGGTGGGGAGTGTCACT– 3′; and *tmem33* exon 4 5′ – GCTGAGT

AGAGCCTTCCTGGgtcatggcgtttaaaccttaattaagctgttgtagCCCAGGCTTTACAGGAGGAC – 3'.

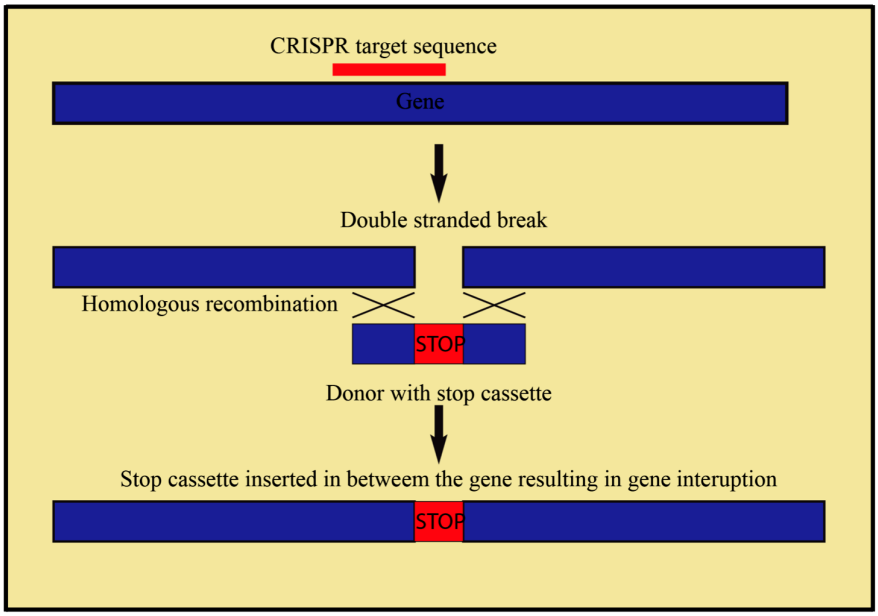

Figure 2.1 – CRISPR methodology using a stop cassette. The sgRNA is injected with a stop cassette containing several stop codons in tandem, and flanked by homology sequences that are complementary to the target region of the gene. After recognition of the target region by the sgRNA and double strand break generated by Cas9, the stop cassette is inserted in the target region through homologous recombination. This results in premature termination of transcription of the gene in the targeted region.

2.4. Fin biopsy and DNA extraction

Zebrafish were anaesthetised in Tricaine methane-sulfonate (3-amino benzoic acid-ethyl ester, Sigma) at a final concentration of 0.16% in E3 embryo medium. Fin clipping was performed with a scalpel (World Precision Instruments) by incision within the pigment gap in 5 dpf larva as per Wilkinson et al. (2018), or cutting a small piece of the caudal fin in adult zebrafish. Zebrafish were subsequently placed in individual wells of a 96-well plate, or small plastic containers if adults, and were kept individually until genotyping was completed. Genomic DNA was extracted using the Hot Shot method from whole embryos or fin clips. Samples were digested with 25 µl of 50mM NaOH at 95 ºC for 20 min, and the high pH of sodium hydroxide was buffered by adding 6.5 µl of 1M Tris HCl pH 8. DNA was stored at 4 ºC.

2.5. Genotyping using PCR

Genotyping was carried out using PCR with a set of primers designed to amplify the region of interest. The primers used were for *uba5* exon 1 (forward primer 5'- ACTCATCCTCGCCAGCTGAT -3' and reverse primers 5' - CTCGTT TGCTGTGGCGGTGG- 3'), for *uba5* exon 3 (forward primer 5' – GAGAATGGGGATAGTGCAAGAC – 3', and reverse primer 5' – TGGTGCTGGGTAATATGAC AAA – 3') and for *tmem33* exon4 (forward primer 5' CTCTGCTTGGGTGAGTCATG - 3', and reverse primer 5' – AAGGATACTTGTGATGGGGTAG – 3'). DNA amplification was performed using a BioRad Thermal Cycler using a standard 35-cycle protocol with a denaturation temperature of 95 ^{o}C, annealing temperature of 58 ^{o}C, and an elongation temperature of 72 ^{o}C. A single PCR reaction (10 µl) consisted of 1 µl DNA (20-50 ng/µl concentration), 5 µl GoTaq DNA Polymerase (Promega), 0.5 µl primer forward, 0.5 µl primer reverse and 3 µl Milli-Q water. To separate the bands of the different alleles, 10 µl of PCR product was run on 2% agarose or 2.5% polyacrylamide gel.

2.6. Genotyping using KASP

Genotyping of the *plexin b3* ^ sa10506 strain was performed using a KASP assay. The KASP assay is a competitive allele-specific PCR-based genotyping system that allows high level of accuracy in distinguishing the three genotypes (wild type, heterozygote and mutant fish). Allele-specific primers were designed by the LGC Group (https://www.lgcgroup.com) based on the supplied gene sequence: ACAGCTGAGCAGGATTGTCCCAGAAAAAGGCCCTTGGCYGGAGRTACGT[T/A] G CT CATGGTGTATGGGTCACAGCTCCTGACAGGACAAAACCTTCAACAAA. A single KASP reaction (8 µl) consisted of 1.5 µl DNA, 0.1 µl of mix of primers, 4 µl of 2x KASP Master Mix and 2.4 µl of Milli-Q water. The thermocycling conditions followed were according to the 65 – 57 ^{o}C touchdown protocol provided by the LGC Group: initial denaturation temperature of 95 ^{o}C, followed by 10 cycles of touchdown with denaturation at 94 ^{o}C and annealing from 65 ^{o}C to 57 ^{o}C and extension of primers, ending with 26 cycles of denaturation at 94 ^{o}C and amplification at 57 ^{o}C. Data analysis was performed using KlusterCaller software.

2.7. PTU treatment

In order to prevent pigment formation, embryos were treated with 1-phenyl-2-thiourea (PTU, 0.03mg/ml) (P3755, Sigma-Aldrich) before the onset of pigmentation at 1 dpf. 1% PTU was added to the embryo medium from a stock solution of 25% PTU. PTU inhibits melanogenesis by blocking all tyrosine-dependent steps in the melanin pathway and the embryos remain transparent as long as the PTU treatment is continued. PTU solution was replaced daily.

2.8. Swimming assays

Touch-evoked response and swimming performance experiments were performed at 2 dpf and 6 dpf, respectively, as previously described (Sztal et al., 2016). Each experiment was carried out blinded and with three biological replicates. Touch-evoked response and locomotor activity was analysed using the ZebraLab software (ViewPoint Life Sciences). To analyse locomotor activity, embryos were tracked in the dark for 10 min with the following parameters: inactivity threshold of 1 mm/s, detection threshold of 25 mm/s, and activity burst threshold of 30 mm/s. To test whether locomotor activity was altered upon a stimulus (darkness) in mutants compared to wild type zebrafish at 6 dpf, embryos were adapted to the device for 10 min in 0% light. Then, their movement was tracked for 5 min 0% light, 5 min 100% light, 5 min 0% light, and 5 min 100% light with the setup described above**.**

The locomotor activity of larvae from 28 dpf onwards was examined using the ZebraCube (Viewpoint) recording device wherein 9 zebrafish were recorded simultaneously in separate tanks (10 cm x 12.5 cm x 6 cm deep). Zebrafish were adapted to the device for 5 min, followed by tracking of their activity for 10 min.

2.9. Survival analysis

For survival analysis, embryos were genotyped at 5 dpf as mentioned in section 2.5 and each genotype raised separately. A maximum of 28 embryos was raised per genotype in each replicate and the number of embryos was recorded daily. Larvae were closely monitored to ensure fish suffering from severe neuromuscular disease were humanely killed before disease resulted in emaciation due to a failure to feed. All fish were maintained in the Fish Core facility at Monash University under license BSCI201618.

2.10. Adult fish brain dissection

Each fish was euthanized in Tricaine methane-sulfonate. The caudal fin was excised and the fish placed upright in ice to exsanguinate and prevent blood clotting on the brain during dissection. The dorsal neurocranium was removed by lifting up the heart-shaped scale that lies over the junction between the cranium and torso and pulling in an anterior direction until the brain was exposed from the telencephalon to the cerebellum. The muscle above the hindbrain was resected to expose the medulla oblongata and spinal cord. The optic nerves were then cut to release the optic chiasm from

the bone, and the lateral portion of the neurocranium was removed. The brain was separated from the spinal cord and immediately placed into the appropriate medium for experimental application.

2.11. Molecular Biology Techniques

2.11.1. RNA extraction

RNA extraction was carried out on wild type embryos at 1 dpf, 2 dpf, 3 dpf, 4 dpf, 5 dpf, and 6 dpf for RT-PCR and to generate *in situ* hybridization RNA probes. Embryos were homogenized in 1 ml of Tri-reagent (Sigma), followed by incubation at room temperature for 5 min. 200 µl of chloroform was added and the sample was vortexed for 15 seconds. This was followed by centrifugation for 20 min at 16,128g. The aqueous phase was then transferred to a new tube and the RNA was precipitated by adding 600 µl of isopropanol. After 10 min incubation at room temperature, the reaction was centrifuged in 18,928g at 4 ^{o}C for 20 min. The supernatant was discarded, and 1ml of 75% ethanol in DEPC-treated water was added and the pellet washed by centrifugation for 10 min in 18,928g at 4 ^{o}C. After discarding the supernatant, the pellet was air dried at room temperature for 10 min. 20 µl of RNA-free water was added to dilute the pellet. RNA was quantified on the Nanodrop®ND-1000 Spectrophotometer (Thermo Scientific) and 1 µl was run on a 1 % agarose gel. To remove remnants of genomic DNA, 2 µl of DNase I (Promega) and 2 µl of DNase buffer (Promega) was added to 6 µl of RNA.

2.11.2. cDNA synthesis and RT-PCR

cDNA synthesis was carried out using the Protoscript III synthesis kit (Invitrogen) according to the manufacturer's instructions. A 20 µl reaction containing 1 µg of template RNA, 1 µl of oligonucleotide primer mix, 1 µl of random primer mix, 10 µl of Protoscript II reaction mix (2X), and 2 µl of Protoscript II enzyme mix (10x) was incubated at 25 ^{o}C for 5 min, and then at 42 ^{o}C for 1 hour, followed by inactivation of the reverse transcriptase enzyme at 80 ^{o}C for 5 min.

RT-PCR was performed in a 20 µl reaction with 10 µl of GoTaq DNA Polymerase (Promega), 1 µl of forward primer, 1 µl of reverse primer and 7 µl of Milli-Q water. Primers used were: *uba5* (forward primer 5'- GCAGGACTTCTTCCCAAGCA-3' and reverse primer 5'- ATGCTTGTCTACACCCA GCC-3'), *plexinb3* (forward primer 5' – GTCACGCAAACCAAACTGGA – 3' and reverse primer 5' – CGCCCATCAACACCTTTAGT – 3'), *tmem33* (forward primer 5' – TTCAGCTGAGTAGAGCCTT CC – 3' and reverse primer 5' – TCGTCAACTATTAGGAGGCAAC – 3'), *β – actin* (forward primer 5' – GCATTGTGACCGTATG CAG-3' and reverse primer 5'-GATCCACATCTGCTGGAAGGTGG-

3′), *myelin basic protein* (forward primer 5′ – AATCAGCAGGTTCTTCGGAGGA – 3′ and reverse primer 5′ – GGGCATACAATCCAAGCCACA – 3′), *sox10* (forward primer 5′ – GACCTACCGAAG TCACCTGTGG – 3′ and reverse primer 5′ – GTTTGTGTCGATTGTGGTGC– 3′), *olig1* (forward primer 5′ – AGGATCAGGAGGACCAGGCTCCAAT – 3′ and reverse primer 5′ – GTAGGCAAGTTTGGTCCTGGAGA – 3′), *olig2* (forward primer 5′ – ATGGACTCTGACACGAGC CGA – 3′ and reverse primer 5′ – GGCTAAGGAAGGTTTGCCATT – 3′), and *aldolase C* (forward primer 5′ – GTCTATAGGCAGTATGGGGAAGC – 3′ and reverse primer 5′ – GCCAGGTCTTCAG AGCCGAG– 3′). The PCR was carried out using the following conditions: denaturation at 94 °C for 2 min, followed by 30 cycles of 94 °C denaturation for 30 secs, 58 °C annealing for 30 secs and extension at 72 °C for 30 secs, and final extension at 72 °C for 5 min.

2.11.3. Cloning of PCR products

2.11.3.1. Ligation reaction

Cloning of PCR products was performed using the Quick protocol and the pGEM®-T Easy vector from Promega. Ligation reaction was set up on ice by mixing 5 µl of 2X Rapid Ligation Buffer, 1 µl of pGEM®-T Easy vector, 1 µl of T4 DNA ligase and 3 µl of PCR product. The reaction was then incubated for 1 hour at room temperature, or overnight at 4°C.

2.11.3.2. Transformation of competent cells using heat shock

Frozen aliquots of competent cells (New England Biolabs) were thawed on ice. Plasmid DNA (1µl) was incubated with 100 µl of cells on ice for 30 minutes. A heat shock was applied at 42 °C during 45 seconds (sec), followed by cooling on ice for 2 minutes. Then, 1ml of LB medium was added to the bacteria solution and the bacterial culture was incubated for 1 hour with agitation at 37 °C. Bacteria were plated in solid medium (LB) containing ampicillin (100µg/µl), X- Gal and IPTG, to select the transformed bacteria, and grown overnight in an incubator at 37 °C.

2.11.3.3. Plasmid DNA Isolation

A single colony of transformed bacteria was collected using a micropipette tip and inoculated in a 15ml falcon containing 2ml of pre-warmed LB medium supplemented with ampicillin (100µg/µl). The bacterial culture was then grown in an incubator for 12 hours at 37 °C. For small scale isolation of plasmid DNA, bacterial cultures were processed using the Miniprep Quick protocol according to Epoch Life Science instructions. Accordingly, the bacterial cultures were centrifuged at 11,200g for

1 min to harvest the pellet. Next, 250 µl of MX1 buffer (RNase A, 100 µg/ml) was mixed with the pellet, and 250 µl of the MX2 buffer was added. The reaction was incubated at room temperature for 5 min, and 350 µl of MX3 buffer was added, followed by centrifugation at 18,928gfor 10 min. After these steps, the supernatant was transferred onto a spin column for further centrifugation at 4,000 for 1 min. The columns were washed with 500 µl of PB buffer, by centrifugation at 16,128g for 1 min, and 500 µl of WS buffer, and another centrifugation at 16,128gfor 1 min. The ethanol contained in both washing solutions was allowed to evaporate by centrifugation at 16,128gfor 2 min. Finally, the DNA was eluted by adding 50 µl of EB buffer to the column and centrifugation for 1 min at 16,128g. The extracted plasmid DNA was run on a 1% Agarose (Sigma) gel to ensure the DNA integrity, quantified using the Nanodrop ®ND-1000 Spectrophotometer (Thermo Scientific), and stored at -20 ^{o}C.

2.11.4. Antisense mRNA probe synthesis

Before mRNA synthesis, plasmid DNA was sequenced to determine the orientation of the insert within the vector by using M13 forward (5' – TGTAAAACGACGGCCAGT – 3') and M13 reverse (5'- CAGGAAACAGCTATGACCATG -3') primers. If the insert was oriented with the 5' end to the T7 site, M13 forward and gene-specific forward primers (section 2.2.3.) were used to amplify the PCR product; if the insert was oriented with the 5' end to the SP6 site, M13 reverse and gene-specific reverse primers (section 2.2.3.) were used to amplify the PCR product. This method ensured that the PCR product contained the T7 or SP6 RNA polymerase transcription start sites.

mRNA probes were synthesized with an appropriate RNA polymerase (T7 or SP6, Promega) following the manufacturer's guidelines. Briefly, 1 µg of PCR product was added to 10x DIG-NTP mix (Promega), RNAse inhibitor (Roche), 10x Transcription Buffer (Roche) and 2 µl of T7 or SP6 RNA polymerase in a final volume of 20 µl with RNase free water. The reaction was incubated at 37 ^{o}C overnight. After synthesis, RNA was treated with 20 U DNase I (Promega) at 37 ^{o}C for 15 min. To stop the reaction 2 µl of 200mM EDTA (pH 8.0) was added, and the RNA was purified by adding 2.5 µl of 4M LiCl and 75 µl pre-chilled ethanol 100% and incubation at -20 ^{o}C for at least 2 hours. RNA was next precipitated by centrifugation at 18,928g for 30 minutes at 4 ^{o}C. The supernatant was removed and the pellet was washed with 1ml of 70% ethanol. The RNA precipitate was centrifuged for a second time at 18,928g for 15 minutes at 4 ^{o}C, and the supernatant discarded. Lastly, the pellet was air dried for 10 min and ressuspended in 100 µl of RNase-free water containing 1 µl of RNase inhibitor, and stored at -80 ^{o}C. RNA integrity was checked by running 2.5 µl of RNA on a 0.8% agarose gel, and RNA concentration was determined using the Nanodrop®ND-1000 Spectrophotometer (Thermo Scientific).

2.11.5. Fixation of embryos

Embryos were fixed overnight in 4% PFA (in PBS) at 4 ºC, or at room temperature for 3 hours. After fixation, embryos were washed 3 times for 15 min in PBST (PBS with 0.01% Tween) to remove residual PFA. Fixed embryos were stored at 4 ºC for immediate use or dehydrated in a methanol series (25% methanol/ 75% PBST, 50% methanol/ 50% PBST, 75% methanol/ 25% PBST and 100% methanol) and stored at -20 ºC until processed. For *in situ* hybridization, embryos were first bleached in 3% peroxide/ 0.5% KOH for 40 min at room temperature before dehydration in methanol and storage at -20 ºC.

2.11.6. Whole-mount *in situ* hybridization

Whole mount *in situ* hybridization was performed as previously described in Thisse and Thisse (2008). Accordingly, embryos were rehydrated for 5 minutes in a methanol series (100% methanol; 75% methanol/PBST; 50% methanol/PBST; 25% methanol/PBST) and washed 4 times in 100% PBST for 5 min. Next, embryos were digested with proteinase K (10 g/ml) for 3 min at 24 hpf, or 10 min when > 48 hpf, and washed in PBST 5 times for 5 min. After the washes, embryos were transferred to pre-hybridization buffer (pre-Hyb) for 2-5 hours at 70 ºC. The pre-Hyb buffer was then replaced with pre-Hyb containing 100 ng of DIG-labelled RNA probe (1:100) and the embryos were incubated at 70°C overnight. Washes were performed at the hybridization temperature with preheated solutions for 15 minutes each with 75% Hyb /2X SSC; 50% Hyb/2X SSC; 25% Hyb/2X SSC; 100% SSC and finally 2 times 30 minutes in 0.2X SSC. A series of washes were performed at room temperature for 10 minutes each in 75% 0.2X SSC/PBST; 50% 0.2X SSC/PBST; 25% 0.2X SSC/PBST and 100% PBST. Embryos were blocked in 2 mg/ml BSA, 2% goat serum in PBST for several hours and then incubated with alkaline-phosphatase (AP)-conjugated anti-DIG Fab fragments (Sigma) diluted 1:1000 in 2 mg/ml BSA, 2% goat serum in PBST at 4°C overnight with agitation. After washing at least 5 times for 15 minutes with PBST, the embryos were rinsed 3 times for 5 minutes in NTMT reaction buffer. Detection was performed using NBT/BCIP (Sigma; 20 µl/ml). After stopping the reaction with 100% PBST twice for 5 min, embryos were re-fixed in 4% PFA for 10 min and again washed with 100% PBST twice for 5 min. Embryos were cleared in an ethanol series in 1x PBST, washed into 80% glycerol and stored at 4 °C. Images were acquired using the Olympus SZX10 dissecting microscope at 50x and 80x magnification, and stacks were processed using Zerene Stacker (https://zerenesystems.com).

2.11.7. Whole-mount immunohistochemistry

For immunohistochemistry, embryos were rehydrated through successive dilutions of methanol in 1x PBST, and washed 3 times for 5 min in 100% PBST. Digestion was first performed with acetone at – 80 ºC for 15 min, and embryos were washed at room temperature in Milli-Q water for 5 min. A second digestion was carried out with 2.5 % trypsin at room temperature for 15 min, and embryos were then placed in blocking buffer at room temperature for at least 1 hour before being incubated in blocking buffer containing primary antibody at 4 ºC for at least 2 nights. Embryos were washed several times in 100% PBST for 2 hours and incubated in blocking buffer with secondary antibody at 4°C overnight. Lastly, embryos were washed six times for 15 min in 100% PBST and stored at 4 °C. The primary antibodies used in this study were anti-synaptic vesicle glycoprotein 2A (DSHB, 1/10), anti-alpha bungarotoxin (Biotium, CF594, 1/500), anti-acetylated alpha-tubulin (Sigma, T6793, 1/1000), anti-GFP (Invitrogen, A-11122, 1/100), and anti-neurofilament associated protein (DSHB, 3A10, 1/10). Alexa Fluor-488 and Alexa Fluor-594 secondary antibodies (Molecular Probes), and Alexa Fluor-594 phalloidin (Thermofisher) were used at 1:150. The samples were embedded in 1 % low melting point agarose (A9414; Sigma) and the images acquired using the Thorlabs confocal microscope (20x objective). The maximum intensity projections were obtained using Fiji (http://fiji.sc).

2.12. Western Blotting

Protein lysates were obtained per (Boglev et al., 2013) and quantified using the Qubit3 Fluorometer (Invitrogen). 30 µg of each sample, along with reducing agent (ThermoFisher) and protein loading dye (ThermoFisher), was heated at 70 °C for 10 min, separated by SDS-PAGE on NuPAGE 4-12 % Bi-Tris gels, and transferred onto PVDF membrane (Millipore). Following transfer, the membrane was blocked with 5 % skimmed milk in PBST for 1 hour, and probed with primary antibody at 4 °C overnight. Primary antibodies used in this study were: anti-Ufm1 (Abcam, ab108062, 1/1000), anti-glutamine synthetase (Merck Millipore, MAB302, 1:1000), anti-GFAP (Abcam, ab154474, 1:1000), and anti-NCAM (Merck Millipore, AB5032, 1:1000). The membrane was washed 5 times for 15 min in 1x PBST and incubated with HRP-conjugated secondary antibody (Southern Biotech, 1/10000) for 1 hour at room temperature. Immunoblots were developed using ECL prime (GE healthcare), washed with stripping buffer twice for 10 min, with 1x PBS twice for 10 min and with 1x PBST twice for 5 min. As loading control, total protein staining was carried out with Direct Blue solution for 10 min at room temperature, and the membrane was washed with wash buffer for 10 min. The blot images were quantified using ImageJ and normalized against the total protein of each sample.

2.13. Preparation of samples for LC-MS analysis

Mixture of ^{13}C, ^{15}N labelled amino acids was received as a suspension (Part number 767964, Lot # MBBC4315). According to the certificate of analysis provided by Sigma Aldrich the concentration of Glutamic acid was 42 mM and Glutamine 20mM. Following dilution to 10 mL in water all solids dissolved. Accordingly, the concentration of labelled Glutamic acid and labelled Glutamine in this dilute solution corresponds to 4.2 mM and 2.0 mM respectively. 162uL of this dilute solution was then diluted to a final volume of 1800uL in 2:6:1 Chloroform:Methanol:Water (v/v/v) used for sample extraction. Accordingly, the concentration of the labelled amino acids was 378 µM and 180 µM respectively.

Frozen samples were crushed while frozen using the bio-pulveriser (biospec products) which had been cooled in liquid nitrogen. Crushed samples were then transferred to pre-cooled Eppendorf tubes on dry ice. Ice cold extraction solvent equivalent to 70 µL per 30 fish was added to each sample. Samples were then sonicated in an ice water bath for 10 minutes and then centrifuged for 10 minutes at 4 degrees and the supernatant transferred to a mass spectrometry sample insert for LC-MS analysis. 10uL of each sample was pooled to provide a quality control sample.

2.14. Electron Microscopy

Zebrafish were anesthetized and immediately fixed in 2% glutaraldehyde/2% PFA, in 0.1 M Na cacodylate buffer (pH 7.4) overnight. Samples were post-fixed in osmium buffer (pH 7.4) for 2 hours at 4 °C in the dark, rinsed in distilled water, and stained with 0.5 % uranyl acetate. Dehydration was carried out in ethanol gradients, and samples were embedded in Epon epoxy resin. After polymerization, ultrathin sections (80 nm) were cut and stained with 2 % uranyl acetate in distilled water and Reynolds lead citrate.

Electron microscopy sectioning and imaging was carried out by Viola Oorschott (Ramaciotti Centre for Cryo-Electron Microscopy, Monash University).

2.15. Brightfield imaging and measurements

Lateral and dorsal images were acquired on an Olympus SZX16 microscope (30-40 larvae per replicate). The forebrain cross-sectional area and body length were measured with Fiji software. For body length measurements (from lateral images), a polyline was drawn beginning at the anterior-most point of the body and terminating at the posterior-most point on the tail; for forebrain area

measurements (from dorsal images) an outline was drawn beginning at the posterior-most point of the eye and tracing around the head to terminate at the start point.

2.16. Statistics

Means, standard deviation (SD), and standard error of the mean (S.E.M.) were calculated using SPSS. Graphs were generated with the Graph Pad Prism software (www.graphpad.com). The statistical analysis and test used are indicated in the respective figure legend.

2.17. Multiple sequence alignment and phylogenetic analyses

Full-length amino acid sequences were retrieved from Ensembl protein database for human, mouse, medaka and zebrafish Plexin Bs, including: human PLXNB1 (ENSDART00000358536.8), human PLXNB2 (ENST00000449103.5), human PLXNB3 (ENST00000538966.5), mouse PLXNB1 (ENSMUST0000072093.12), mouse PLXNB2 (ENSMUST00000109331.8), mouse PLXNB3 (ENSMUST00000002079.6), medaka Plxnb1a (ENSORLT00015024445.1), medaka Plxnb1b (ENSORLT00015012464.1), medaka Plxnb2a (ENSORLT00020005105.1), medaka Plxnb2b (ENSORLT00020026625.1), medaka Plxnb3 (ENSORLT00020011162.1), zebrafish Plxnb1a (ENSDART00000166663.2), zebrafish Plxnb1b (ENSDART00000161257.3), zebrafish Plxnb2a (ENSDART00000159447.2), zebrafish Plxnb2b (ENSDART00000042781.8) and zebrafish Plxnb3 (ENSDART00000026965.11). Multiple sequence alignment was carried out using T-Coffee (http://tcoffee.crg.cat/apps/tcoffee/do: regular) using clustalW_msa alignment method. The generated alignment was formatted using BoxShade (http://www.ch.embnet.org/software/BOX_form.html). The maximum likelihood phylogenetic tree was generated using the LG+G model and MEGA 6.0 software (Tamura et al., 2013).

2.18. Solutions

E3 embryo medium: 5 mM NaCl, 0.17 mM KCl, 0.33 mM CaCl, 0.33 mM MgSO4 in water.

EB buffer (Elution buffer): 10 mM Tris-HCl pH 8.5.

Hybridization (Hyb) buffer: 50% Formamide, 20X SSC, 20% Tween 20, 1M Citric acid.

Immunohistochemistry blocking buffer: 2% goat serum, 1% BSA, 1% DMSO and 1% PBST.

MX1 buffer (Suspension buffer): 50 mM Tri-HCl, 10 mM EDTA pH 8.0, 100 µg/ml RNase A

MX2 buffer (Lysis solution): 0.2 M NaOH and 1% SDS

MX3 buffer (Neutralization and Binding solution): 4 M guanidine hydrochloride and 0.5 M potassium acetate, pH 4.2

NTMT reaction buffer: 1 M Tris-HCl pH 9.5, 1 M MgCl2, 5 M NaCl, 20% Tween 20.

PB buffer (Wash buffer): 5 M guanidine hydrochloride, 20 mM Tris-HCl, pH 6.6

Pre-hybridization (pre-Hyb) buffer: 50% formamide, 20X SSC, 50 ug/µl yeast RNA,100 µg/µl heparin, 20% Tween 20, 1M citric acid to pH 6.0-6.5.

RIPA buffer: 50 mM Tris-HCl pH 7.4, 150 mM NaCl, 22 mM EDTA, 1% NP-40 and 0.1% SDS.

Stripping buffer: 0.75 g Glycine, 0.5 mL 10% SDS, 0.5 mL Tween20 in 50 mL final volume with Milli-Q water.

Wash solution and direct blue for Western blot: 200 mL Ethanol, 5 mL Acetic Acid and 25 mL of Milli-Q water. 800 µl of 0.1% direct blue is added to 9.2 mL of wash solution.

WS buffer (Wash buffer): 10 mM Tris-HCl pH 7.5 with 80% ethanol

Chapter 3. Characterization of *tmem33* mutant zebrafish to investigate the potential role of *TMEM33* in cerebellar ataxia

Introduction

Cerebellar ataxias are clinically defined by cerebellar dysfunction and difficulties with tandem walking. The patients' symptoms can range in severity, age of onset and may be associated with both the central and peripheral nervous systems (Anheim et al., 2012). Autosomal recessive cerebellar ataxia patients, in particular, may exhibit, other than cerebellar atrophy, oculomotor impairment, mental retardation, decreased or absent tendon reflexes, and decreased sensibility in the ankles (Anheim et al., 2012). These disorders are currently incurable and associated with high incidence of disability and morbidity.

Collaborators of the Bryson-Richardson lab have identified a novel disease candidate gene associated with cerebellar ataxia using linkage analysis and exome sequencing. A homozygous recessively inherited mutation in the *TMEM33* gene (*p. T109P*) was identified in two siblings presenting weakness around the ankles, wasting of calf muscles, poor balance, saccadic interruption of eye movements, and chronic cough at age of 54 and 55 years, respectively. Nerve conduction studies showed a severe sensorimotor peripheral neuropathy. Brain MRI revealed that the patients presented progressive atrophy of the cerebellum, and of the brainstem (Novak et al., personal communication). To our knowledge this is the first report on this particular combination of symptoms in cerebellar ataxia patients, representing a new type of autosomal recessive cerebellar ataxia.

TMEM33 has not been previously associated with neurological disease. *TMEM33* encodes for a transmembrane protein that is abundantly expressed in the brain, liver, and kidneys in mammals (Nakadai et al., 1998). *In vitro* studies demonstrated that TMEM33 is mainly localized to the endoplasmic reticulum (ER), and is involved in maintaining the ER tubular structure by binding and inhibiting the action of ER-membrane shaping proteins, known as reticulons (Urade et al., 2014). TMEM33 is also involved in regulation of the unfolded protein response triggered under ER stress conditions (Sakabe et al., 2015). TMEM33 is required to modulate the activity of IRE1 that is crucial to initiate the unfolded protein cascade, and induces the PERK pathway that is involved in the inhibition of protein synthesis to maintain cellular homeostasis (Sakabe et al., 2015). ER-shaping proteins have been linked with neurodegenerative diseases, like ALS and Hereditary spastic paraplegia (Westrate et al., 2015). As an example, overexpression of reticulon-4A was revealed to protect against neurodegeneration in a SOD1 (*p. G93A*) transgenic mouse model of ALS, whereas knockout of reticulon-4A further exacerbates disease (Yang et al., 2009). Of importance, ER stress is a common mechanism associated with disease in the nervous system (Cabral-Miranda and Hetz,

2018). Disruption of the ER homeostasis could therefore be a potential pathomechanism associated with *TMEM33* dysfunction. Still, the biological significance of TMEM33 remains largely unknown, and additional studies have suggested that TMEM33 may play a role in other cellular processes. In particular, proteomic studies have demonstrated that TMEM33 is one of the interactors of two-pore ions channels (Lin-Moshier et al., 2014), which are localized to the membrane of endosomes and lysosomes. Two-pore channels regulate the release of Ca^{2+} from these organelles and have been implicated in regulation of the autophagic pathway (Lin et al., 2015). *In vitro* analysis, using melanoma cell lines, further revealed that TMEM33 is co-expressed with Neutral Endopeptidase (Velazquez et al., 2007), an enzyme associated with the metabolism of several peptides in the brain (Carson and Turner, 2002). Additionally, TMEM33 was also implicated in the degradation of the major histocompatibility complex class I molecules (MHC I) pathway (Chapman et al., 2015). Furthermore, in yeast, Tts1, the TMEM33 homologue, is involved in the reshaping of the nuclear envelope during mitosis (Zhang and Oliferenko, 2014). More recently, TMEM33 was shown to contribute to angiogenesis in response to VEGF (vascular endothelial growth factor) signalling (Savage et al., 2019).

Although TMEM33 has never been associated with a role in the nervous system, the involvement of TMEM proteins in ataxia disorders has been reported. Namely, *TMEM240* mutations are known to cause spinocerebellar type 21 (Delplanque et al., 2014), and mutations in *TMEM67* (Huynh et al., 2018), *TMEM216* (Edvardson et al., 2010), *TMEM237* (Huang et al., 2011), *TMEM138* (Lee et al., 2012), and *TMEM231* (Srour et al., 2012) were identified in patients with Joubert syndrome, a disorder characterized by abnormal ocular movements, ataxia, and hindbrain-midbrain malformations. Thus, *TMEM33* is a strong candidate for cerebellar ataxia.

In this study, we aimed to generate and characterize *tmem33* mutant zebrafish to evaluate *TMEM33* as a candidate for cerebellar ataxia. We investigated the conservation of zebrafish Tmem33 amino acid sequence, followed by functional characterization of *tmem33* mutants. We conclude that loss of Tmem33 does not lead to motor deficits and cerebellar defects at early stages of zebrafish development. However, further work is required before we can exclude *TMEM33* as a candidate of cerebellar ataxia.

Results

3.1. Zebrafish have a single *TMEM33* orthologue

In humans, the *TMEM33* gene (ENSG00000109133) is located between *PHOX2B* and *DCAF4L1* on chromosome 4. We searched the Ensembl database using the human *TMEM33* coding sequence and identified a single *TMEM33* homologue in zebrafish (*E-value* = 0.033; ENSDART000000193707.1) on chromosome 14. A reciprocal search on the Ensembl human database using the zebrafish *tmem33* coding sequence was additionally performed to confirm that *tmem33* is the correct homologue of human *TMEM33*. The chromosomal region harbouring the zebrafish *tmem33* gene was found to be flanked by the *cryba1l1* and *ccna2* genes and showed no conserved synteny with the human genomic region spanning 20 genes upstream and downstream to *tmem33*. Though, *bend4*, *shisa3*, and *atp8a1*, which are located downstream of human *TMEM33*, are located upstream of zebrafish *tmem33* following an interval of 28 genes (Fig. 3.1).

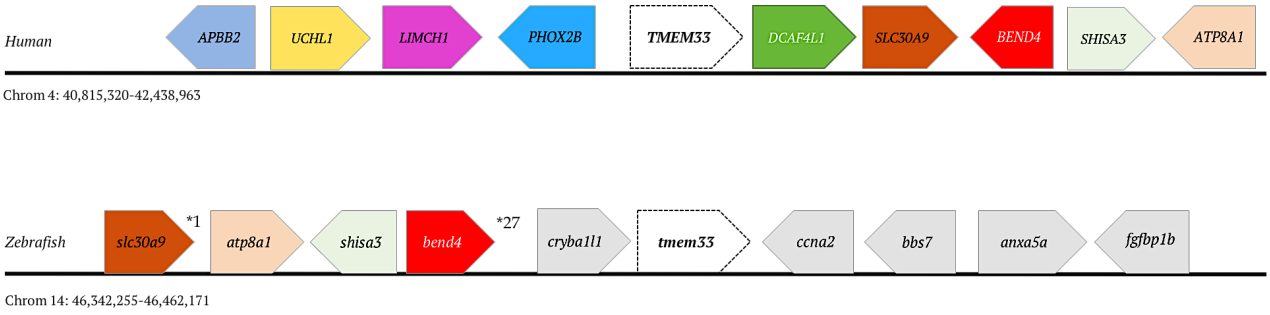

Figure 3.1. Genes flanking TMEM33 in the human genome and corresponding chromosomal region in zebrafish. Each line represents a contiguous sequence and the arrowhead indicates the direction of transcription for each gene. TMEM33/tmem33 genes are shown in white.

To examine the conservation at the protein level, the amino acid sequences of zebrafish Tmem33 and human TMEM33 were retrieved from the Ensembl protein database (version GRCz11) and aligned based on sequence homology. Human TMEM33 and zebrafish Tmem33 protein sequences demonstrate high conservation with 80% overall amino acid identity, and 88% similarity. Similar to human, zebrafish Tmem33 is a protein with three transmembrane helix spanning domains with 81.8%, 85.5% and 100% amino acid conservation, respectively (Fig. 3.2, green boxes). The high degree of conservation between human TMEM33 and zebrafish Tmem33 sequences suggests a conserved function.

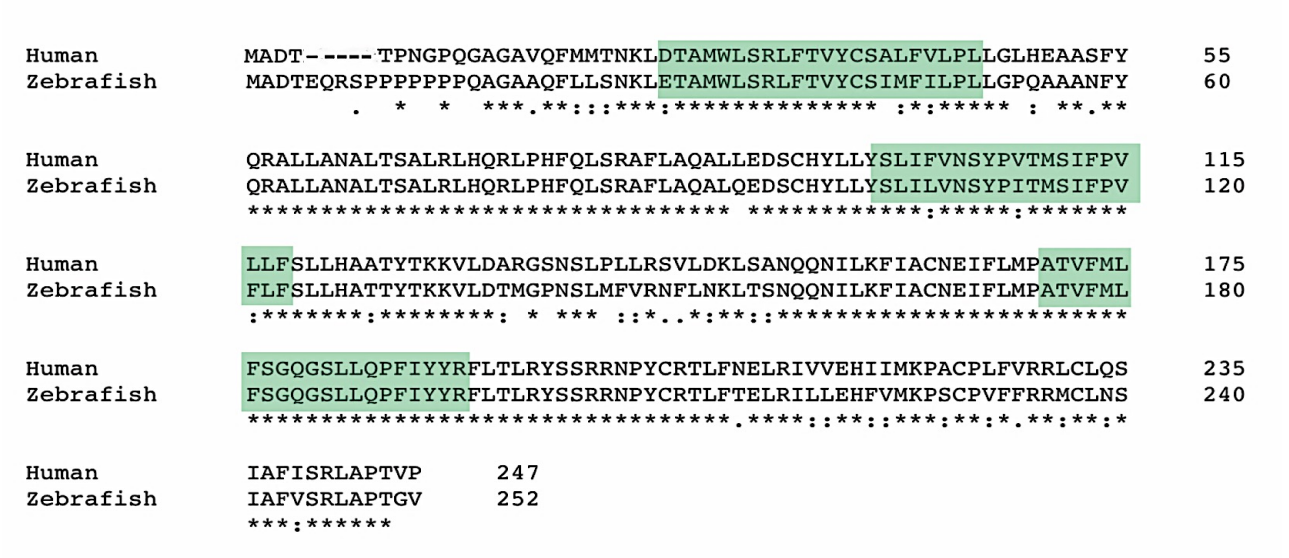

Figure 3.2. Zebrafish Tmem33 and human TMEM33 protein sequences. Zebrafish Tmem33 and human TMEM33 protein sequences alignment using Clustal Omega. The three transmembrane helix domains are highlighted in green. * (asterisk) denote the conserved amino acids, : (colon) indicates conservation between groups of strongly similar properties - scoring > 0.5 in the Gonnet PAM 250 matrix, and . (period) indicates conservation between groups of weakly similar properties - scoring =< 0.5 in the Gonnet PAM 250 matrix. Numbers on the right of sequences indicate positions relative to the translation start site.

3.2. *tmem33* expression during embryonic development

The expression pattern of *tmem33* has never been reported in zebrafish. To investigate the temporal and spatial expression pattern of *tmem33*, we performed semi-quantitative RT-PCR and whole mount *in situ* hybridization during zebrafish embryonic development. RT-PCR analyses showed that *tmem33* transcripts are detected from 10-somite to 5 dpf stages (Fig. 3.3 A). Notably, *tmem33* expression level is higher at 2 dpf and 3 dpf. *In situ* hybridization analyses showed that *tmem33* is predominantly expressed in the forebrain, midbrain, and hindbrain at 1 dpf (Fig. 3.3 B & C). At 3 dpf, *tmem33* remains expressed throughout the brain and is also detected in the neural tube, notochord, liver, pancreas, and gut (Fig. 3.3 B). *tmem33* expression was not observed in the zebrafish skeletal muscle. This data suggests that Tmem33 may play a function in several tissues including in the brain and neural tube, which are the areas of interested in cerebellar ataxia.

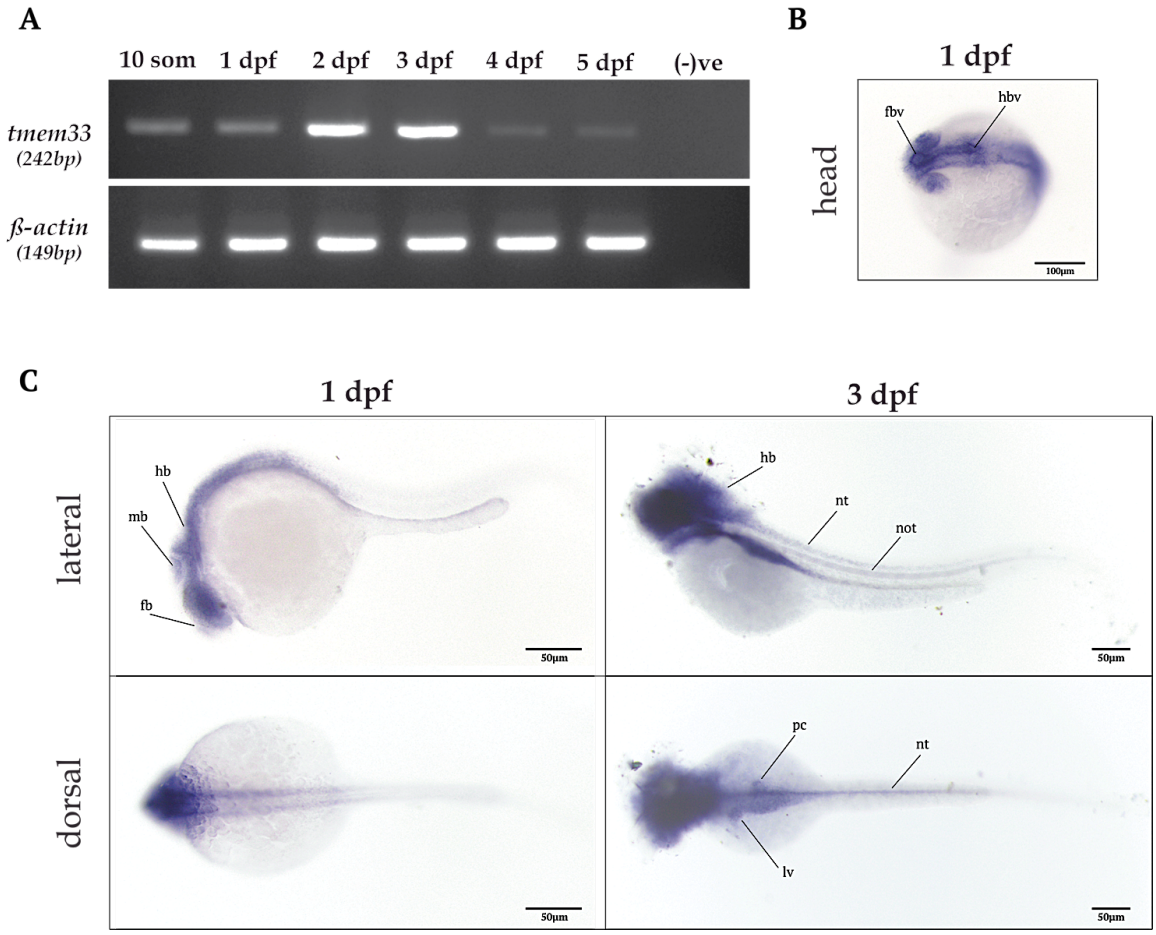

Figure 3.3. Expression of *tmem33* during zebrafish development. (A) RT-PCR analysis of *tmem33* mRNA in zebrafish from 10-somites to 5 dpf. (B & C) Whole-mount *in situ* hybridization on zebrafish embryos at 1 dpf and 3 dpf. Abbreviations: fbv – forebrain ventricle, hbv – hindbrain ventricle, fb – forebrain, hb – hindbrain, mb – midbrain, nt – neural tube, not – notochord, pc – pancreas, lv - liver.

3.3. Generation of *tmem33* mutant zebrafish

The *TMEM33* variant identified in the patients results in a substitution of a threonine residue to a proline within the second transmembrane helix domain of the protein. The mutation is predicted to significantly impair TMEM33 protein structure, preventing TMEM33 from adopting its native helical conformation (Novak et al., personal communication). To gain insight into the potential role of *TMEM33* in causing cerebellar ataxia, we mutated the *tmem33* gene in zebrafish using CRISPR mutagenesis. Since patients with the *TMEM33* variant exhibit a late disease-onset, we generated a *tmem33* loss-of-function mutant. The *tmem33* loss of function is expected to result in an earlier phenotype compared to the patients.

We selected a target site located within exon 4 of zebrafish *tmem33* and designed a stop cassette, consisting of a 35-base pair region with stop codons, flanked by 20-base pairs homologous sequences to the target site. The sgRNA targeting exon 4 and the stop cassette were co-injected into one-cell stage zebrafish embryos. Injected embryos were confirmed to include a mutated sequence in the target site, and the remaining embryos were raised to adulthood. From the outcross of F0 with wild type zebrafish, we identified an F0 that transmitted a mutation to the offspring. Sequencing revealed that the F0 carries an in-frame insertion of 90 base pairs (*c.268_359 ins (90); p. Ser94**) that included part of the stop cassette sequence, resulting in a premature stop codon (Fig. 3.4 A). RT-PCR was used to verify that the mutation leads to reduction of *tmem33* mRNA in mutant zebrafish compared to siblings (Fig. 3.5). As zebrafish only has one predicted protein isoform reported in the Ensembl database, the mutation made in zebrafish is predicted to result in a loss of function (Fig. 3.4 A&B). However, due to the lack of suitable zebrafish Tmem33 antibody we were not able to confirm reduction of Tmem33 protein levels.

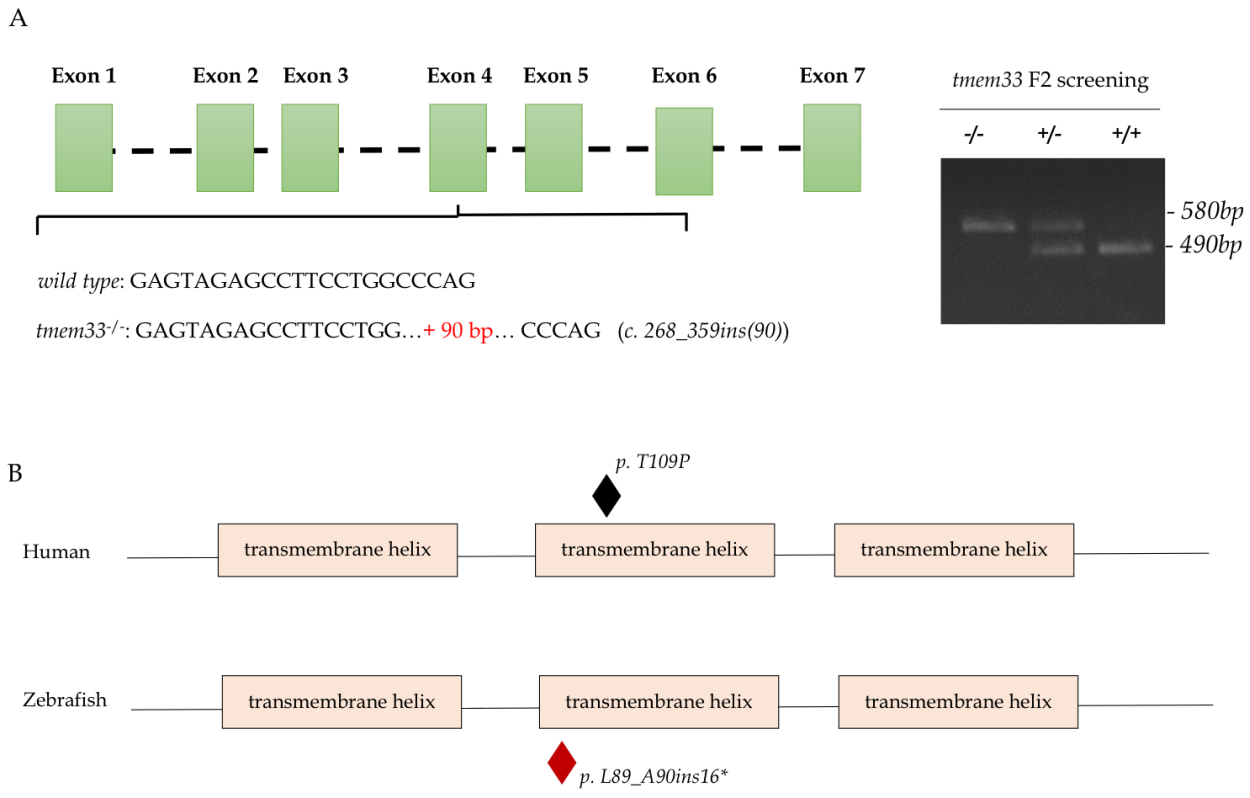

Figure 3.4. Targeted disruption of zebrafish *tmem33* gene. (A) Diagram of *tmem33* genomic DNA, showing the CRISPR target site in exon 4. CRIPSR mutagenesis resulted in the insertion of 90 base pairs, including a stop codon. On the right, representative genotyping results of the F2 generation. (B) A diagram of the human TMEM33 and zebrafish Tmem33 protein domains, showing the mutation site in the patients with cerebellar ataxia and the mutation generated in zebrafish.

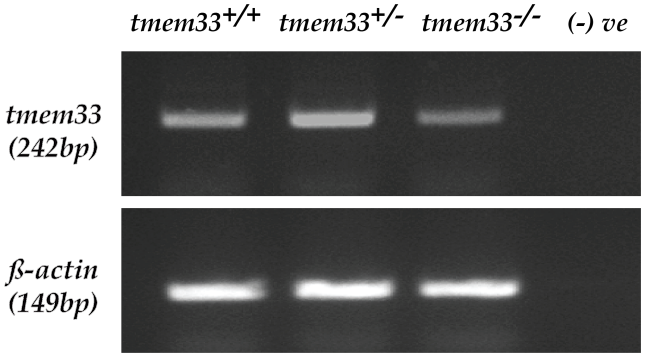

Figure 3.5. RNA analysis of *tmem33* mRNA in the progeny of *tmem33*$^{+/-}$ incrosses. Semi-quantitative RT-PCR using total RNA extracted from 6 days post fertilization embryos shows reduced *tmem33* mRNA levels in *tmem33* mutants. *β*-actin expression level was used as control.

3.4. *tmem33*$^{-/-}$ zebrafish show normal movement patterns

The clinical symptoms of *TMEM33* patients include locomotor abnormalities. To examine this in the *tmem33*$^{-/-}$ fish, F2 heterozygotes were in-crossed to obtain embryos for swimming analysis at 6 dpf. Locomotor activity was tracked for 10 minutes, and data of *tmem33*$^{-/-}$ larvae were compared to the wild type values (Fig. 5.6). *tmem33*$^{-/-}$ larvae showed no significant alterations in distance travelled ($p = 0.807$), number of movements ($p = 0.128$), duration of activity ($p = 0.877$), or speed ($p = 0.760$) compared to siblings. These data suggest that *tmem33* loss of function does not result in motor dysfunction at early stages of zebrafish development.

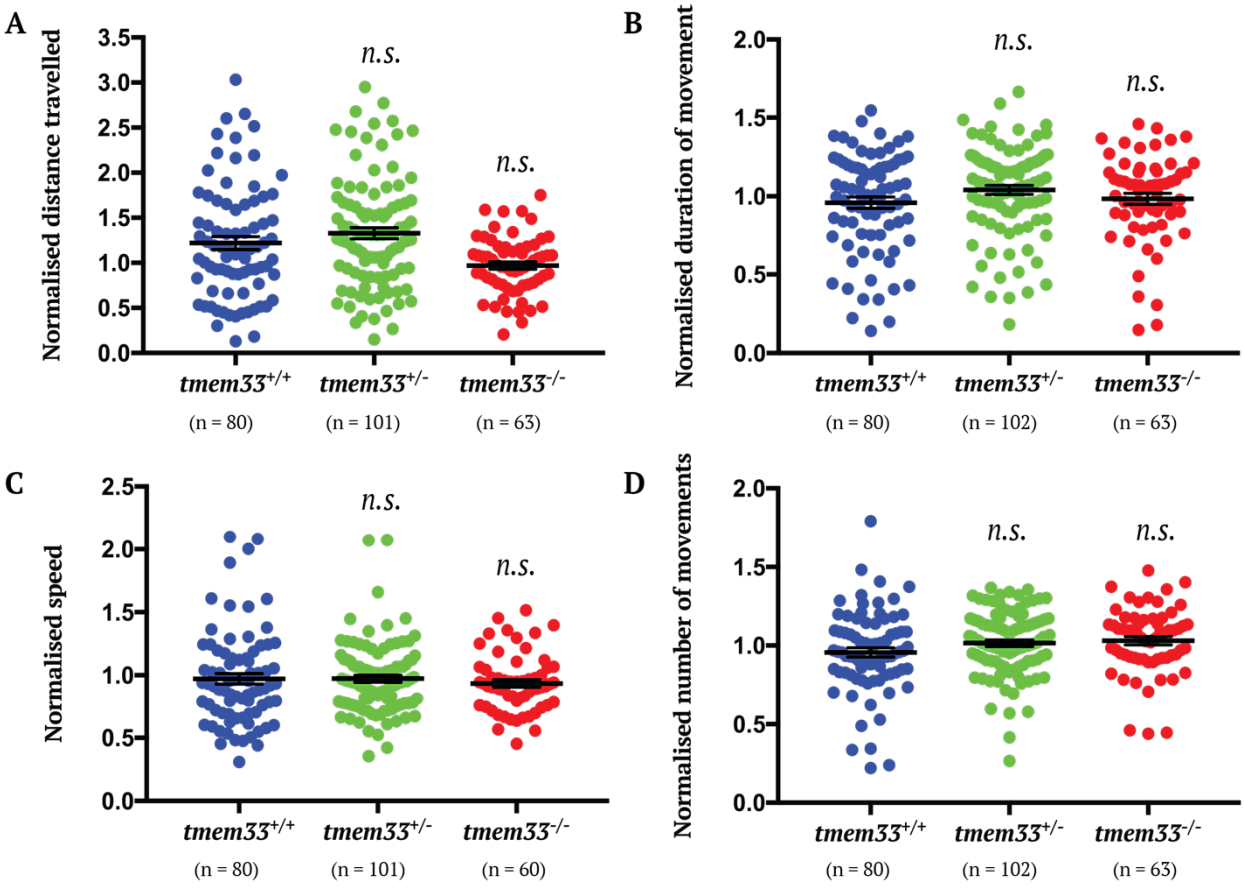

Figure 3.6. Loss of *tmem33* function does not result in motility deficiency at 6 days post fertilization. Quantification of the distance travelled (A), duration of activity (B), speed of movement (C) and number of movements (D) by *tmem33*$^{-/-}$ and sibling controls. Data are represented as mean ± SEM for 3 independent replicate experiments. Statistical significance was assessed using one-way ANOVA with Tukey's multiple comparison test. *n.s. not significant*. Replicate 1: $n = 11$ wildtype, $n = 27$ heterozygotes and $n = 17$ mutants. Replicate 2: $n = 33$ wildtype, $n = 40$ heterozygotes and $n = 26$ mutants. Replicate 3: $n = 36$ wildtype, $n = 35$ heterozygotes and $n = 20$ mutants. Each dot represents an individual zebrafish. Data is normalized to the mean of each biological replicate.

3.5. *aldolase C* expression in *tmem33*$^{-/-}$

Expression analysis of *tmem33* in zebrafish revealed that *tmem33* mRNA is abundantly expressed in the brain. As the most striking neuropathology in cerebellar ataxia is observed in the cerebellum, characterized by loss of Purkinje cells, we analysed the expression pattern of *aldolase C* (a Purkinje cells marker) in *tmem33* mutants at 6 dpf. Expression of *aldolase C* was evident in the cerebellum of *tmem33*$^{-/-}$ embryos, which showed no visible alterations in *aldolase C* expression pattern compared to wild type embryos (Fig. 3.7).

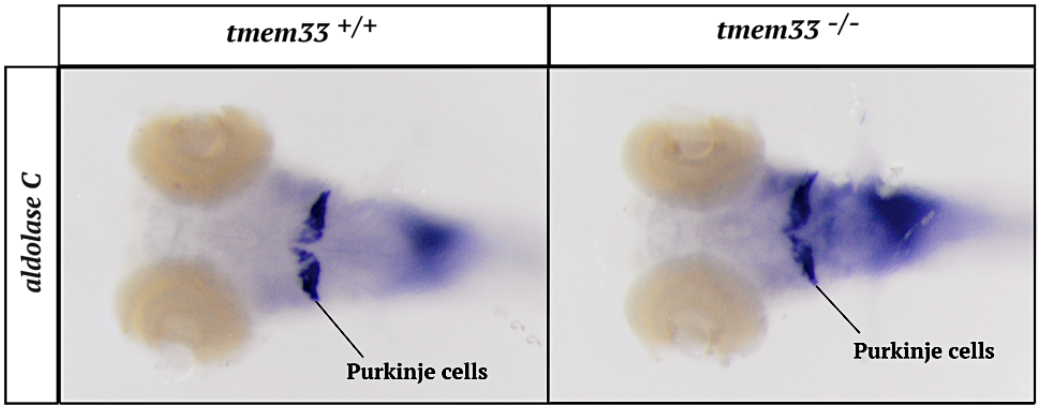

Figure 3.7. *aldolase C* expression pattern in *tmem33* mutants at 6 days post fertilization. Whole mount *in situ* hybridization on zebrafish embryos shows that *aldolase C* mRNA is restricted to the cerebellum in both wild type and *tmem33* mutant embryos, and no significant alterations are observed between the expression patterns. Representative images of *tmem33*$^{+/+}$ and *tmem33*$^{-/-}$ embryos at 6 dpf, for one experiment carried out with 20 embryos. Dorsal view. Anterior to the right. Images recorded by brightfield microscope.

Discussion

A recessive variant in *TMEM33* was identified in two siblings diagnosed with cerebellar ataxia, suggesting *TMEM33* as a novel gene associated with the disorder. We aimed to functionally characterize *tmem33* loss of function in zebrafish to evaluate whether mutation in *TMEM33* would recapitulate the phenotype of the patients.

The function of TMEM33 in the nervous system has not yet been investigated. We found that *tmem33* is predominantly expressed in the zebrafish brain, suggesting a potential role of Tmem33 in the nervous system. However, characterization of *tmem33* loss of function fish did not detect structural abnormalities in the cerebellum, or movement deficits, two of the main symptoms presented by the patients, during early zebrafish development. Since the patients are asymptomatic during childhood and develop the phenotype as adults, it remains to be answered if *tmem33* mutant zebrafish develop phenotypic alterations later in life. Presumably, if the mutation in *TMEM33* is the cause of cerebellar ataxia in the patients, a difference in locomotor activity between *tmem33* mutants and wild type siblings could possibly be detected at later stages. Though, as the disease onset in *TMEM33* patients is at 54 and 55 years of age, it is not feasible to predict when phenotypic alterations would be observed in zebrafish compared to the patients.

Recently, a study by Savage et al. (2019) revealed that *tmem33* mutant zebrafish exhibit no phenotypical alterations compared to *tmem33* morphants. The authors showed that *tmem33* knockdown results in deficient vascular development, with delayed angiogenesis, impaired segmental arteries lateral migration, and absence of thoracic duct. Conversely, *tmem33*^{sh443} mutants, with a premature stop within exon 4, have normal vascular development, and are protected against *tmem33* morpholino knockdown. They conclude that *tmem33* mutants represent an example of genetic compensation or transcriptional adaptation (Savage et al., 2019).

Genetic compensation is a phenomenon that has been recently investigated in zebrafish, with several authors reporting differences between the phenotype of mutant zebrafish and morphants for the same gene (El-Brolosy et al., 2018; Rossi et al., 2015; Sztal et al., 2018). It has been demonstrated that upregulation of a set of genes with similar sequence and/or function with the gene under investigation acts as a compensatory mechanism in mutant zebrafish carrying a premature stop, which is not observed in morphants (El-Brolosy et al., 2018; Rossi et al., 2015; Sztal et al., 2018). As an example, Sztal et al. (2018) reported that knockdown of *actc1b* leads to formation of nemaline bodies in the skeletal muscle and reduced locomotor activity that is not detected in *actc1b* mutants. Instead, *actc1b* mutants display upregulation of *actc1a*, an α-actin paralogue, to compensate for the loss of Actc1b. While the mechanism of genetic compensation remains unclear, El-Brolosy et al. (2018) demonstrated that the level of mutant mRNA degraded through nonsense-mediated decay is

proportional to the transcriptional upregulation of paralogues in mutant zebrafish, and that degradation of the mRNA may act as a signal for transcriptional adaptation.

Here we generated *tmem33* mutant zebrafish with a premature stop within exon 4, and showed through RT-PCR analysis that *tmem33* mRNA levels are reduced in *tmem33* mutants indicating that mRNA is degraded via nonsense-mediated decay. Similar to previous studies, it is possible that loss of *tmem33* causes transcriptional adaptation and other TMEM proteins are capable to compensate for the absence of Tmem33. For example, like TMEM33, TMEM170A is a transmembrane protein predominantly found in the ER that is involved in the formation of the ER shape, and that is as well required for the nuclear envelope expansion (Christodoulou et al., 2016). Comprehensive investigation will be needed to determine whether genetic compensation is the reason for the absence of phenotype in *tmem33* mutants observed in this study. A possible approach is to use CRISPR-Cas9 mutagenesis to delete the entire promotor region of *tmem33*, impeding RNA transcription, a method previously shown to circumvent transcriptional adaptation (El-Brolosy et al., 2018). Generation of such mutant will allow the confirmation of whether cerebellar and locomotor defects are being masked through transcriptional adaptation. Alongside this approach, injection of *tmem33* morpholino into the progeny of *tmem33*$^{+/-}$ incrosses can be used to assess the phenotypic differences between *tmem33* mutants and their siblings, and evaluate whether *tmem33* mutants are protected against morpholino knockdown. Depending on the results of the above experiments, we could then determine the consequences of the variant identified in the patients by injecting a construct with *T109P* into *tmem33* mutant zebrafish and analyse the resulting phenotype. It is possible that the *T109P* variant may lead to misfolding of the second transmembrane domain of the TMEM33 protein, resulting in a protein with altered function instead of loss of function.

Although transcriptional adaptation is a feasible hypothesis that may explain the absence of phenotype in *tmem33* mutants, we cannot also rule out the possibility that the *TMEM33* variant may not be the cause of cerebellar ataxia in the patients. Despite the increasing number of reports using exome sequencing on single patients or single families to identify novel genes associated with disease (Wang et al., 2011; Weisz Hubshman et al., 2018), it is difficult to prove causality with information based on a single family. In fact, some authors propose that a prerequisite for novel gene identification should include genetic information based in more than one pedigree (Lyon and Wang, 2012). Thus, while the *T109P* variant is found at a lower incidence (0.001%) in the population (https://gnomad.broadinstitute.org), and only in the heterozygous state, the identification of an additional family with a similar phenotype is imperative and would support the involvement of TMEM33 dysfunction in cerebellar ataxia.

Chapter 4. Characterization of *plxnb3* mutant zebrafish to investigate the potential role of *PLXNB3* in cerebellar ataxia

Introduction

Cerebellar ataxias are clinically and genetically heterogeneous disorders characterized by progressive loss of balance and motor coordination as primary symptoms (Sullivan et al., 2019). Collaborators of the Bryson-Richardson lab identified a 24kb deletion in plexinB3 (*PLXNB3*) in two individuals of a single family diagnosed with adult-onset spinocerebellar ataxia. The 24kb deletion was identified in the heterozygous state in the female individual and hemizygous state in the male individual, and it was not previously reported. To our knowledge this is the first report on the association of mutation in *PLXNB3* with cerebellar ataxia.

PlexinB3 belongs to a family of transmembrane receptors that activate semaphorins, which act as signalling cues in the nervous system. Semaphorins and Plexins are involved in axon guidance and neuronal migration in both the central and peripheral nervous system (CNS & PNS). These proteins play important roles in neuronal patterning and homeostasis (Alto and Terman, 2017), and have been proposed as prospective targets to treat disease in the nervous system (Worzfeld and Offermanns, 2014). The function of PlexinB3 in the CNS and PNS is not fully characterized. PlexinB3 is a receptor for semaphorin 5A (Sema5A), which mainly functions as a repelling cue in axon guidance (Artigiani et al., 2004). *Sema5A* has been previously associated with Cri-du-chat syndrome, characterized by severe intellectual disability and developmental delay (Simmons et al., 1998), and demonstrated to have a role in oligodendrocyte cells (Goldberg et al., 2004) *PLXNB3* is mainly expressed postnatally in oligodendrocytes, suggesting a potential role in oligodendrogenesis (Worzfeld et al., 2004). In support of this hypothesis, a specific *PLXNB3* haplotype is associated with increased volumes of myelin in human brains (Rujescu et al., 2007). The same *PLXNB3* haplotype is additionally correlated with enhanced verbal performance, indicating that PlexinB3 may have a function in cognitive ability (Rujescu et al., 2007).

In neurons, Plexin-B3 has been further implicated in regulation of glutamatergic and GABAergic synapses (Laht et al., 2015). Plexin-B3, similar to other plexin-B members, inhibits glutamatergic (excitatory) synapses, while also acting to stimulate GABAergic (inhibitory) synapses (Laht et al., 2015). Alterations in glutamate-GABA signalling is one of the mechanisms mediating neurodegeneration and motor dysfunction in neurodegenerative diseases, including Alzheimer's and Huntington disease, spinocerebellar ataxia type 1, and spinocerebellar ataxia type 5 (André et al., 2010; Danysz and Parsons, 2012; Duenas et al., 2006). Therefore, this may be a potential mechanism by which *PLXNB3* mutation may cause cerebellar ataxia.

Due to the potential role in oligodendrocyte cells development, and its affinity for Sema5A, *PLXNB3* is a strong candidate for cerebellar ataxia. However, previous work analysing the functional consequences of loss of PlexinB3 in mice revealed that absence of PlexinB3 is compatible with normal locomotor function and morphology of the CNS and PNS (Worzfeld et al., 2009). This suggested that PlexinB3 may play a redundant role in the nervous system. Still, contradictory results obtained in mice and zebrafish regarding phenotypes associated with the Plexin-B family have been described previously, suggesting that the Plexin-B subfamily may have functionally diverged in these organisms. In particular, *PlexinB2* null mice were shown to die before birth, exhibit defects in closure of the neural tube, and smaller cerebellum with abnormal cell layers (Deng et al., 2007); whereas, *plxnb2a* and *plxnb2b* double knockdown in zebrafish resulted in normal neurulation and locomotor activity (Perälä et al., 2010). Therefore, we wanted to investigate the consequences of *plxnb3* loss of function in zebrafish.

In this study, we sought to investigate the role of Plexin-B3 in the nervous system using *plexinb3*^{sa10506} nonsense mutant zebrafish. We examined the conservation of zebrafish Plexinb3 (Plxnb3) amino acid sequence, followed by immunological and functional characterization of *plexinb3* mutants.

Results

4.1. Zebrafish have a single *PLXNB3* orthologue

In the human genome, *PLXNB3* is located between *ABDC1* and *SRPK3* on the X chromosome. To identify zebrafish *plxnb3*, we searched the Ensembl genome database and found an orthologue of *PLXNB3* adjacent to *abdc1* and *srpk3* on chromosome 8. Similar to the human genome, zebrafish *plxnb3* is flanked by *mecp2, irak1, hcf1b, bcap31, slc6a8,* and *pnck* showing a conserved synteny with human *PLXNB3*. Although, the genomic regions including the *pnck*, *slc6a8,* and *bcap31*, and *hcf1b*, *irak1* and *mecp2*, respectively, are on opposite sides of *plxnb3* in the zebrafish genome (Fig. 4.1).

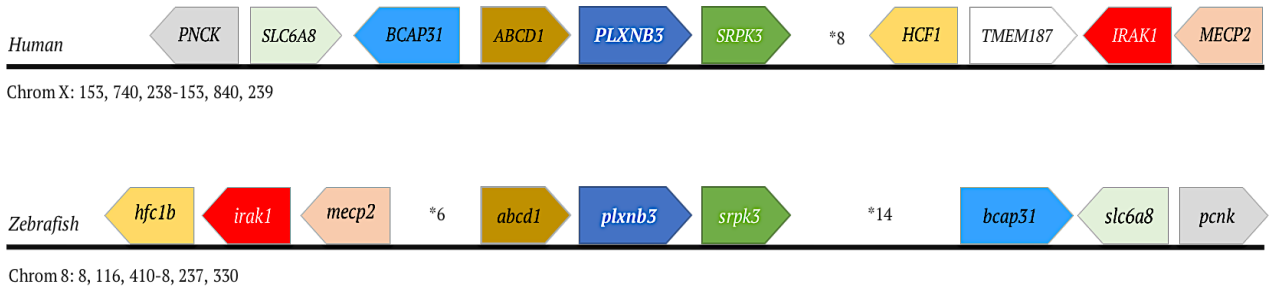

Figure 4.1. Genes flanking *PLXNB3* in the human genome and corresponding syntenic regions in zebrafish. Each line represents a contiguous sequence and the arrowhead indicates the direction of transcription for each gene. *PLXNB3/plxnb3* is highlighted in dark blue and syntenic regions are shown in the same colour in human and zebrafish genomes. *6, *8 and *14 indicate the number of skipped genes.

Next, the amino acid sequences of zebrafish, human, mouse, and medaka PlexinB1, PlexinB2, and PlexinB3 were retrieved from the Ensembl protein database (version GRCz11) and aligned based on sequence homology. The protein alignment was used to generate a maximum likelihood phylogenetic tree to investigate the relationship between the different Plexin B proteins. Zebrafish Plexinb3 clustered together with the respective vertebrate orthologue sequences, into an individual clade with n = 66 bootstrap support, confirming that zebrafish *plxnb3* is the orthologue of mammalian *PLXNB3* (Fig. 4.2).

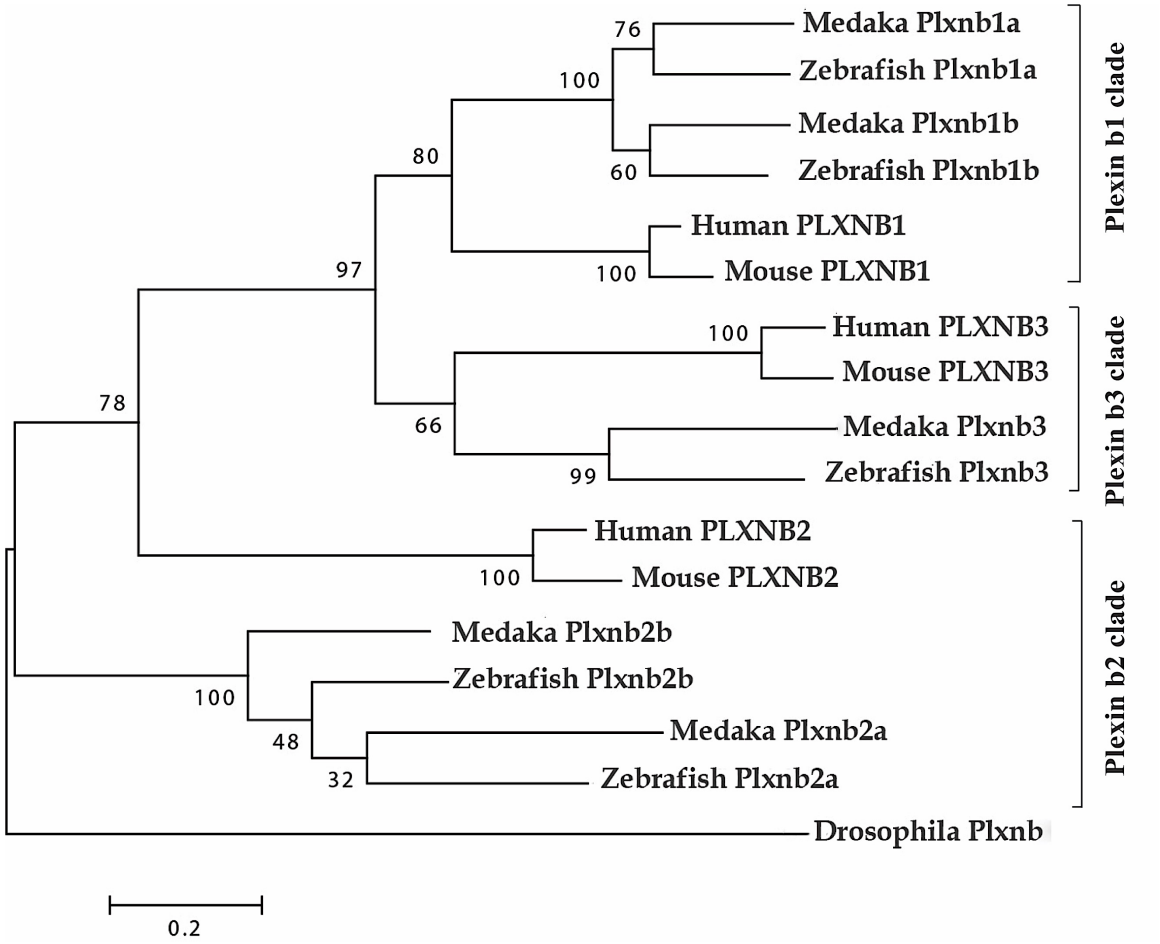

Figure 4.2. Phylogenetic comparison between zebrafish, human, mouse, and medaka Plexin B protein sequences. The percentage of replicate trees in which the sequences clustered together in the bootstrap test (1000 replicates) is shown at the left of each branch. *Drosophila melanogaster* homologue, Plxnb, was used as the outlier.

Further analysis comparing amino acid sequences of zebrafish Plxnb3 and human PLXNB3 revealed an overall identity of 52%, and similarity of 65% (Figure 4.3). To identify PlexinB3 protein domains and examine the conservation of PlexinB3 protein domain structure, the amino acid sequences of zebrafish and human were then analysed using the Conserved Domain Database (Marchler-Bauer et al., 2007).

A

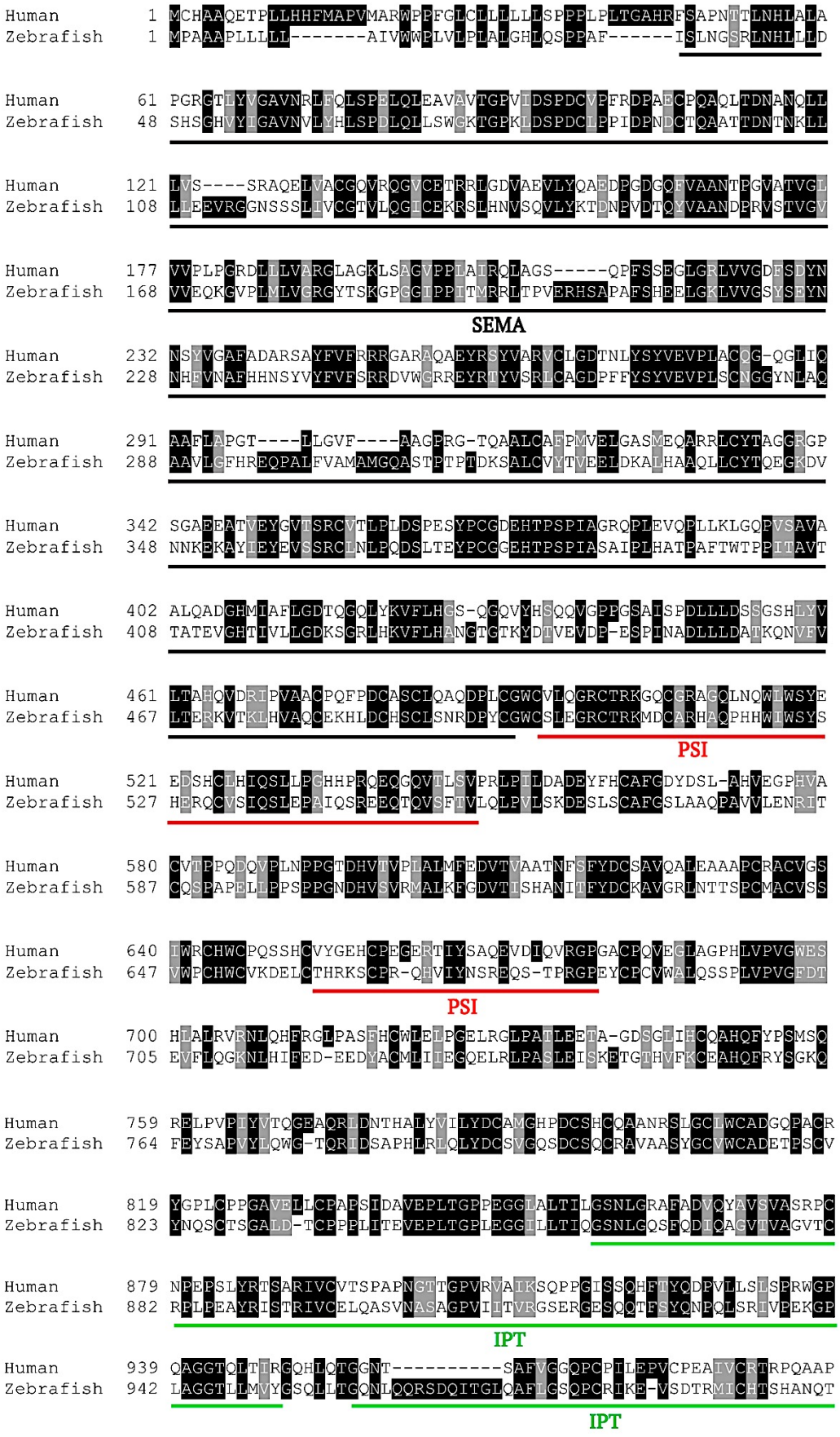
Human 1 MCHAAQETPLLHHFMAPVMARWPPFGLCLLLLLLSPPPLPLTGAHRFSAPNTTLNHLALA
Zebrafish 1 MPAAAPLLLLL-------AIVWWPLVLPLALGHLQSPPAF------ISLNGSRLNHLLLD
Human 61 PGRGTLYVGAVNRLFQLSPELQLEAVAVTGPVIDSPDCVPFRDPAECPQAQLTDNANQLL
Zebrafish 48 SHSGHVYIGAVNVLYHLSPDLQLLSWGKTGPKLDSPDCLPPIDPNDCTQAATTDNTNKLL
Human 121 LVS----SRAQELVACGQVRQGVCETRRLGDVAEVLYQAEDPGDGQFVAANTPGVATVGL
Zebrafish 108 LLEEVRGGNSSSLIVCGTVLQGICEKRSLHNVSQVLYKTDNPVDTQYVAANDPRVSTVGV
Human 177 VVPLPGRDLLLVARGLAGKLSAGVPPLAIRQLAGS-----QPFSSEGLGRLVVGDFSDYN
Zebrafish 168 VVEQKGVPLMLVGRGYTSKGPGGIPPITMRRLTPVERHSAPAFSHEELGKLVVGSYSEYN
SEMA
Human 232 NSYVGAFADARSAYFVFRRRGARAQAEYRSYVARVCLGDTNLYSYVEVPLACQG-QGLIQ
Zebrafish 228 NHFVNAFHHNSYVYFVFSRRDVWGRREYRTYVSRLCAGDPFFYSYVEVPLSCNGGYNLAQ
Human 291 AAFLAPGT----LLGVF----AAGERG-TQAALCAFPMVELGASMEQARRLCYTAGGRGP
Zebrafish 288 AAVLGFHREQPALFVAMAMGQASTPTPTDKSALCVYTVEELDKALHAAQLLCYTQEGKDV
Human 342 SGAEEATVEYGVTSRCVTLPLDSPESYPCGDEHTPSPIAGRQPLEVQPLLKLGQPVSAVA
Zebrafish 348 NNKEKAYIEYEVSSRCLNLPQDSLTEYPCGGEHTPSPIASAIPLHATPAFTWTPPITAVT
Human 402 ALQADGHMIAFLGDTQGQLYKVFLHCS-QGQVYHSQQVGPPGSAISPDLLLDSSGSHLYV
Zebrafish 408 TATEVGHTIVLLGDKSGRLHKVFLHANGTGTKYDTVEVDP-ESPINADLLLDATKQNVFV
Human 461 LTAHQVDRIPVAACPQFPDCASCIQAQDPLCGWCVLQGRCTRKGQCGRAGQLNQWLWSYE
Zebrafish 467 LTERKVTKLHVAQCEKHLDCHSCLSNRDPYCGWCSLEGRCTRKMDCARHAQPHHWIWSYS
PSI
Human 521 EDSHCLHIQSLLPGHHPRQEQGQVTLSVPRLPILDADEYFHCAFGDYDSL-AHVEGPHVA
Zebrafish 527 HERQCVSIQSLEPAIQSREEQTQVSFTVLQLPVLSKDESLSCAFGSLAAQPAVVLENRIT
Human 580 CVTPPQDQVPLNPPGTDHVTVPLAIMEEDVTVAATNFSFYDCSAVQALEAAAPCRACVGS
Zebrafish 587 CQSPAPELLPPSPPGNDHVSVRMAIKFGDVTISHANITFYDCKAVGRLNTTSPCMACVSS
Human 640 IWRCHWCPQSSHCVYGEHCPEGERTIYSAQEVDIQVRGPGACPQVEGLAGPHLVPVGWES
Zebrafish 647 VWPCHWCVKDELCTHRKSCPR-QHVIYNSREQS-TPRGPEYCPCVWALQSSPLVPVGFDT
PSI
Human 700 HLALRVRNLQHFRGLPASEHCWLELPGELRGLPATLEETA-GDSGLIHCQAHQFYPSMSQ
Zebrafish 705 EVFLQGKNLHIFED-EEDYACMLIIEGQELRLPASLEISKETGTHVFKCEAHQFRYSGKQ
Human 759 RELPVPIYVTQGEAQRLDNTHALYVILYDCAMCHPDCSHCQAANRSLGCLWCADGQPACR
Zebrafish 764 FEYSAPVYLQWG-TQRIDSAPHLRLQLYDCSVGQSDCSQCRAVAASYGCVWCADETPSCV
Human 819 YGPLCPPGAVELLCPAPSIDAVEPLTGPPEGGLALTILGSNLGRAFADVQYAVSVASRPC
Zebrafish 823 YNQSCTSGALD-TCPPPLITEVEPLTGPLEGGILLTIQGSNLGQSFQDIQAGVTVAGVTC
Human 879 NPEPSLYRTSARIVCVTSPAPNGTTGPVRVAIKSQPPGISSQHFTYQDPVLLSLSPRWGP
Zebrafish 882 RPLPEAYRISTRIVCELQASVNASAGPVIITVRGSERGESQQTFSYQNPQLSRIVPEKGP
IPT
Human 939 QAGGTQLTIRGQHLQTGGNT----------SAFVGGQPCPILEPVCPEAIVCRTRPQAAP
Zebrafish 942 LAGGTLLMVYGSQLLTGQNLQQRSDQITGLQAFLGSQPCRIKE-VSDTRMICHTSHANQT
IPT

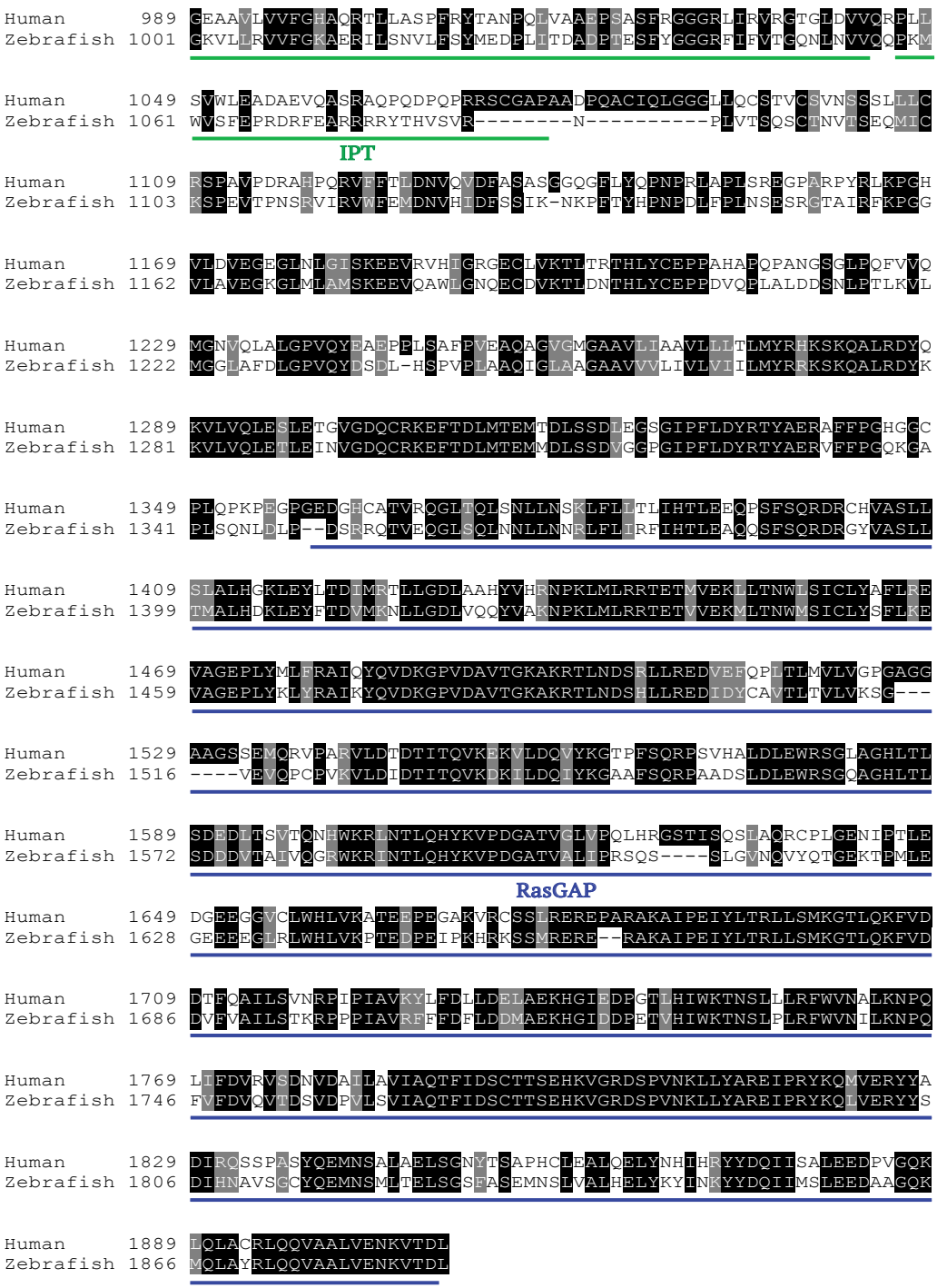
Human 989
Zebrafish 1001
Human 1049
Zebrafish 1061
IPT
Human 1109
Zebrafish 1103
Human 1169
Zebrafish 1162
Human 1229
Zebrafish 1222
Human 1289
Zebrafish 1281
Human 1349
Zebrafish 1341
Human 1409
Zebrafish 1399
Human 1469
Zebrafish 1459
Human 1529
Zebrafish 1516
Human 1589
Zebrafish 1572
RasGAP
Human 1649
Zebrafish 1628
Human 1709
Zebrafish 1686
Human 1769
Zebrafish 1746
Human 1829
Zebrafish 1806
Human 1889
Zebrafish 1866

B

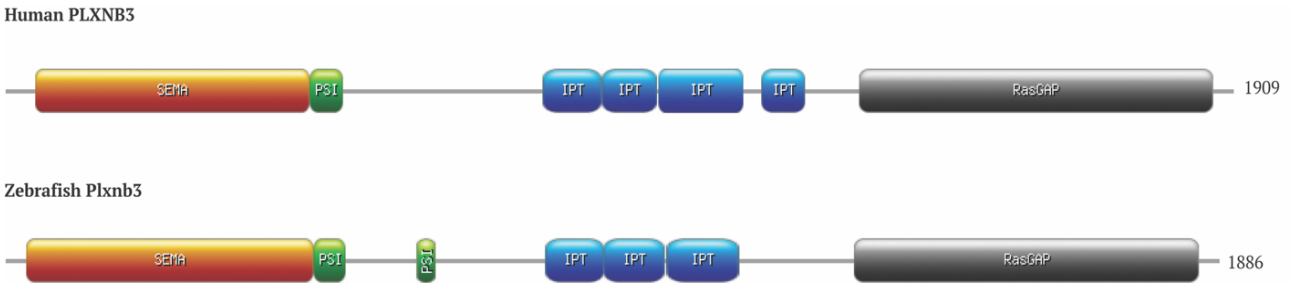

Figure 4.3. Zebrafish Plxnb3 and human PLXNB3 protein domain structure. (A) Zebrafish Plxnb3 and human PLXNB3 protein alignment using T-Coffee. Identical residues are highlighted in black and conserved substitutions in grey. (B) Zebrafish Plxnb3 contains a SEMA-plexin domain, one PSI domain, four IPT domains and a RasGAP C-terminal domain. The SEMA domain is highlighted in orange, PSI domains are highlighted in green, IPT domains are highlighted in blue, and the RasGAP domain is highlighted in dark grey. The image was created using MyDomains from Prosite.

Both human and zebrafish amino acid sequences comprise a SEMA domain, which is an extracellular region that binds to semaphorin, and a cytoplasmic RasGAP domain at the C terminus that is required for downstream signalling. Moreover, human PLXNB3 contains a PSI domain, which consists of a cysteine-rich domain, and four IPT (transcription factors immunoglobin) domains. In contrast, zebrafish Plxnb3 includes two PSI domains and three IPT domains (Fig. 4.3). Zebrafish Plxnb3 demonstrates a high conservation in the cytoplasmic RasGAP domain with 70% identity, indicating that both orthologues most likely mediate similar intracellular signalling pathways. The SEMA domain shows only 45.3% identity, while the single PSI domain and the three IPT domains shared between zebrafish and human proteins revealed 51%, 49.5%, 42.4%, and 32.5% identity homology, respectively.

4.2. *plexinb3* is expressed in the CNS of the developing zebrafish embryo

The expression pattern of *plxnb3* has not been characterized in zebrafish. To examine the temporal expression pattern of *plxnb3*, RT-PCR was performed using total cDNA from the 10-somite stage, 1 day post fertilization (dpf), 2 dpf, 3 dpf, 4 dpf and 5 dpf embryos. *plxnb3* mRNA expression was detected at all stages analysed (Fig. 4.4 A), demonstrating that *plxnb3* is expressed throughout zebrafish embryonic development. To investigate the spatial expression pattern of *plxnb3*, whole mount *in situ* hybridization was subsequently performed at 1dpf, 2 dpf, and 3dpf. *plxnb3* mRNA was found to be restricted to the central nervous system. *plxnb3* expression is initially detected in

the hindbrain at 1 dpf, and is seen widely expressed throughout the brain at 2 dpf. At 3 dpf, *plxnb3* remains expressed in the forebrain, midbrain, and in the cerebellum (Fig. 4.4 B).

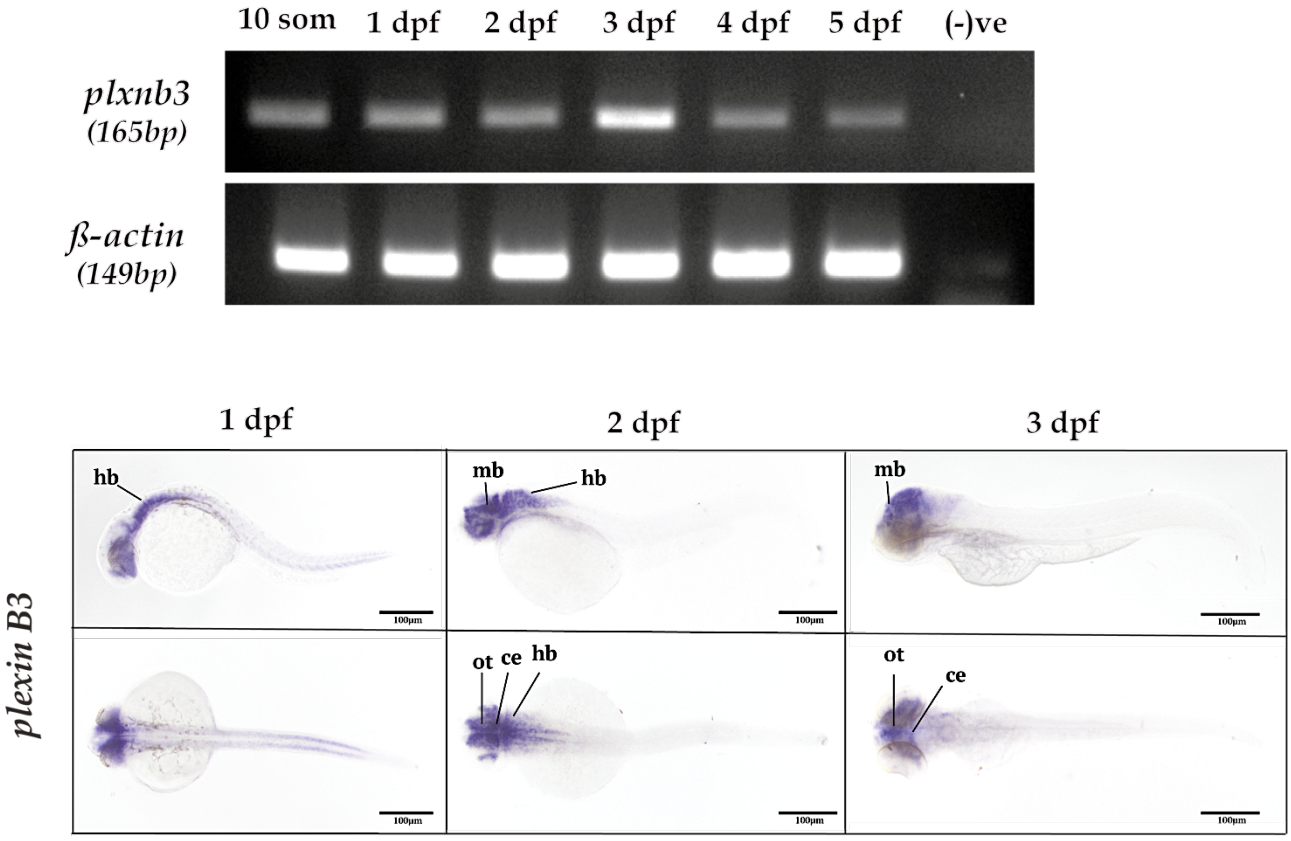

Figure 4.4. *plxnb3* expression analysis performed on wild type embryos. (A) RT-PCR analysis of *plxnb3* expression in developing zebrafish reveals *plxnb3* transcripts from the 10-somite stage to 5 dpf. Expression of *β*-actin was used as a control. (B) Whole mount *in situ* hybridization for zebrafish *plxnb3* at 1 dpf, 2 dpf and 3 dpf. Abbreviations: hb – hindbrain, mb – midbrain, ot – optic tectum, ce – cerebellum.

4.3. Wild type and *plxnb3* mutant zebrafish show similar oligodendrogenesis

The evidence that *Plxnb3* is expressed in the white matter of the CNS in mice, including in the cerebellum, suggests that Plxnb3 may have a role during maturation and/or survival of oligodendrocyte cells. Given that oligodendrocyte cells form the myelin sheath in the CNS, essential for nerve conduction, and oligodendrocyte dysfunction is associated with motor function impairment in disorders, such as ALS (Philips et al., 2013), we hypothesized that defects in these cells may result in ataxia in the patients.

Oligodendrocyte cells are first detected in the brain and expand throughout the spinal cord. *Olig2* is a transcription factor involved in oligodendrocyte progenitor cells formation (Zhou et al., 2001), while *Olig1* and *Sox10* are required for oligodendrocyte differentiation and transcriptional activation of myelin basic protein expression (Li et al., 2007). To investigate whether oligodendrocyte cell development is compromised in the absence of Plxnb3, we used a *plxnb3* mutant strain (sa10506 allele, ZIRC) that carries a point mutation resulting in a premature stop (*c.2840 T>A*; *p. Leu947**). *plxnb3* mRNA level in homozygous *plxnb3* mutants carrying the loss of function alleles was confirmed to be reduced compared to expression levels detected in wild type embryos by semi-quantitative RT-PCR at 6 dpf (Fig. 4.5).

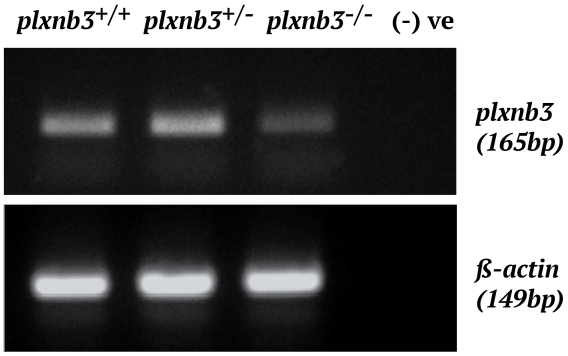

Figure 4.5. RNA analysis of *plxnb3* mRNA in the progeny of *plxnb3*$^{+/-}$ incrosses. Semi-quantitative RT-PCR using total RNA extracted from 6 days post fertilization embryos shows reduced *plxnb3* mRNA levels in *plxnb3* mutants. *β*-actin expression level was used as control.

We next examined the expression of *olig1, olig2,* and *sox10* by whole-mount *in situ* hybridization at 1, 2, 3, and 4 dpf. *Sox10* expression was detected throughout the brain and in the lateral line in both *plxnb3* mutants and sibling controls. Similarly, *olig1* and *olig2* expression was observed in the midbrain and hindbrain, in the three genotypes. Furthermore, there was also no evidence of altered expression of *mbp* in *plxnb3* mutants, suggesting that oligodendrocyte formation is not impaired (Fig. 4.6).

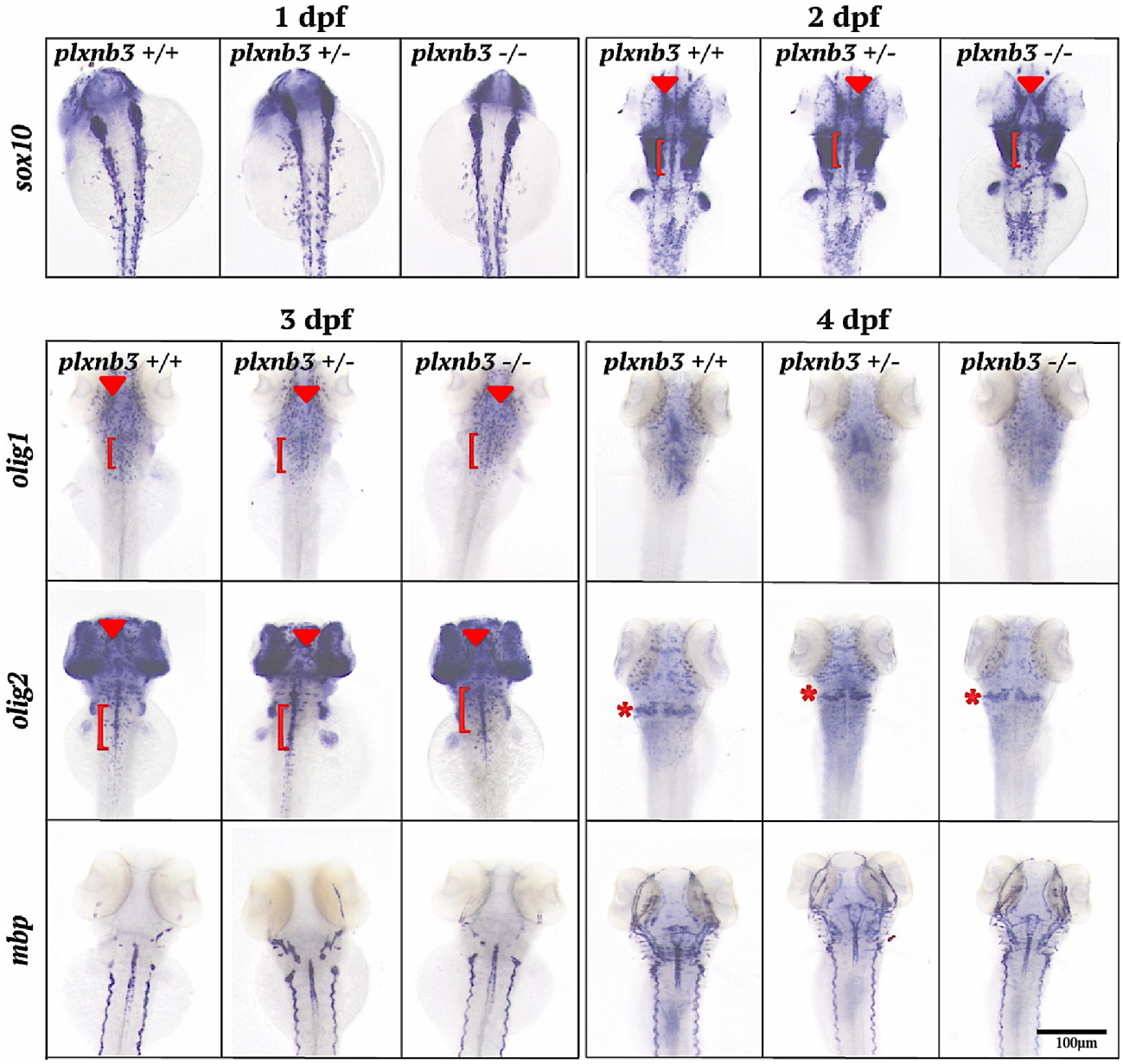

Figure 4.6. Expression analysis shows that *olig1*, *olig2*, *sox10* and *mbp* expression pattern is not altered in *plexinb3* mutants. Red bracket marks hindbrain oligodendrocytes, red asterisk marks the cerebellum and red arrowhead marks midbrain oligodendrocytes.

To further examine the pattern of oligodendrocytes, we analysed *olig2*-expressing cells in the progeny of a *plxnb3*$^{+/-}$; Tg (*olig2*: *gfp*) incross at 4 dpf. As a result, we found no noticeable differences in the pattern of *olig2*-expressing cells in *plxnb3* mutants compared to controls (Fig. 4.7).

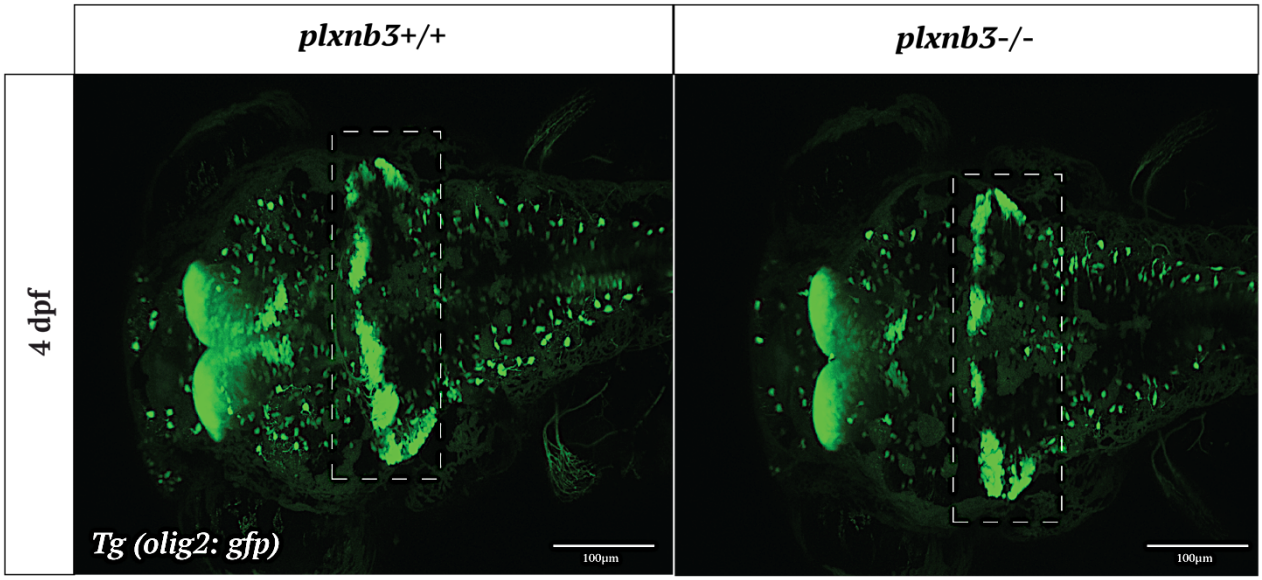

Figure 4.7. Oligodendrocyte progenitor cells pattern in *plxnb3* mutant brains show no difference to wild type siblings at 4 days post fertilization. Maximum projections of confocal z-series to visualize oligodendrocyte cells using Tg (*olig2: gfp*). White dashed line marks the cerebellum.

Previous studies demonstrated that *PLXNB3* is expressed throughout the CNS, including in the spinal cord (Worzfeld et al., 2004). As oligodendrocytes support axonal function, and plexins have a known function also in axon guidance, the organization of the axonal tracts in the spinal cord was analysed by staining with acetylated alpha-tubulin. The neuronal network in *plxnb3* mutants had no gross abnormalities compared to wild type controls at 6 dpf, showing that axonal guidance and integrity is not affected (Fig. 4.8).

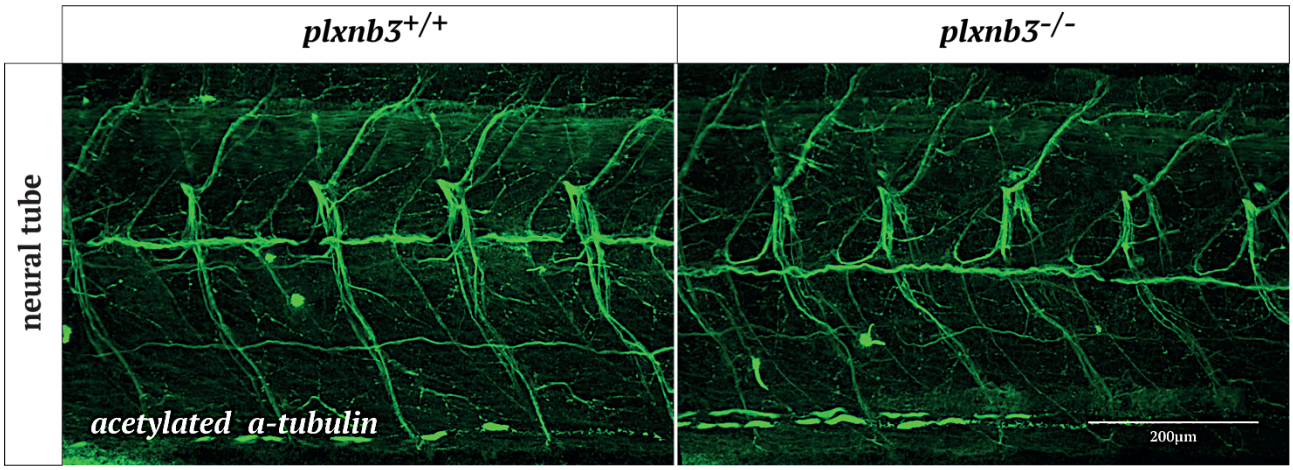

Figure 4.8. Axonal morphology is not altered in the absence of Plxnb3. Whole-mount staining with acetylated alpha-tubulin antibody to view axonal projections coming from the spinal cord in 4 dpf embryos.

4.4. *plxnb3* mutants show normal gross cerebellar morphology

Since *plxnb3* mRNA is detected in the zebrafish cerebellum, the main area of the brain affected in cerebellar ataxia patients, we next examined the expression pattern of *aldolase C*. Aldolase C is a marker of the Purkinje cells of the cerebellar cortex. Dysfunction or degeneration of Purkinje cells is directly associated with loss of motor coordination (ataxia), and is a common finding in cerebellar ataxia (Hoxha et al., 2018; Tara et al., 2018). We detected *aldolase C*-expressing cells in *plxnb3* mutants in a similar pattern to wild type controls (Fig. 4.9). This result suggests that the main neuronal cells in the cerebellum, which are required for control of motor function, are not absent or largely reduced in the absence of Plxnb3.

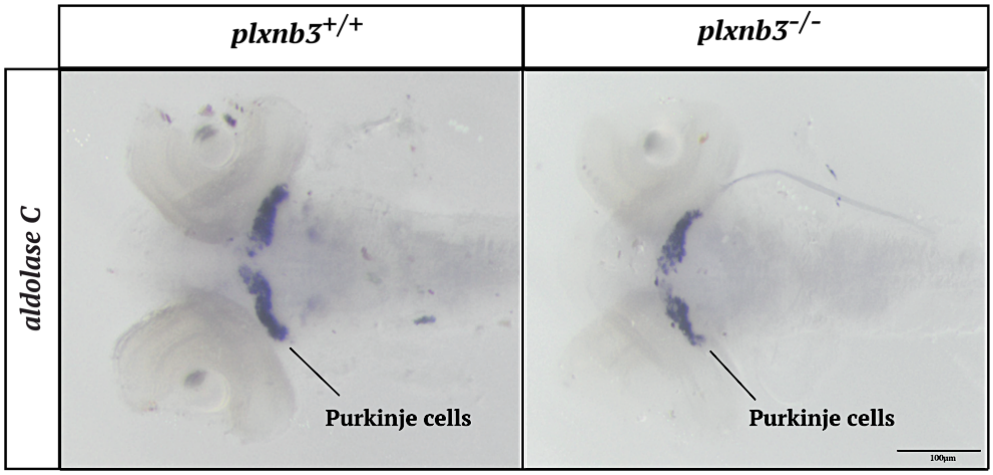

Figure 4.9. Expression pattern analysis of *aldolase C* in *plexinb3* mutants. Whole-mount *in situ* hybridization on zebrafish embryos at 6 dpf using RNA probe specific to zebrafish *aldolase C*. *Aldolase C* expression pattern in *plxnb3* mutants is comparable to wild type embryos.

To assess possible morphologic defects at later stages of development, we extracted the brains of 18 weeks-old zebrafish and observed the shape of the cerebellum. We found that the cerebellum exhibited no gross changes in shape, and the brain showed no obvious alterations in size, in *plxnb3* mutants compared to wild type zebrafish (Fig. 4.10).

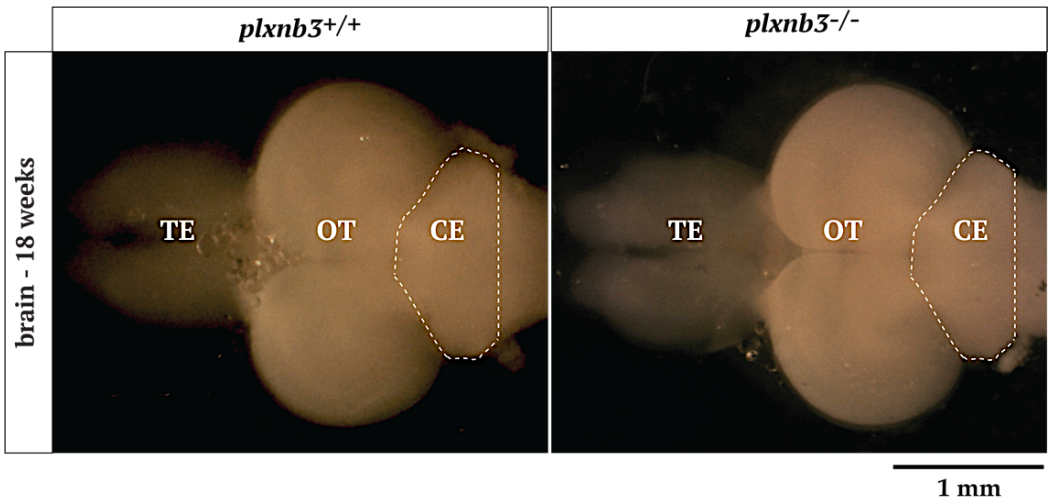

Figure 4.10. Normal brain morphology in *plxnb3* mutant zebrafish at 18 weeks post fertilization. Brightfield images of the dorsal view of the brain, oriented anterior to the left and posterior to the right. TE – telencephalon, OT – optic tectum, CE – cerebellum. White line outlines the cerebellum.

4.5. Swimming analysis of *plexinb3* mutant zebrafish reveals no motor deficits

The absence of structural abnormalities in *plxnb3* mutants does not preclude functional deficits, therefore we investigated the motor function of *plxnb3* mutants. Two motor function assays were conducted on the progeny of a *plxnb3*$^{+/-}$ incross. A touch-evoked response assay at 2 dpf to quantify the maximum acceleration, which is a measure of muscle force (Fig. 4.11). Further, the number of movements, distance swam, duration, and speed of movement were quantified at 6 dpf (Fig 4.12). The main clinical symptom associated with SCA is the progressive decline of motor control. This deficit in motor control can be manifested in different forms, including undershooting or overshooting of movement, impaired ability to rapidly alternate movements or general decreased number of movements. However, the swimming performance of *plxnb3* mutants was comparable to wild type zebrafish both with respect to muscle force and locomotor activity, demonstrating that loss of Plxnb3 does not lead to motor deficits during early stages of zebrafish development.

As the onset of cerebellar ataxia ranges from childhood to adulthood, and cerebellar ataxia is slowly progressive, the motor function of *plxnb3* mutants was also investigated later in zebrafish development. *plxnb3*$^{+/-}$ incrosses were carried out and a total of sixteen fish were raised per genotype from 5 dpf. Survival and locomotor activity of the progeny was examined at 18 weeks post fertilization (approximately 4.5 months), when zebrafish reach their sexual maturity. *Plxnb3* mutants were phenotypically indistinguishable from wild type and heterozygote fish. Although survival amongst *plxnb3* mutants was 68.8% (11 out of 16) compared to 87.5% (14 out 16) wild type and 81.3% (13 out of 16) heterozygote fish, *plxnb3* mutants were indistinguishable also from wild type controls

with respect to motor activity (Fig. 4.13). We, therefore, conclude that Plexinb3 is not essential for normal locomotor activity in zebrafish.

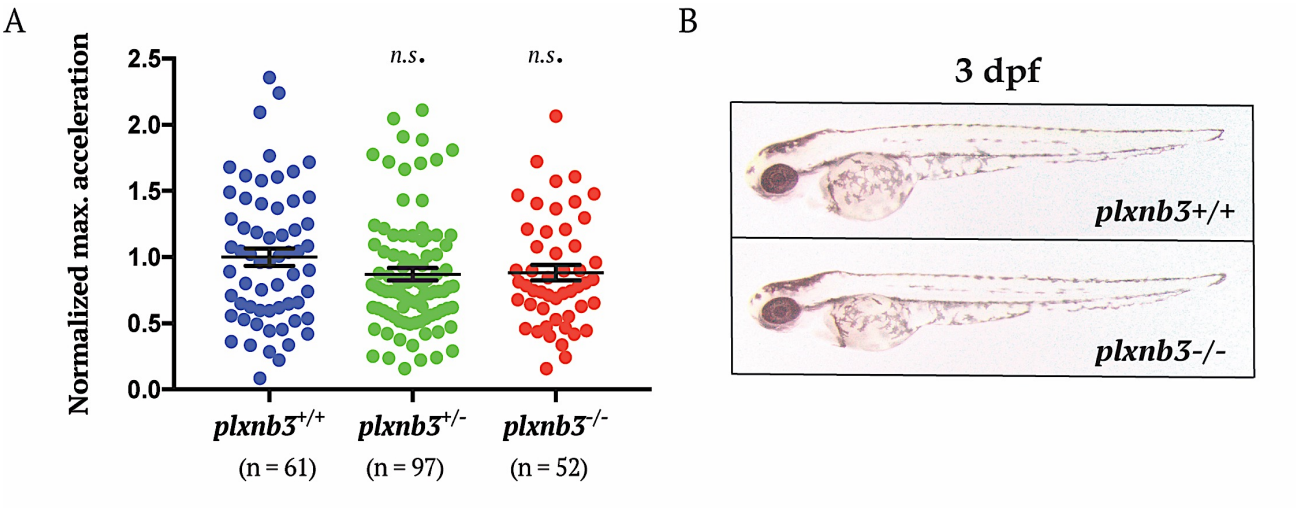

Figure 4.11. ***plxnb3*** **mutants show no motor impairment at 2 days post fertilization**. (A) Quantification of the maximum acceleration recorded from touch-evoked response assays of *plxnb3*$^{-/-}$ embryos compared to wild type siblings. Data are represented as mean ± SEM for 3 independent replicate experiments and statistical significance was assessed using one-way ANOVA, with Tukey's multiple comparison test. *n.s. not significant*. (A) Replicate 1: n = 11 wild type, n = 22 heterozygotes and n = 17 mutants. Replicate 2: n = 9 wild type, n = 23 heterozygotes and n = 11 mutants. Replicate 3: n = 8 wild type, n = 25 heterozygotes and n = 6 mutants. Each dot represents individual zebrafish. (B) Brightfield image of wild type and *plxnb3* mutant embryos at 3 dpf.

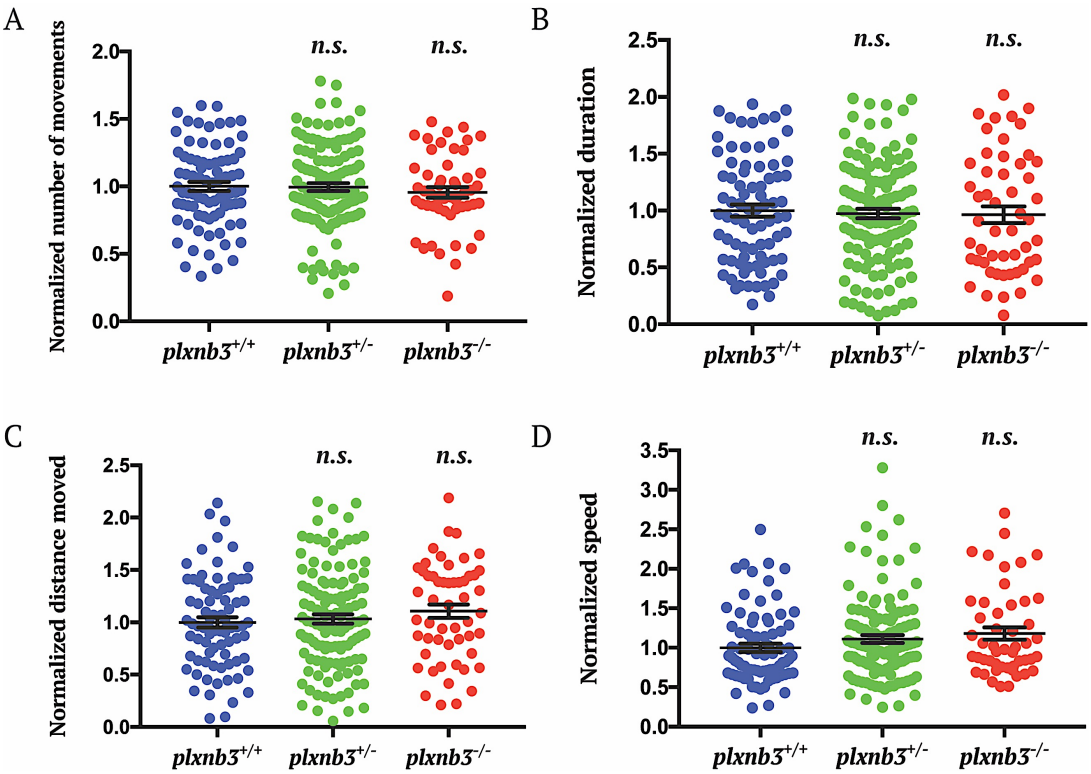

Figure 4.12. The swim tracks of *plxnb3* mutants revealed no abnormal swim behaviour at 6 days post fertilization. Quantification of the number of movements (A), duration of movement (B), distance travelled (C) and speed of movement (D) by *plxnb3* mutants compared to wild type embryos. Data are represented as mean ± SEM for 3 independent replicate experiments. Statistical significance was assessed using one-way ANOVA with Tukey's multiple comparison test. *n.s. not significant*. Replicate 1: n = 27 wild type, n = 38 heterozygotes and n = 14 mutants. Replicate 2: n = 22 wild type, n = 48 heterozygotes and n = 20 mutants. Replicate 3: n = 29 wild type, n = 34 heterozygotes and n = 15 mutants. Each dot represents an individual zebrafish.

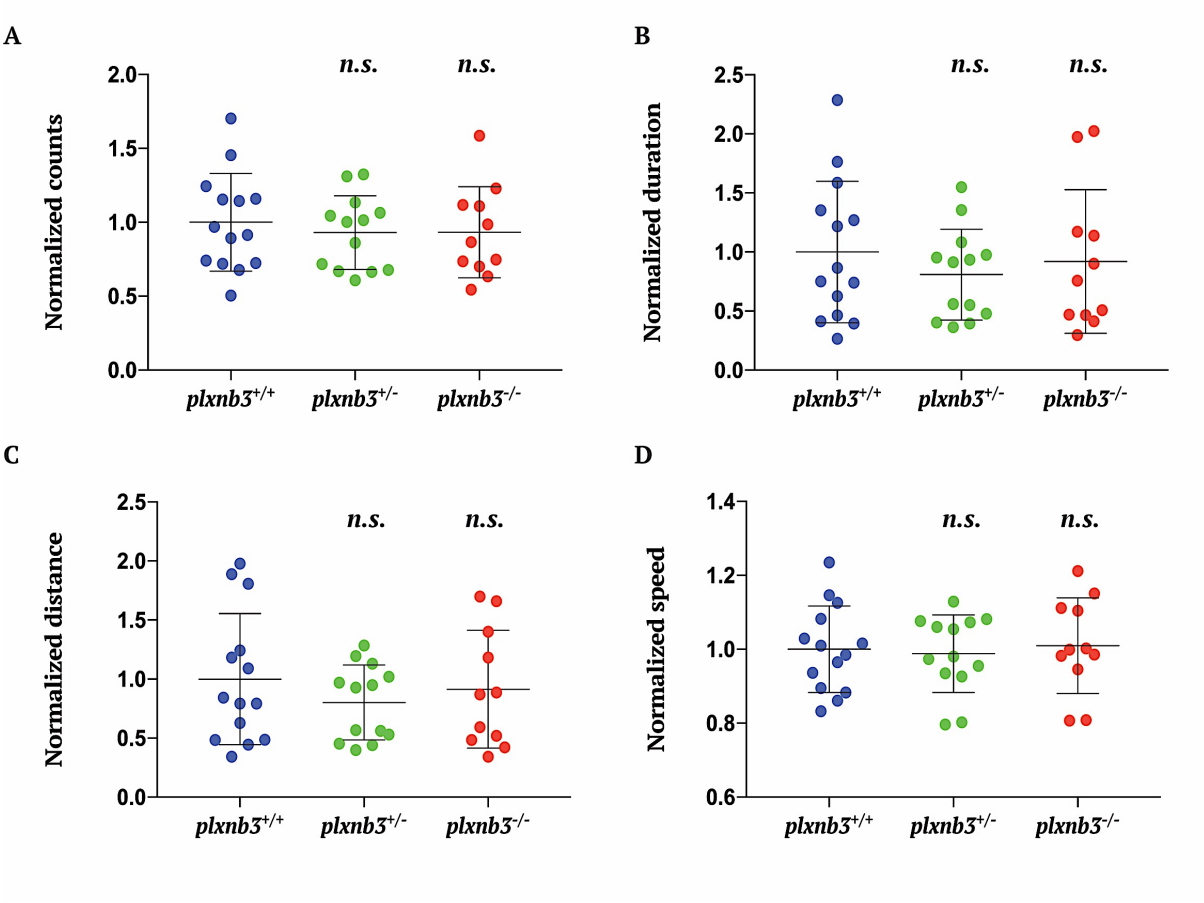

Figure 4.13. The swim tracks of *plxnb3* mutants revealed no abnormal swim behaviour at 18 weeks post fertilization. Quantification of the number of movements (A), duration of movement (B), distance travelled (C) and speed of movement (D) by *plxnb3* mutants compared to wild type embryos. Data are represented as mean ± SD for 14 wild type, 13 heterozygotes and 11 mutant fish. Statistical significance was assessed using one-way ANOVA with Tukey's multiple comparison test. *n.s. not significant*. Each dot represents an individual zebrafish.

Discussion

A 24kb deletion in *PLXNB3* was identified in two individuals diagnosed with adult-onset spinocerebellar ataxia, suggesting *PLXNB3* as a candidate gene associated with the disorder. In this study, we functionally characterized *plxnb3* loss of function in zebrafish to evaluate whether loss of *plxnb3* would result in locomotor deficits and abnormal cerebellar development, two of the main symptoms associated with cerebellar ataxia.

While the biological function of PlxnB3 remains elusive, previous studies have suggested that PlexinB3 may have a role in the CNS (Laht et al., 2015; Rujescu et al., 2007; Worzfeld et al., 2004). Here we found that *plxnb3* is predominantly expressed in the zebrafish brain, consistent with a potential role of PlxnB3 in the CNS. However, characterization of *plxnb3* loss of function fish did not detect motor deficits, or obvious brain structural abnormalities, up to 18 weeks post fertilization (adult zebrafish). Moreover, we did not detect altered expression of *aldolase C* in cerebellar Purkinje cells, suggesting that absence of Plxnb3 does not compromise the main neuronal cells affected in cerebellar ataxia patients.

Previous work on genes associated with cerebellar ataxia has shown evidence that zebrafish models are able to recapitulate cerebellar abnormalities observed in the patients (Aspatwar et al., 2013; Namikawa et al., 2019). While aldolase C has been used to demonstrate cerebellar neuronal deficits in zebrafish (Bae et al., 2009; Su et al., 2014; Yanicostas et al., 2012), it does not allow to detect changes in the number or pattern of other cells in the cerebellum. To investigate potential cerebellar structural abnormalities, markers labelling the different cerebellar cell layers like, for example, *vlgut1* that labels the cerebellar granule cell layer, would need to be used. Still, based on the absence of locomotor dysfunction, it is unlikely that the cerebellum is affected in *plxnb3* mutant fish.

Due to the increasing number of examples of genetic compensation in zebrafish (El-Brolosy et al., 2018; Rossi et al., 2015; Sztal et al., 2018), it is possible that *plxnb3* loss of function may result in upregulation of similar plexin-encoding genes to compensate for the absence of Plxnb3. We showed through RT-PCR analysis that *plxnb3* mRNA levels are reduced in *plxnb3* mutants indicating that mRNA is likely degraded through nonsense-mediated decay, a signal that is hypothesized to initiate transcriptional adaptation (El-Brolosy et al., 2018). Based on structural similarities (Tamagnone et al., 1999), PlexinB1 and PlexinB2 are prospective candidates to be upregulated as result of transcriptional adaptation in *plxnb3* mutants. However, comprehensive investigation will be needed to determine whether upregulation of similar plexins is the reason for the absence of phenotypic alterations in *plxnb3* mutant fish. A possible approach is to determine the mRNA levels of the different plexins through quantitative RT-PCR in *plxnb*3 mutants in relation to wild type fish. Alongside this approach, is necessary to evaluate whether *plxnb3* mutant fish are protected against

plxnb3 morpholino knockdown.

Recent evidence has demonstrated that the same plexin can serve as receptor for different semaphorins, and that semaphorins can interact with different plexin receptors, and exert distinct or similar functions in the same cell type (Ben-Zvi et al., 2008; Suto et al., 2005; Yaron et al., 2005). As an example, Sema3A binds to PlexinA3 to induce neuronal cell death, whereas it binds to PlexinA4 to promote axonal guidance, in the dorsal root ganglia (Ben-Zvi et al., 2008). Furthermore, plexins were reported to interact with signalling molecules of other families of ligands, such as Netrins and Slits (Delloye-Bourgeois et al., 2015; Negishi et al., 2005). These findings indicate that there is a high level of redundancy in semaphorin-plexin interaction. Therefore, we cannot rule out the possibility that the semaphorin that binds to PlxnB3 may have the ability to interact with a different receptor, or other semaphorin-plexin complexes functionally compensate, in the absence of PlxnB3.

Sema5A is the sole ligand described to interact with PlxnB3 (Artigiani et al., 2004). However, Sema5A has been reported to interact with additional transmembrane receptors (Duan et al., 2014; Matsuoka et al., 2011). For example, Sema5A signalling is mediated through PlexinA2 to regulate synaptogenesis in the hippocampus (Duan et al., 2014), whereas PlexinA1 and PlexinA3 act as receptors for both Sema5A/5B and induce neurite outgrowth in the retina (Matsuoka et al., 2011). In addition, while *PlxnB3* knockout mice are viable and exhibit no phenotypic alterations (Worzfeld et al., 2009), *Sema5A* knockout mice were shown to present abnormal branching of the cardinal veins in the brain and die during embryonic development (Fiore et al., 2005). At E11.5 embryonic stage, when *Sema5A* knockout mice die, *PlexinB3* expression is not observed (Fiore et al., 2005). This indicates that Sema5A signalling can be mediated in a PlexinB3-independent manner.

Work conducted by Worzfeld et al. (2004) revealed that *PlxnB3* is expressed in the white matter of the CNS, coinciding with migration and maturation of oligodendrocyte progenitor cells. The contribution of PlexinB3 to oligodendrocyte cells is unknown. However, several semaphorins and plexins have been previously implicated in the development of oligodendrocyte cells (Okada et al., 2007; Okada and Tomooka, 2012; Piaton et al., 2011; Xiang et al., 2012). Namely, Piaton et al. (2011) showed that Sema3A and Sema3F are required for migration of oligodendrocyte precursor cells after demyelination. Xiang et al. (2012) further demonstrated that PlexinA3, a receptor for Sema3A and Sema3F, is implicated in migration of oligodendrocyte precursor cells, and is expressed in immature oligodendrocytes. Moreover, PlexinA4, a receptor for Sema3A and Sema6A, was revealed to participate in the correct positioning of oligodendrocyte cells (Okada and Tomooka, 2012). Therefore, assuming that PlxnB3 is involved in oligodendrogenesis, different semaphorin-plexin complexes may be able to intervene in its absence.

The *PLXNB3* variant was identified in a family with history of dominantly inherited spinocerebellar

ataxia. The two individuals with the *PLXNB3* variant were from the branch of the family in Western Australia, while the remaining individuals affected were from South Australia. Based on diagnostic screening in the two individuals from Western Australia, *PLXNB3* was suggested as the likely candidate gene associated with disease. However, after the zebrafish functional work, screening of members of the South Australia branch family revealed that the *PLXNB3* variant does not segregate with the disease. The genetic cause of spinocerebellar ataxia in this family remains inconclusive. Therefore, the potential genetic compensation in *plxnb3* mutant zebrafish was not further explored.

Since the 24kb deletion identified in the affected individuals spans the entire sequence of the *PLXNB3* gene, resulting in a null allele, and does not contribute to the cerebellar ataxia in patients, we can conclude that PLXNB3 is likely dispensable for normal brain development and function. Notably, 100 hemizygote individuals for loss of function variants in *PLXNB3* are found in the gnomAD database (https://gnomad.broadinstitute.org/), further suggesting that PLXNB3 may have a redundant role in the nervous system.

Chapter 5. Characterization of zebrafish *uba5* loss of function mutants

Introduction

Compound heterozygous variants were recently identified in *UBA5* as cause of childhood-onset cerebellar ataxia (Duan et al., 2016) and infantile-onset epileptic encephalopathy (Arnadottir et al., 2017; Colin et al., 2016; Daida et al., 2018; Low et al., 2018; Mignon-Ravix et al., 2018; Muona et al., 2016). *UBA5* patients with cerebellar ataxia show progressive cerebellar atrophy and ataxia as primary symptoms, and developmental delay during childhood (Duan et al., 2016). In contrast, patients with epileptic encephalopathy are characterised by a range of symptoms that include irritability, mild to severe intellectual disability, microcephaly, failure to achieve developmental milestones, short stature, motor impairment and recurrent seizures which are refractory to antiepileptic drugs, ultimately resulting in death of the patients before the age of twenty. Epileptic encephalopathy patients reveal brain abnormalities, including mildly delayed myelination and atrophy of regions of the brain including the thalamus, corpus callosum, cerebellum, or brain stem; but, these findings are inconsistent amongst *UBA5* patients (Arnadottir et al., 2017; Colin et al., 2016; Daida et al., 2018; Low et al., 2018; Mignon-Ravix et al., 2018; Muona et al., 2016).

UBA5 mutations reported in patients are inherited in an autosomal recessive manner, and are found in individuals as missense/missense or missense/nonsense biallelic variants (Arnadottir et al., 2017; Colin et al., 2016; Daida et al., 2018; Low et al., 2018; Mignon-Ravix et al., 2018; Muona et al., 2016). To date, no correlation has been identified between phenotype and genotype in *UBA5* patients, and the mechanism by which mutations in *UBA5* cause these two nervous system disorders is not understood.

It has been hypothesized that disease in the nervous system due to *UBA5* mutations could arise due to dysfunction of the UFM1- protein modification system (Colin et al., 2016; Muona et al., 2016). The *UBA5* gene encodes an activating enzyme (*E1*) for UFM1, which is a small ubiquitin-like protein that is conjugated to target proteins (Komatsu et al., 2004). This is a controlled mechanism that occurs through an enzymatic cascade that comprises an activator (*E1*), a conjugator (*E2*) and a ligase (*E3*) enzyme. The consequences of modification by the highly conserved UFM1 system are largely unknown but it is hypothesized that UFM1 post-translationally modifies proteins in a similar manner to ubiquitin. The UFM1 pathway has been associated with functions in fatty acids metabolism (Gannavaram et al., 2012), erythrocytes development (Tatsumi et al., 2011), breast cancer (Yoo et al., 2014), stress response and protection against apoptosis (Lemaire et al., 2011). Yet, the role of UFM1 in these cellular processes, and its targets, remains largely uncharacterised.

Previous studies have suggested an association between the UFM1 pathway and the nervous system (Homrich et al., 2014b; Martin et al., 2015). Martin et al. (2015) showed that the UFM1 pathway is impaired in oligodendrocytes and neurons derived from Huntington patients. Additionally, *in vitro* studies showed that components of the UFM1 pathway co-localize with NCAM140, a neural cell adhesion molecule involved in axon guidance and neuronal differentiation, in the brain (Homrich et al., 2014b). Recently, *UFM1* mutations were also associated with a severe infantile neurological disorder similar to the epileptic encephalopathy in *UBA5* patients (Hamilton et al., 2017; Nahorski et al., 2018). These findings indicate that the UFM1 pathway is essential for normal function of the nervous system.

To investigate the pathophysiology associated with *UBA5* mutation and to identify pathways that could reduce disease progression we are using the zebrafish. We generated *uba5* mutants to investigate the consequences of *uba5* loss-of-function on zebrafish locomotion, survival, and nervous system development and homeostasis. We show that Uba5 loss of function leads to significant decrease in locomotor activity, recapitulating the motor dysfunction observed in *UBA5* patients. Notably, motor dysfunction is not accompanied by microcephaly or developmental impairment at early stages of embryonic development. Through immuno-labelling, we demonstrate that the overall neuronal network and muscle morphology is also intact, but signs of nerve dysfunction are observed within the peripheral nervous system (PNS). Similar to *UBA5* patients, *uba5* mutants exhibit developmental delay at later stages of development and have reduced lifespan.

Results

5.1. *Uba5* is conserved in zebrafish

A nucleotide search of the Ensemble genome database (www.ensemble.org) identified a single *UBA5* orthologue in zebrafish encoding a 399-amino acid protein that is 80% identical, and 90% similar, to the human UBA5 protein. Human and zebrafish UBA5 proteins have a highly conserved adenylation domain that includes the ATP-binding site and the putative active cysteine domains, both required for UFM1 activation, and the UFM1-interacting sequence domain and UFC1-binding site domain at the N terminus (Figure 5.1).

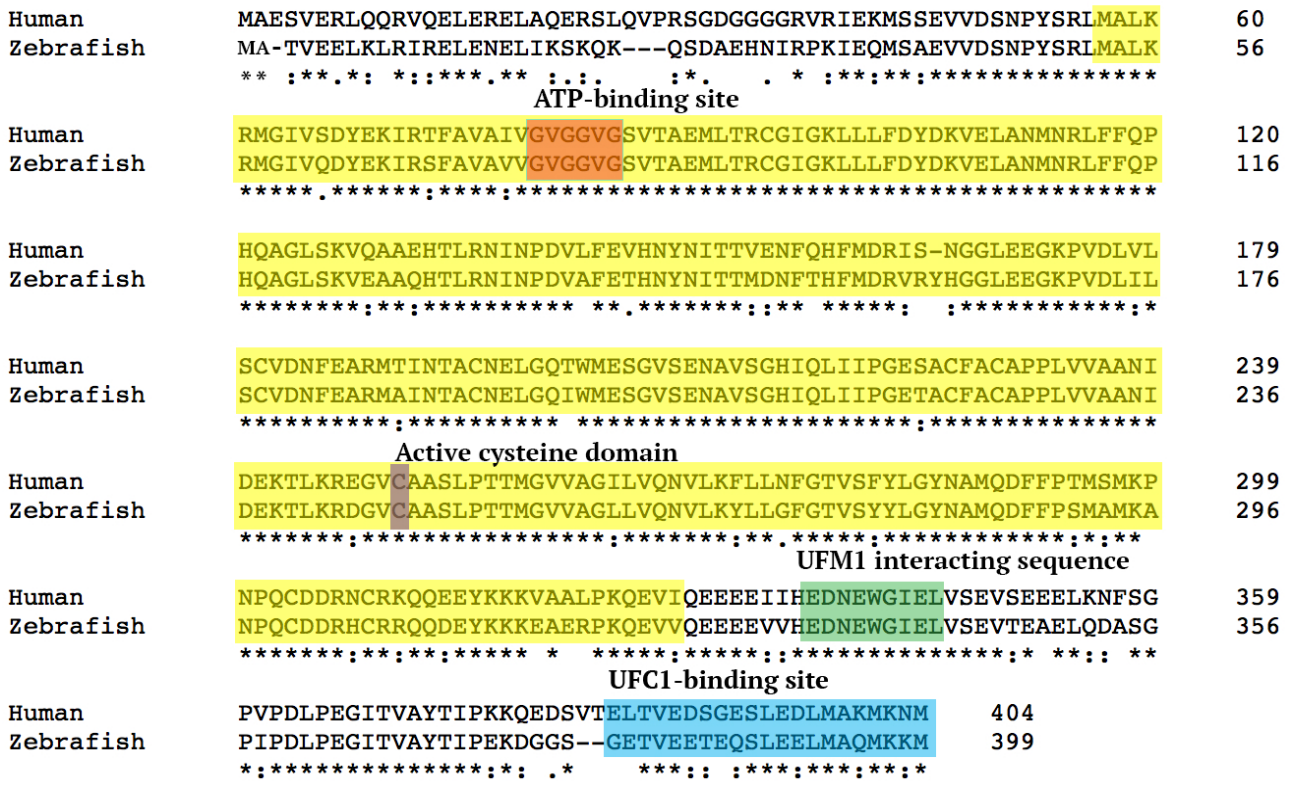

Figure 5.1. Alignment of human UBA5 and zebrafish Uba5. The different colours highlight the relevant domains. In yellow the adenylation domain, in orange the ATP-binding domain, in brown the putative active site (Cys residue), in green the UFM1-interacting sequence, and in blue the UFC1-binding site. * (asterisk) denote the conserved amino acids, : (colon) indicates conservation between groups of strongly similar properties - scoring > 0.5 in the Gonnet PAM 250 matrix, and . (period) indicates conservation between groups of weakly similar properties - scoring =< 0.5 in the Gonnet PAM 250 matrix. Numbers on the left of sequences indicate positions relative to the translation start site.

5.2. *uba5* is expressed in the nervous system during zebrafish development

To investigate the temporal expression pattern of zebrafish *uba5*, we performed RT-PCR analysis. We found that *uba5* is expressed during zebrafish embryonic development at all stages analysed (Figure 5.2 A). Additionally, to identify the spatial expression pattern of zebrafish *uba5*, we carried out whole mount *in situ* hybridization on embryos at 1 and 2 days post fertilization (dpf). At 1 dpf, expression of *uba5* is evident at the midbrain-hindbrain boundary, hindbrain, and at the somite boundaries. At 2 dpf, *uba5* is expressed throughout the zebrafish brain (Figure 5.2 B). This pattern is consistent with a role of Uba5 in the nervous system.

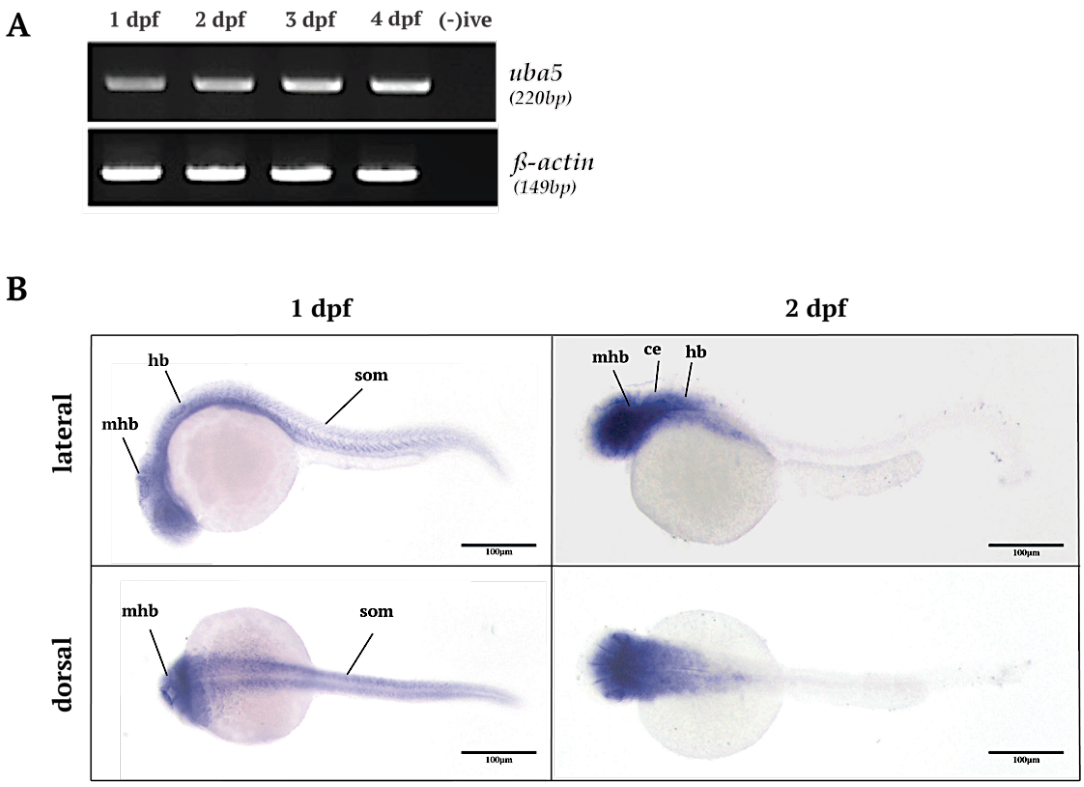

Figure 5.2. *uba5* expression analysis performed on wild type embryos. (A) RT-PCR analysis of *uba5* expression in developing zebrafish reveals *uba5* transcripts from 1 dpf to 4 dpf. Expression of *β*-actin was used as a control. (B) Whole mount *in situ* hybridization for zebrafish *uba5* at 1 dpf and 2 dpf. Abbreviations: mhb – midbrain-hindbrain boundary, mb – midbrain, hb – hindbrain, som – somites, ce – cerebellum.

5.3. Generation of zebrafish *uba5* loss of function mutants

To determine the role of UBA5 in the nervous system we used CRISPR/Cas9 genome editing to generate *uba5* mutant zebrafish. Given that in humans *UBA5* is transcribed as 2 isoforms (Zheng et al., 2008), which encode a full-length protein and a shorter protein lacking the first coding exon, we selected target sites within the first and third exons of zebrafish *uba5*. Each sgRNA was co-injected

with Cas9 protein into one-cell stage embryos, and F0 were screened to determine the sgRNAs efficiency to create double strand breaks within *uba5* coding sequence. Two sgRNAs were selected, which created mutations in 72% and 60% of injected fish, respectively, targeting the first and third exon of *uba5*. From F0 outcrosses that transmitted a mutation to the offspring, we raised and genotyped adult F1 fish for the presence of *uba5* mutant alleles. From the recovered germline alleles, we kept three heterozygous strains. The first strain (*uba5*$^{+/ex1d}$, *c.1_6del*) carries a deletion of 6 base pairs at the start of the coding sequence that deletes the transcription start site in exon 1 and 24 base pairs of the 5'UTR, disrupting the Kozac sequence (Figure 5.3 B). This mutation is predicted to result in absence of Uba5 protein. The second strain (*uba5*$^{+/ex1s}$, *c.4_77ins*) carries an insertion of 73 base pairs within exon 1 that results in a frameshift and generates a premature stop codon, predicted to produce a significantly truncated Uba5 protein without the essential catalytic cysteine (Cys250) domain required for UFM1 activation. Finally, the third strain (*uba5*$^{+/ex3d}$, *c.217_240del*) carries an in-frame deletion of 24 base pairs in exon 3 that leads to deletion of 8 amino acids within the catalytic domain of Uba5 (Figure 5.3 B). Since this mutation is within the ATP-binding site, and UBA5-UFM1 intermediates are formed in an ATP-dependent manner, it is expected to result in a non-functional Uba5 protein. The three strains were used for further analysis.

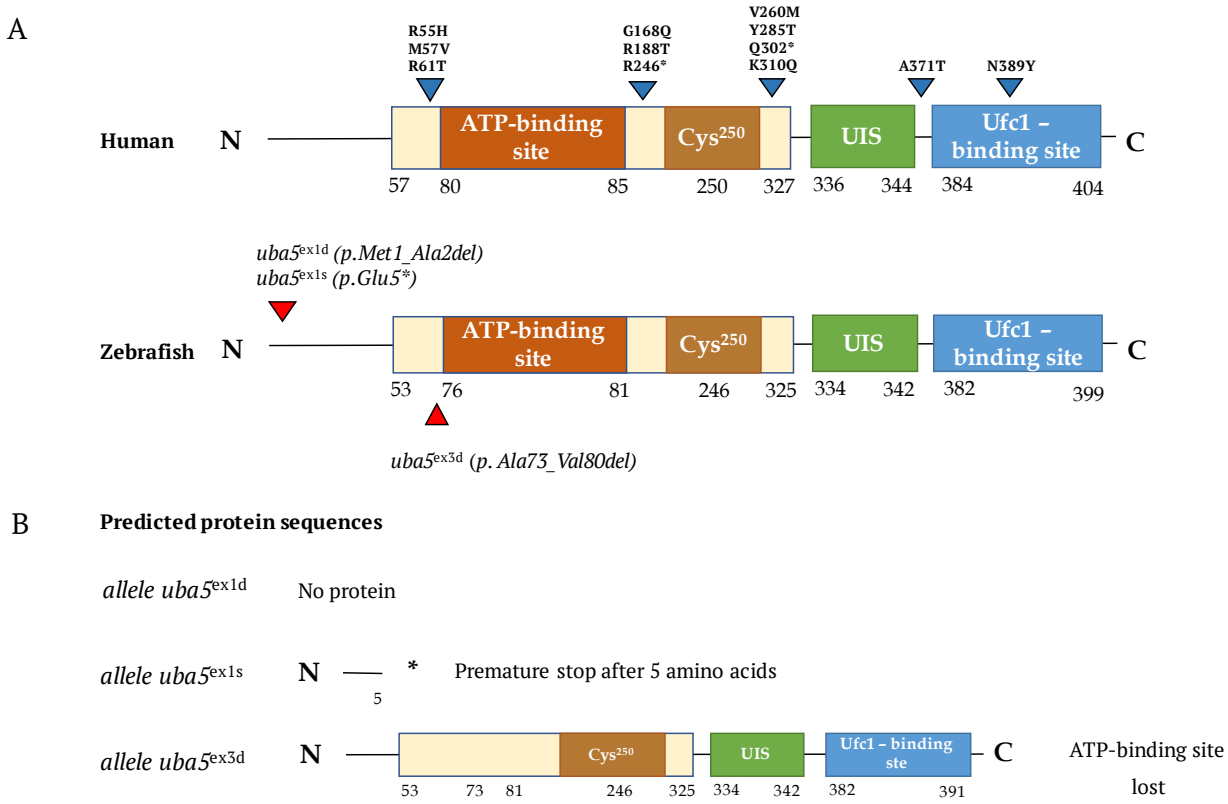

Figure 5.3. The domain structure of Uba5 and the mutant alleles in zebrafish. (A) Schematic representation of human UBA5 and zebrafish Uba5. Red arrowheads indicate the mutation sites in the three zebrafish mutant strains used in this study. Blue arrowheads indicate the mutations identified in

UBA5 patients. (B) The *uba5*^{ex1d} mutation affects the N-terminus of the protein and deletes Met1 and Ala2. The *uba5*^{ex1s} mutation also affects the N-terminus of the protein, due to insertion of 73 base pairs following the start codon, and leads to a frameshift and stop after 5 amino acids. The *uba5*^{ex3d} mutation is present in the ATP-binding site and deletes Ala73 to Val80.

5.4. Loss of Uba5 results in impaired locomotor activity at early stages of development

Given the reduced motor function in patients, we examined the motor function of *uba5* mutants at 2 dpf and 6 dpf. Using a touch-evoked response assay, we were able to determine the maximum acceleration of 2 dpf embryos as a direct measure of muscle force. We found that *uba5*$^{ex1s/ex1s}$ and *uba5*$^{ex3d/ex3d}$ generate the same muscle force as sibling controls, showing no apparent motor impairment at 2 dpf (Fig. 5.4).

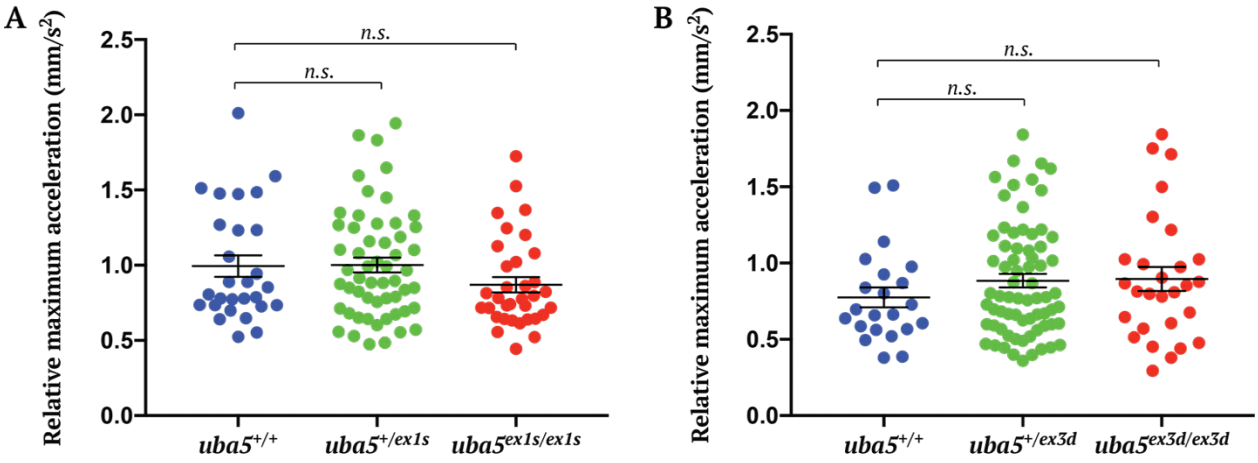

Figure 5.4. *uba5* mutants do not show motor impairment at 2 days post fertilization. Quantification of the maximum acceleration recorded from touch-evoked response assays of *uba5*$^{ex1s/ex1s}$ (A) *and uba5*$^{ex3d/ex3d}$ (B) zebrafish compared to control zebrafish at 2 dpf. Data are represented as mean ± SEM for 3 independent replicate experiments and statistical significance was assessed using one-way ANOVA, with Tukey's multiple comparison test. *n.s. not significant*. (A) Replicate 1: *n*=9 wildtype, *n*=18 heterozygotes and *n*=16 mutants. Replicate 2: *n*=6 wildtype, *n*=16 heterozygotes and *n*=10 mutants. Replicate 3: *n*=13 wildtype, *n*=23 heterozygotes and *n*=9 mutants. (B) Replicate 1: *n*=4 wildtype, *n*=11 heterozygotes and *n*=5 mutants. Replicate 2: *n*=9 wildtype, *n*=26 heterozygotes and *n*=13 mutants. Replicate 3: *n*=13 wildtype, *n*=34 heterozygotes and *n*=10 mutants. Each dot represents an individual zebrafish.

Next, we recorded the swimming performance of 6 dpf embryos to measure their locomotor activity. While *uba5*$^{ex1d/ex1d}$ embryos had 13% less movements, the distance travelled was comparable to wildtype and heterozygous embryos (Fig. 5.5 A & A'). Instead, both *uba5*$^{ex1s/ex1s}$ and *uba5*$^{ex3d/ex3d}$ embryos showed a significant decrease in the number of movements and in the distance travelled. Overall, *uba5*$^{ex1s/ex1s}$ embryos had 20% less movements and travelled 30% less distance (Fig. 5.5 B & B'), and *uba5*$^{ex3d/ex3d}$ embryos showed 40% less movements and travelled 30% less distance (Fig. 5.5 C & C'), than wildtype siblings.

To confirm that the decrease in swimming activity was consequence of mutation in *uba5* and not due to random off-target mutations generated during CRISPR mutagenesis, we also examined the swimming performance of double compound heterozygous embryos. As observed for *uba5*$^{ex1s/ex1s}$ and *uba5*$^{ex3d/ex3d}$ mutants, we found that *uba5*$^{ex1s/ex3d}$ compound heterozygous show a decrease in number of movements and in distance travelled at 6 dpf (Fig. 5.5 E & F). Furthermore, although *uba5* $^{ex1d/ex1d}$ mutants have no dramatic swimming impairment, both *uba5* $^{ex1d/ex1s}$ and *uba5* $^{ex1d/ex3d}$ compound heterozygous revealed a significant decrease in swimming activity at 6 dpf (Fig. 5.6 A-D). These results confirm that the decrease in locomotor activity observed in *uba5*$^{ex1s/ex1s}$ and *uba5*$^{ex3d/ex3d}$ mutants is due to mutation of *uba5.* Additionally, these results suggest that the *uba5*^{ex1d} mutant allele potentially results in a protein able to carry out sufficient function to allow normal movement.

Previous work on *C. elegans* demonstrated that the sensory system is impaired in the absence of components of the UFM1 pathway (Colin et al., 2016). To assess if the sensory ability of zebrafish *uba5* mutants is similarly compromised, embryos were exposed to two cycles of 5 min darkness followed by 5 min 100% light and the locomotor activity was analysed. From this data, we found that *uba5* mutants are able to respond to both light and dark stimuli in an analogous manner to sibling controls at 6 dpf (Figure 5.7). This demonstrates that the perception of a stimulus and response to a stimulus is not affected.

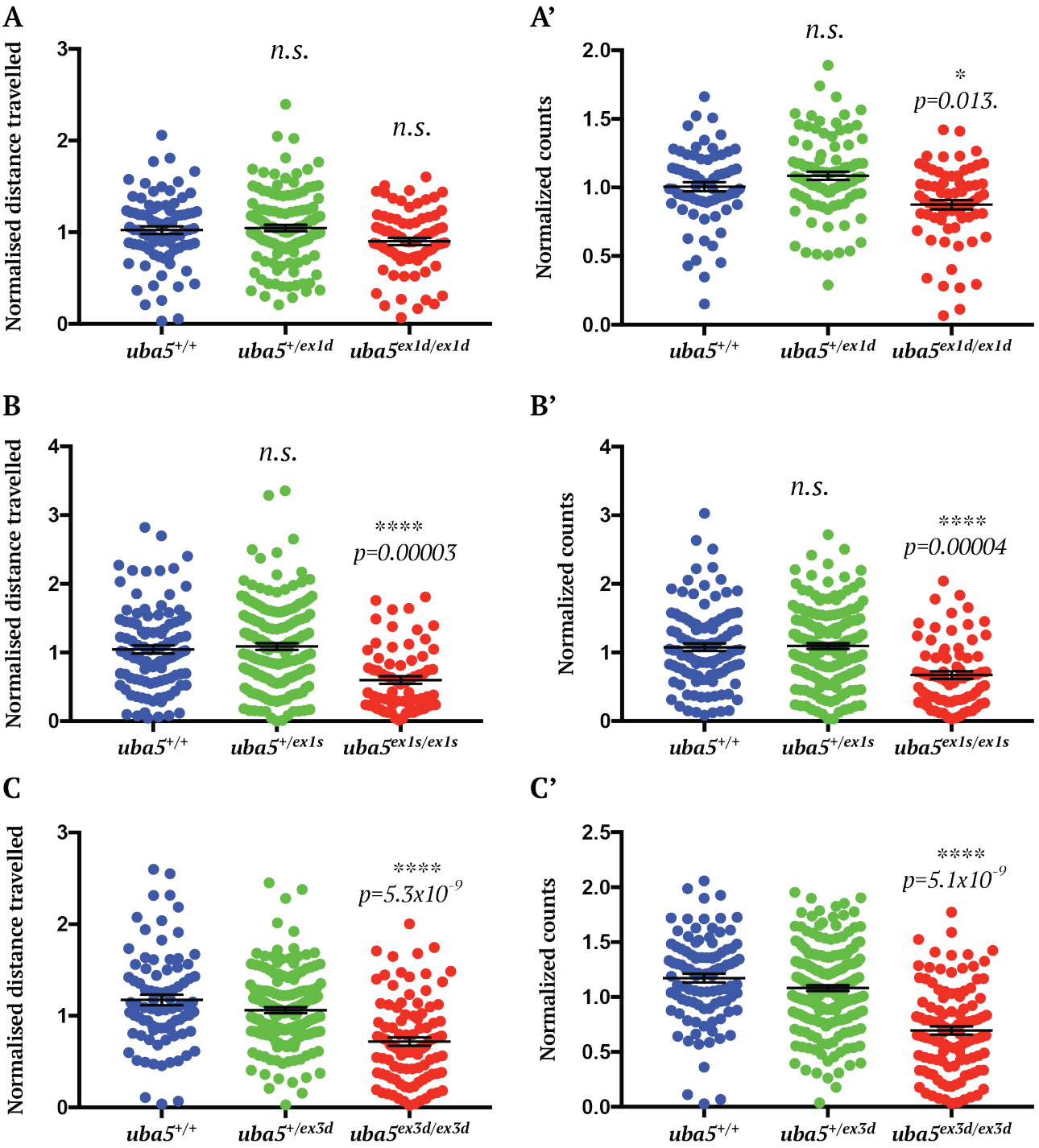

Figure 5.5. *uba5* mutants show decreased locomotor activity at 6 days post fertilization. Quantification of the number of movements and distance travelled by *uba5*$^{ex1d/ex1d}$ (A, A'), *uba5*$^{ex1s/ex1s}$ (B, B') and *uba5*$^{ex3d/ex3d}$ (C, C') mutants. Data are normalised to the mean value of each replicate to exclude potential variation between different biological replicates, and represented as mean ± SEM for 4 independent replicate experiments. Statistical significance was assessed using one-way ANOVA with Tukey's multiple comparison test. * < 0.05, ** < 0.01, *** < 0.001 and **** < 0.0001, comparing wild type and *uba5* mutants. *n.s.* not significant. (A & A') Replicate 1: *n* = 15 wildtype, *n* = 23 heterozygotes and *n* = 13 mutants. Replicate 2: *n* = 33 wildtype, *n* = 36 heterozygotes and *n* = 26 mutants. Replicate 3: *n* = 16 wildtype, *n* = 35 heterozygotes and *n* = 21 mutants. Replicate 4: *n* = 21 wildtype, *n* = 38 heterozygotes

and n = 30 mutants. (B & B') Replicate 1: n = 24 wildtype, n = 57 heterozygotes and n = 25 mutants. Replicate 2: n = 27 wildtype, n = 25 heterozygotes and n = 17 mutants. Replicate 3: n = 26 wildtype, n = 40 heterozygotes and n = 15 mutants. Replicate 4: n = 28 wildtype, n = 49 heterozygotes and n = 18 mutants. (C & C') Replicate 1: n = 31 wildtype, n = 55 heterozygotes and n = 27 mutants. Replicate 2: n = 31 wildtype, n = 79 heterozygotes and n = 27 mutants. Replicate 3: n = 32 wildtype, n = 60 heterozygotes and n = 44 mutants. Replicate 4: n = 22 wildtype, n = 24 heterozygotes and n = 20 mutants. Each dot represents an individual zebrafish.

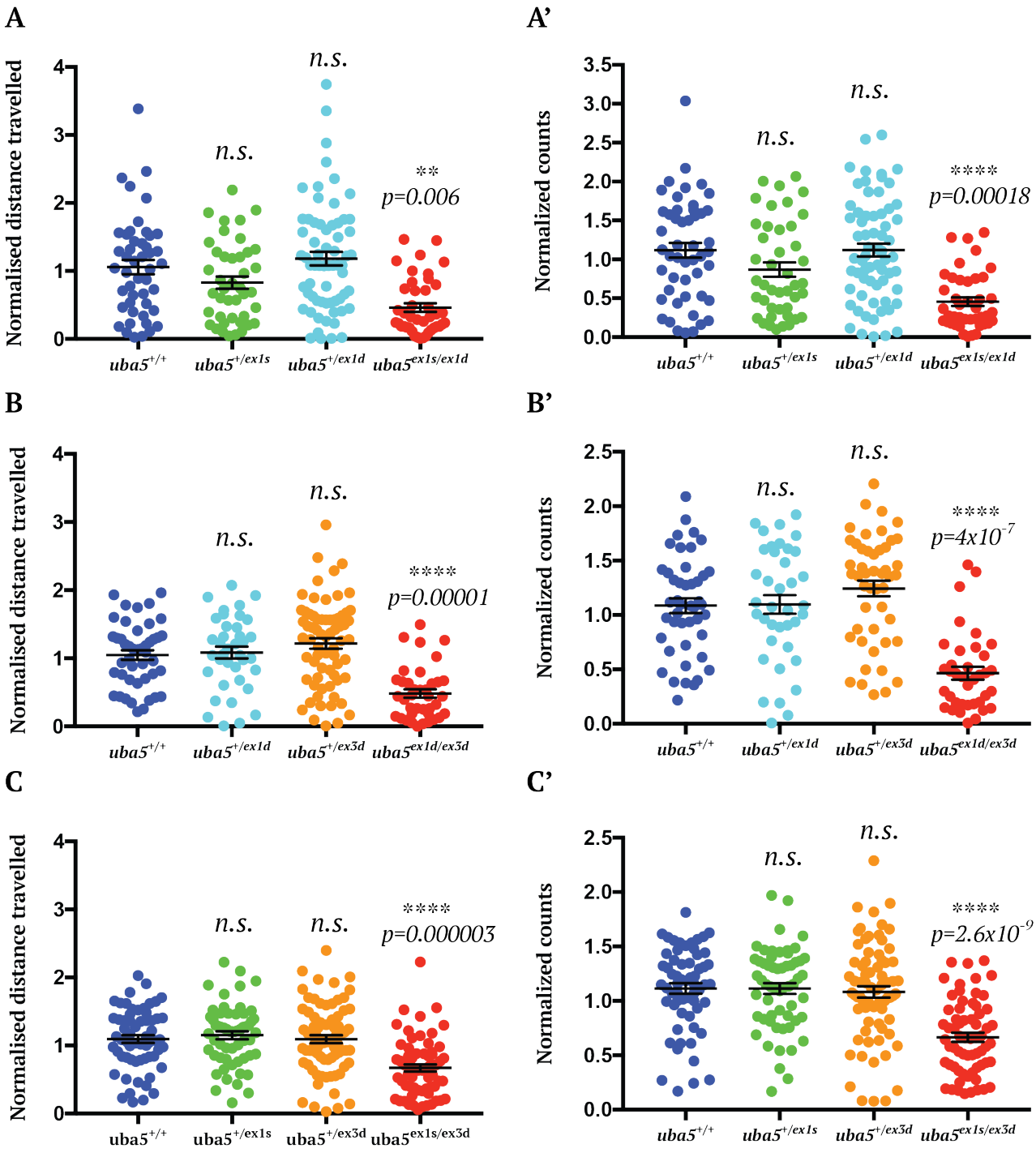

Figure 5.6. *uba5* compound heterozygous show decreased locomotor activity at 6 days post fertilization. Quantification of the number of movements and distance travelled by *uba5*$^{ex1d/ex1s}$ (A, A'), *uba5*$^{ex1d/ex3d}$ (B, B') and *uba5*$^{ex1s/ex3d}$ (C, C') mutants. Data are normalised to the mean value of each replicate to exclude potential variation between different biological replicates, and represented as mean ± SEM for 2-3 independent replicate experiments. Statistical significance was assessed using one-way ANOVA with Tukey's multiple comparison test. * < 0.05, ** < 0.01 and **** < 0.0001, comparing wild type and *uba5* mutants. *n.s.* not significant. (A & A') Replicate 1: *n* = 20 wildtype, *n* = 30 heterozygotes for *uba5*^{ex1d}, *n* = 17 heterozygotes for *uba5*^{ex1s} and *n* = 27 compound heterozygotes. Replicate 2: *n* = 29

wildtype, *n* = 36 heterozygotes for *uba5*^{ex1d}, *n* = 27 heterozygotes for *uba5*^{ex1s} and *n* = 17 compound heterozygotes. (B & B') Replicate 1: *n* = 7 wildtype, *n* = 8 heterozygotes for *uba5*^{ex1d}, *n* = 7 heterozygotes for *uba5*^{ex3d} and *n* = 5 compound heterozygotes. Replicate 2: *n* = 24 wildtype, *n* = 9 heterozygotes for *uba5*^{ex1d}, *n* = 23 heterozygotes for *uba5*^{ex3d} and *n* = 20 compound heterozygotes. Replicate 3: *n* = 14 wildtype, *n* = 21 heterozygotes for *uba5*^{ex1d}, *n* = 18 heterozygotes for *uba5*^{ex3d} and *n* = 13 compound heterozygous. (C & C') Replicate 1: *n* = 23 wildtype, *n* = 15 heterozygotes for *uba5*^{ex1s}, *n* = 26 heterozygotes for *uba5*^{ex3d} and *n* = 23 compound heterozygotes. Replicate 2: *n* = 14 wildtype, *n* = 25 heterozygotes for *uba5*^{ex1s}, *n* = 10 heterozygotes for *uba5*^{ex3d} and *n* = 23 compound heterozygotes. Replicate 3: *n* = 24 wildtype, *n* = 18 heterozygotes for *uba5*^{ex1s}, *n* = 39 heterozygotes for *uba5*^{ex3d} and *n* = 19 compound heterozygotes. Each dot represents an individual zebrafish.

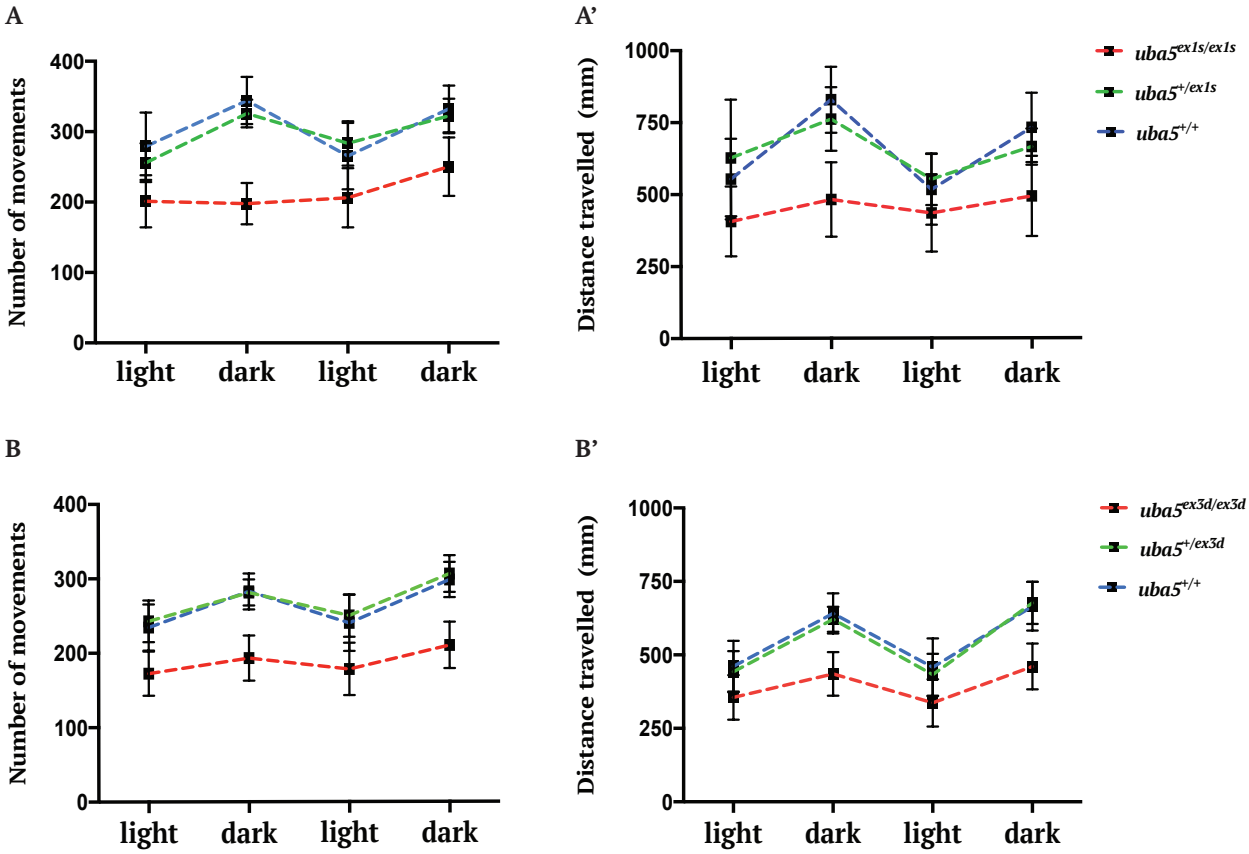

Figure 5.7. Photomotor response analysis show *uba5*$^{ex1s/ex1s}$ and *uba5*$^{ex3d/ex3d}$ mutants respond to light and dark stimuli at 6 days post fertilization. Quantification of the number of movements and distance travelled by *uba5*$^{ex1s/ex1s}$ (A, A') and *uba5*$^{ex3d/ex3d}$ (B, B') mutants. Data are represented as mean ± 95%CI for 2 independent replicate experiments. *n* = 96 per biological replicate. Each dot represents the mean of 2 independent replicates.

5.5. Impaired motor function is not preceded by gross morphological abnormalities

To investigate the pathological changes underlying the observed motor phenotype, we performed immunohistochemistry and confocal microscopic analyses of the muscle and axonal structure from mutant and control zebrafish. The Tg (*olig2*: *EGFP*) reporter line was further used to examine the primary motor neurons. At 6 dpf, *uba5* mutants showed no obvious abnormalities in the muscle or axonal morphology (Fig. 5.8). Additionally, no differences were observed in the patterning of primary neurons (Fig. 5.9). To assess whether the axons were capable of forming synapses on the muscle fibres, we next analysed the acetylcholine receptors (AChR) clusters at 6 dpf (Fig. 5.10). Using rhodamine conjugated α-bungarotoxin (α-BTX), we found that the axons in *uba5*$^{-/-}$ co-localized with AChR clusters, demonstrating that there are no signs of denervation of the muscle.

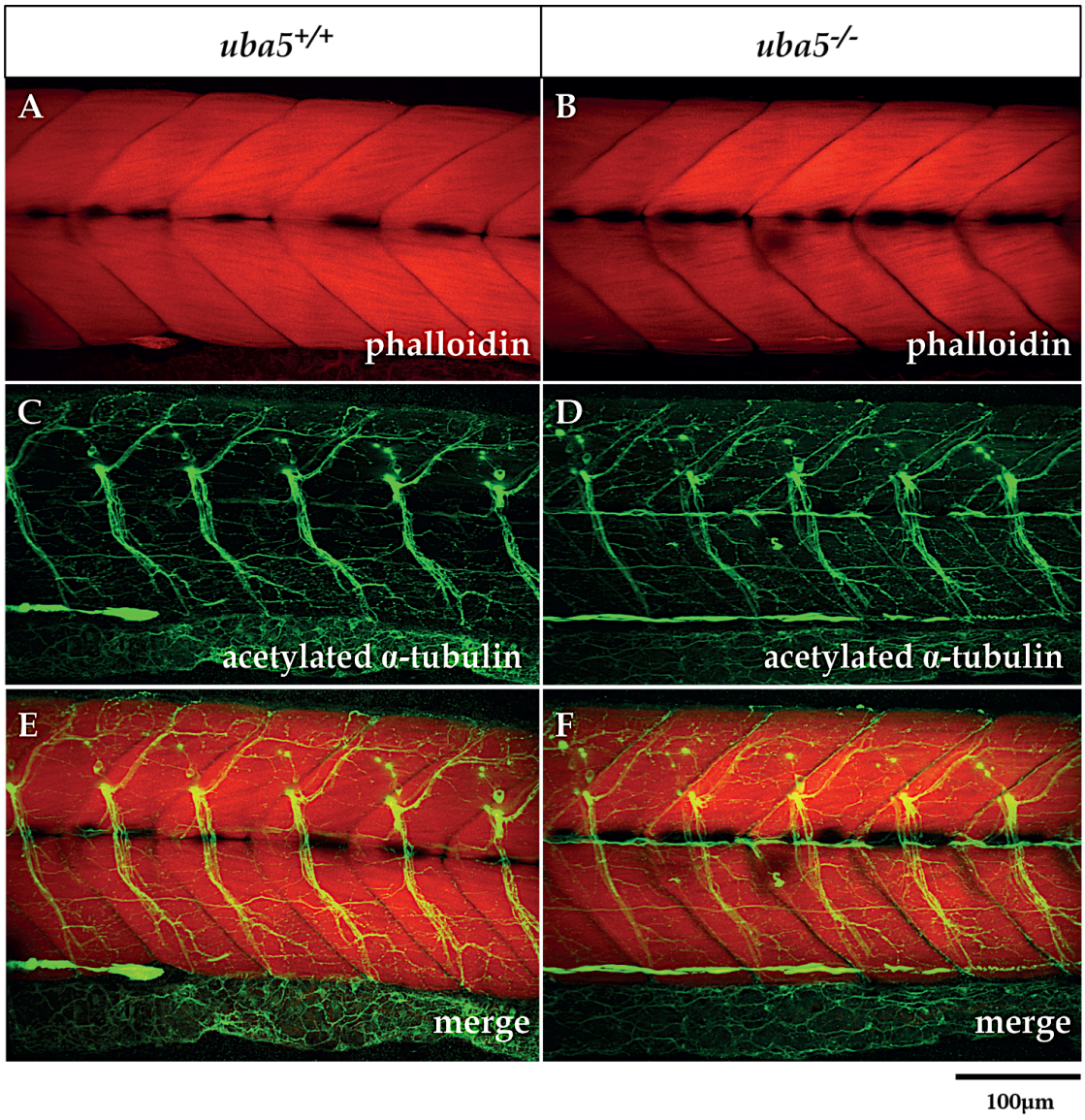

Figure 5.8. The muscle morphology and axonal network is unaffected in *uba5*$^{-/-}$ mutants at 6 dpf. Maximum projections of confocal z-series to visualize the muscle (A, B) and axonal morphology (C, D) of *uba5* mutants and wild type siblings.

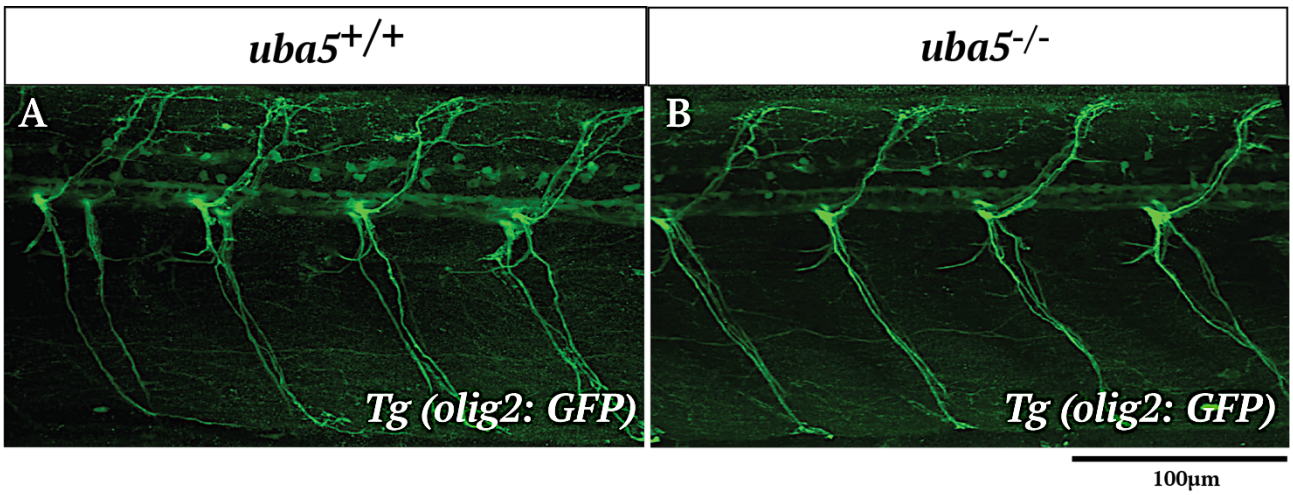

Figure 5.9. Normal patterning of the motor neurons in *uba5* mutants at 6 dpf. Maximum projections of confocal z-series to visualize the motor neurons in *uba5* mutants (B) and wild type siblings (A).

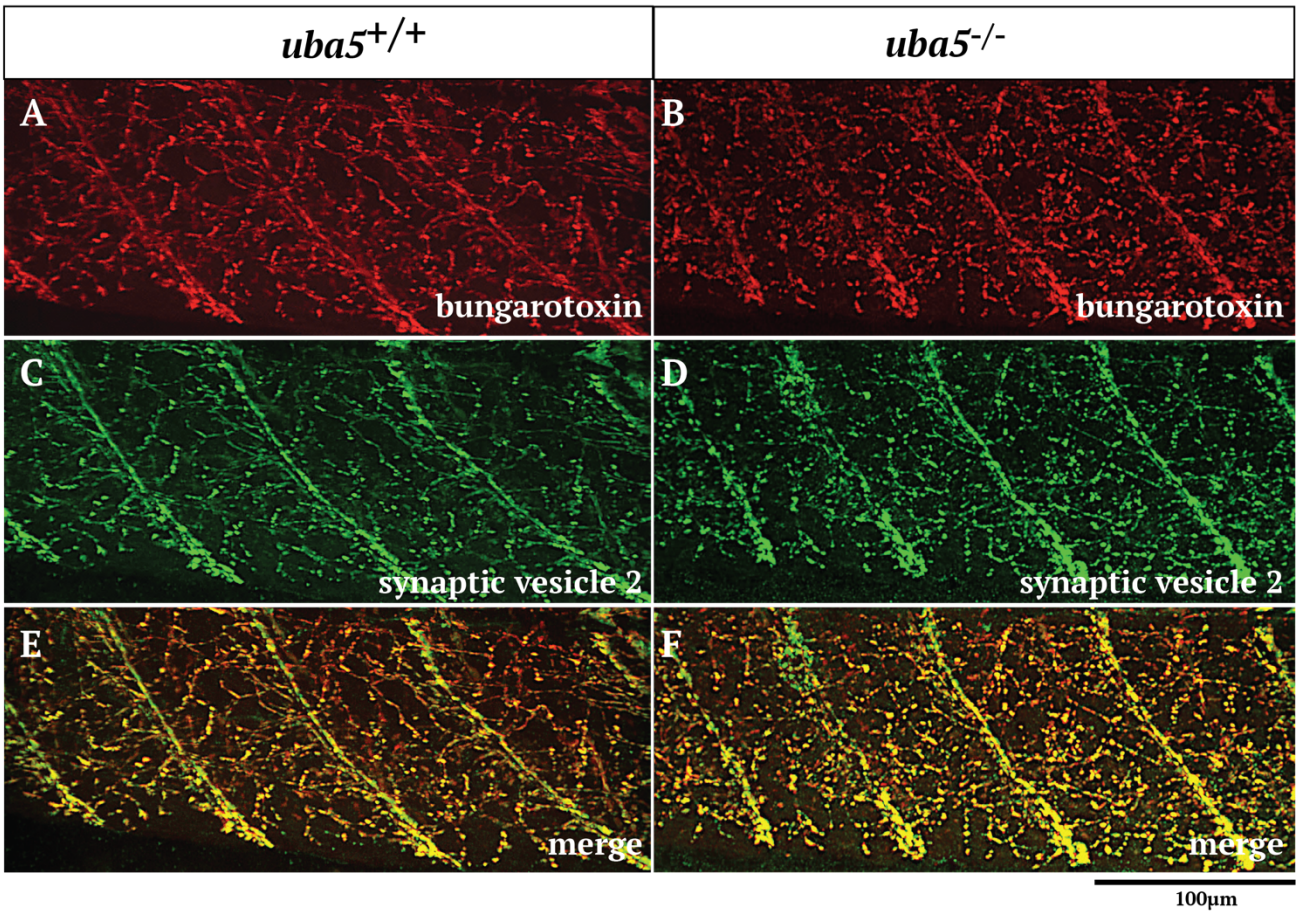

Figure 5.10. Neuromuscular junctions are intact in *uba5* mutants at 6 dpf. Maximum projections of confocal z-series to visualize the neuromuscular junctions in *uba5* mutants (B, D & F) and wild type siblings (A, C & E). Lateral views of synaptic vesicle 2 (motor axons, green), α-BTX (AChR, red) stained, and merge (yellow).

In addition to impaired motility, most *UBA5* patients exhibit delayed myelination in the brain. Myelin is well-known to have an essential role for speed of signal conduction and, consequently, coordination of movement. Hence, the motor function impairment in *uba5* mutants could be the result of delayed myelination. To investigate this hypothesis, we examined *myelin basic protein* (*mbp*) expression pattern by *in situ* hybridization at several stages of development. We found no obvious signs of delayed myelination in *uba5* mutants compared to sibling controls (Figure 5.11).

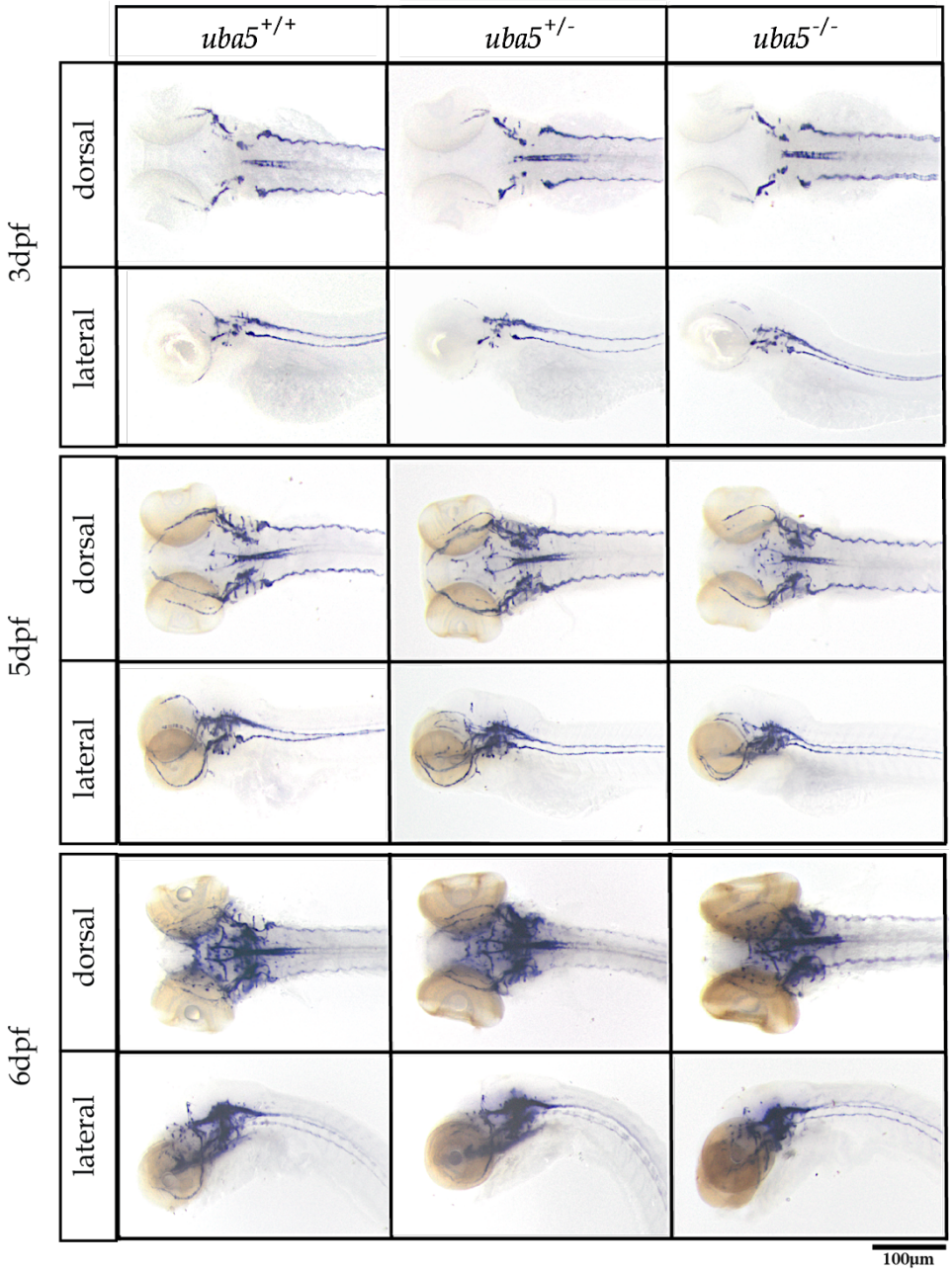

Figure 5.11. ***Myelin basic protein*** **expression pattern.** Whole mount *in situ* hybridization for zebrafish *mbp* at 3 dpf, 5 dpf and 6 dpf shows that *mbp* expression pattern in *uba5* mutants is similar to sibling controls.

As epileptic encephalopathy patients with *UBA5* mutations develop postnatal microcephaly, and fail to thrive, lateral and dorsal brightfield images were subsequently acquired for morphometric analyses of the body length and area of the head at 5 dpf. This time point was chosen to assess whether potential developmental deficits would arise before the impaired motility observed at 6 dpf. As a result, *uba5* mutants could not be phenotypically distinguished from wild type embryos, showing comparable body length and forebrain cross-sectional area (Fig. 5.12).

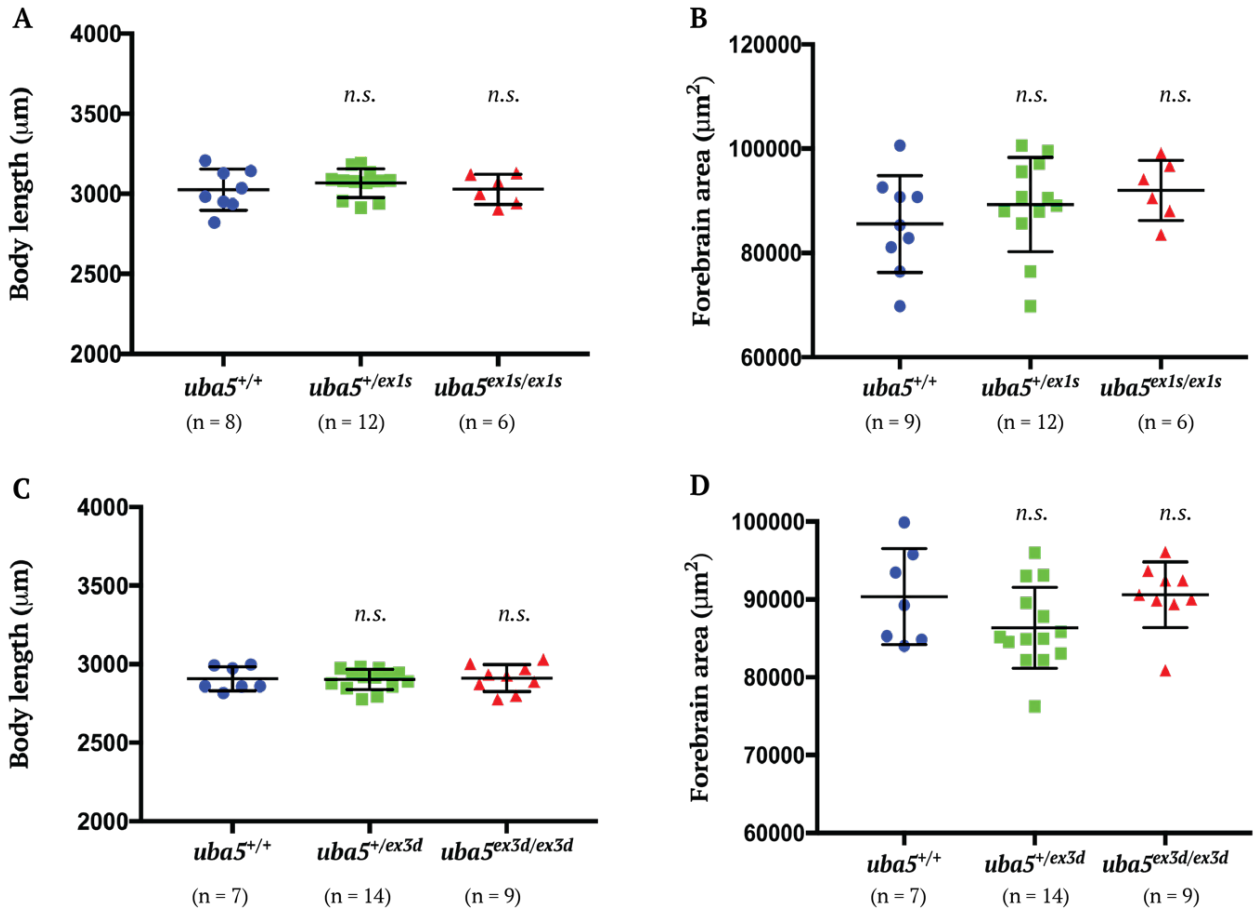

Figure 5.12. Body length and forebrain area at 5 dpf. Quantification of the body length and forebrain cross-sectional area in *uba5*$^{ex1s/ex1s}$ (A, B) and *uba5*$^{ex3d/ex3d}$ (C, D) and sibling controls. Data are represented as mean ± SD and statistical significance was assessed a one-way ANOVA. *n.s.* not significant. Each dot represents individual zebrafish.

While *uba5* mutants lack gross morphological abnormalities early in development, it is possible that subtle structural defects still exist. To search for subtle structural abnormalities in *uba5* mutant brains, we used the *Tg* (*huc*: *EGFP*) reported line to label the neuronal cells and maximum projection images from confocal series were used to measure the length of the cerebellum, the optic tectum and the telencephalon. Similar to the previous analysis, *uba5* mutants showed no signs of morphological alterations in the brain compared to wild type siblings (Fig. 5.13). Thus, *uba5* mutants show no signs of microcephaly at 6 dpf.

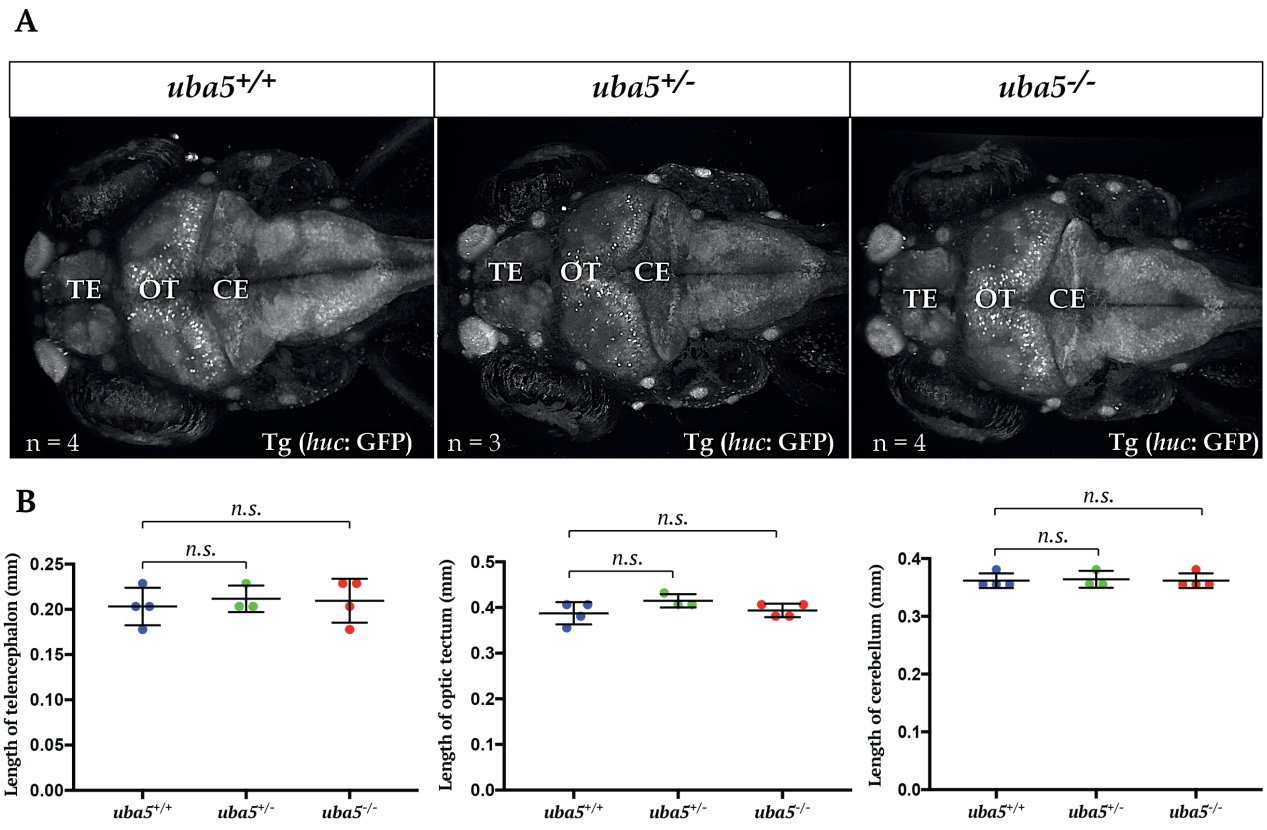

Figure 5.13. Brain morphology is not compromised in *uba5* mutants at 6 dpf. (A) Maximum projections of confocal z-series to visualize the brain of *uba5* mutants and sibling controls. (B) Quantification of the length of the telencephalon, optic tectum and cerebellum in *uba5* mutants normalized to wild type zebrafish. Data are represented as mean ± SD and statistical significance was assessed using a one-way ANOVA. *n.s.* not significant. Each dot represents an individual zebrafish.

5.6. *uba5* mutants show signs of peripheral nerve dysfunction at 6 dpf

To further characterize the pathological changes in *uba5* mutants, we performed electron microscopic (EM) analyses of the skeletal muscle and peripheral nerves at 6 dpf. Similar to wild type controls, *uba5* mutants exhibit highly organized sarcomeres composed of thin and thick filaments flanked by distinct Z-disks. However, *uba5* mutants presented abnormalities at the nerves innervating the skeletal muscle that were not observed in control embryos. Autophagic structures and large vesicles enclosing debris were identified within the peripheral nerves (Fig. 5.14 D), representing signs of active degradation of nerve cellular components. Plus, *uba5* mutants presented elongated mitochondria (Fig. 5.14 C) and 'onion-ring' membranous structures at the nerve terminals (Fig. 5.14 E), which are features of mitochondrial degeneration. Consistent with this finding, we also identified autophagic structures associated with a small number of mitochondria in the skeletal muscle, which further suggests an overall impairment of mitochondrial function in *uba5* mutant fish.

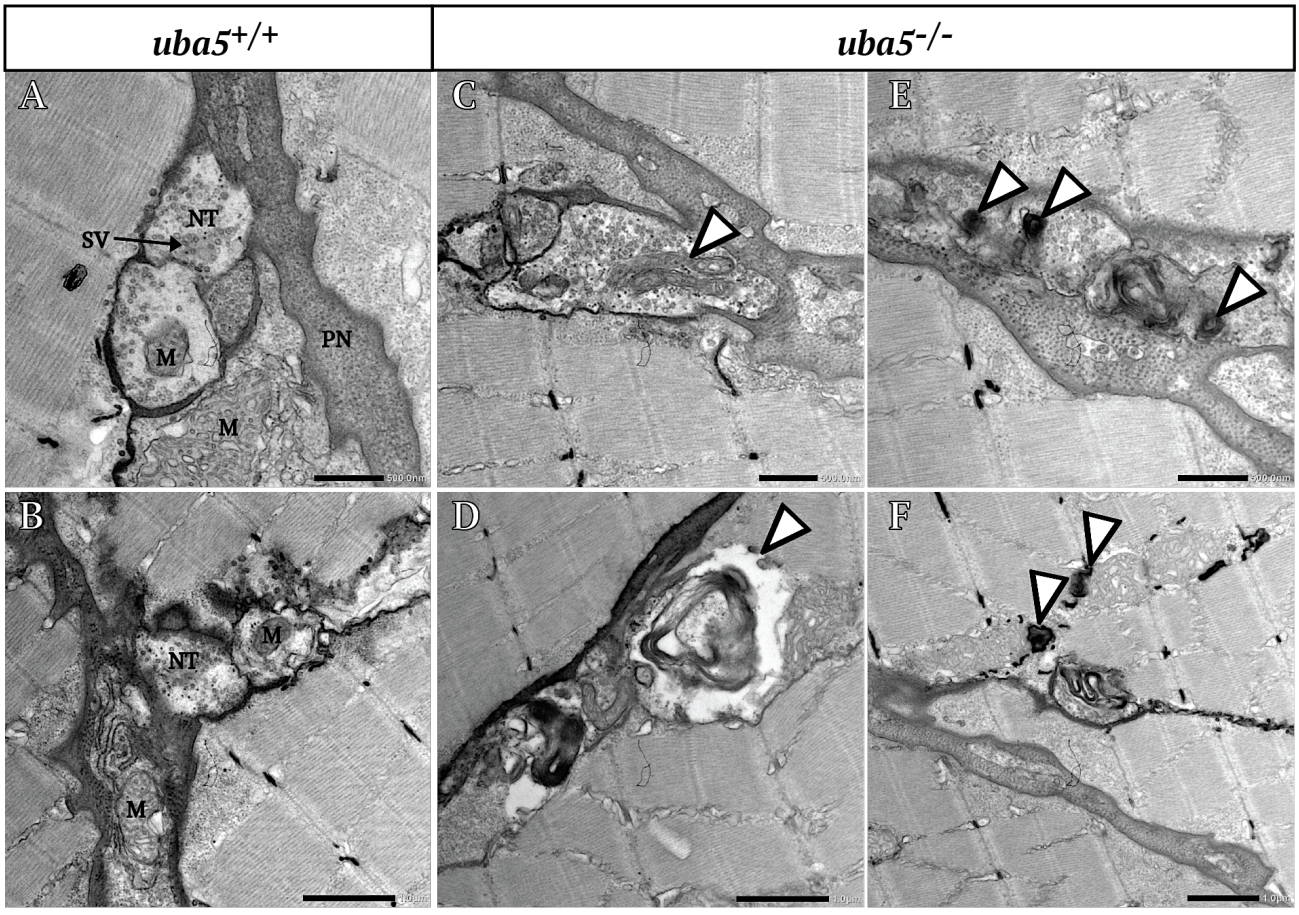

Figure 5.14. Ultrastructural changes of the peripheral nerves in *uba5* mutants at 6 days post fertilization. (A & B) Normal patterning of the peripheral nerves in *uba5*$^{+/+}$ embryos. (C - F) EM sections of the peripheral nerves in *uba5* mutants, showing abnormal findings. EM images illustrate mitochondrial abnormalities, including (C) elongated mitochondria (arrowhead) and (E) degenerating mitochondria in the nerve terminals (arrowhead). (D) Degradation vacuole enclosing debris (arrowhead). (F) Autophagic

structures associated with mitochondria in the skeletal muscle (arrowhead). M, mitochondria; NT, nerve terminal; PN, peripheral nerve; SV, synaptic vesicles. Scale bars are 500 nm in (A, C & E) and 1 µm in (B, D & F).

5.7. *uba5* mutants' survival and growth is compromised from 14 dpf

As *UBA5* patients show a decline in motor skills and significantly reduced lifespan, we carried out *uba5*$^{+/ex1s}$ in-crosses and monitored survival and locomotor activity of the offspring after 6 days post fertilization. The analysis revealed that the number of *uba5* mutants declines approximately from 15 dpf, with only 50% of the mutants surviving up to 25 dpf, and the maximum lifespan ranged between 35 dpf and 70 dpf (Fig. 5.15 A). By examining the swimming performance, it was clear that *uba5* mutants show a severe decline in motor function at 14 dpf, with only 20% of the distance swum compared to wild type values. The locomotor activity was continuously reduced in *uba5* mutant fish compared to wild type throughout the mutants' lifespan. (Fig. 6.15 B). In contrast, wild type zebrafish showed 88% survival, and no significant differences in locomotor activity were detected between wild type and heterozygotes, until the end of the experiment (70 days).

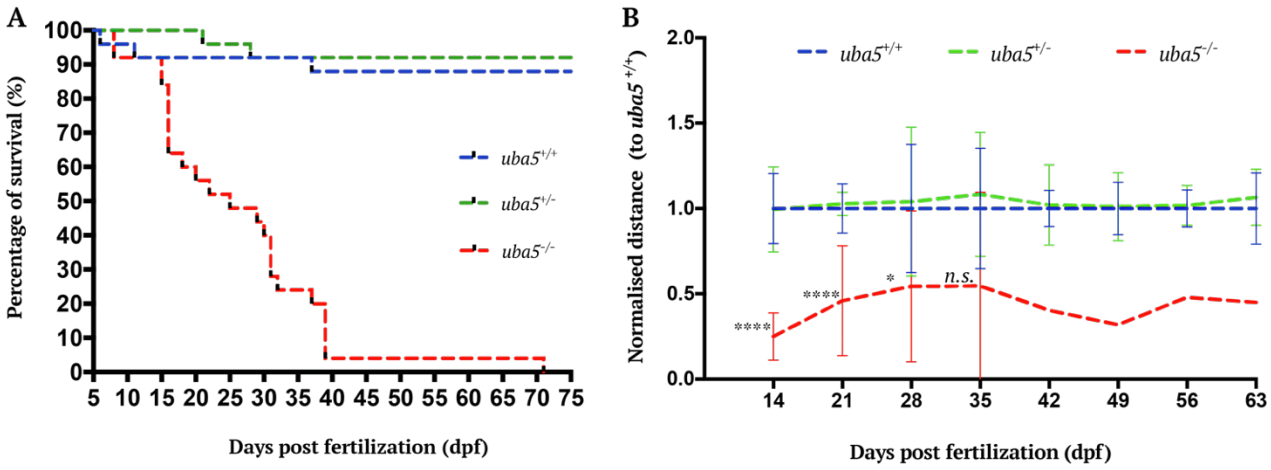

Figure 5.15. Characterization of survival and locomotor activity in embryos from 5 days fertilization. (A) 25 wild type, 25 heterozygotes, and 25 mutant embryos were raised and used for the survival analysis. Survival curve shows loss of viability from 15 dpf. (B) Quantification of the distance travelled in *uba5* mutant zebrafish and sibling controls. Data are represented as mean ± SD and statistical significance was assessed using one-way ANOVA with Tukey's multiple comparison test. * $p < 0.05$ and **** $p < 0.0001$, comparing wild type and *uba5* mutants. *n.s.* not significant.

Of note, while no difference in size was observed between *uba5* mutants and wild type siblings at 5 dpf, *uba5* mutants are clearly smaller than wild type and heterozygote larvae from 14 dpf (Fig. 5.16 A). In average, the body length of *uba5* mutants was 40-50% less compared to wild type values at equivalent developmental stages throughout their lifespan (Fig. 5.16 B). This finding is consistent with the phenotype of *UBA5* patients who show normal growth rate at an early age followed by growth arrest at the onset of disease.

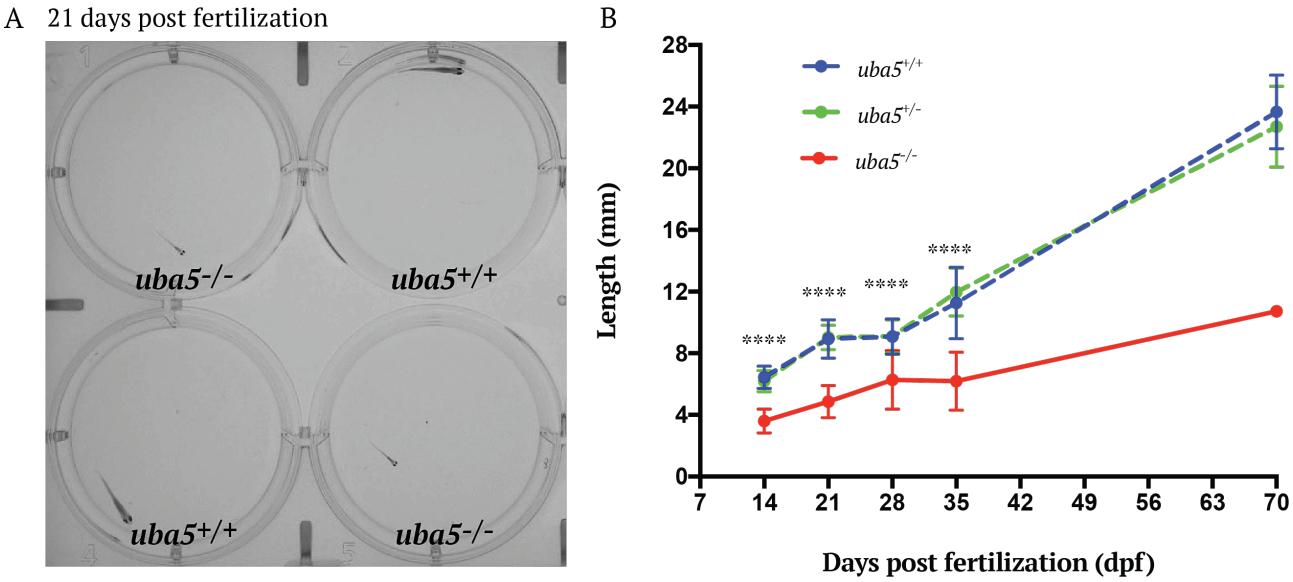

Figure 5.16. *Uba5* mutants are smaller in size. (A) Representative images of *uba5*$^{+/+}$ and *uba5*$^{-/-}$ at 21 dpf, showing significant difference in size at 21 days post fertilization. (B) Length of wild type, heterozygote and mutant larvae measured at 14, 21, 28, 35 and 70 dpf. *Uba5* mutants remain smaller than wild type siblings throughout development. Data are represented as mean ± SD and statistical significance was assessed using one-way ANOVA with Tukey's multiple comparison test. **** $p < 0.001$, comparing wild type and *uba5* mutants. 14 dpf: n=23 wild type, n=25 heterozygotes and n=23 mutants; 21 dpf: n=23 wild type, n=25 heterozygotes and n=14 mutants; 28 dpf: n=23 wild type, n=23 heterozygotes and n=12 mutants; 35 dpf: n=23 wild type, n=23 heterozygotes and n=6 mutants; 42 dpf to 70 dpf: n=22 wild type, n=23 heterozygotes and n=1 mutant.

5.8. Loss of Uba5 results in neurodegeneration in the cerebellum and mitochondrial abnormalities at 14 dpf

Ultrastructural analysis of the brain by EM revealed significant axonal pathology in the cerebellum at 14 dpf. Axonal degeneration was indicated by the presence of abnormal myelin swirls, which appeared as darkly stained ovals, consistent with myelin remaining after axonal loss (Fig. 5.17 D & D′). Dark cytoplasmic condensation of glial cells was also particularly abundant in the cerebellum of *uba5* mutants (Fig. 5.17 F & F′). Condensed cytoplasm is characteristic of dying glial cells and neurons, and is observed in neurodegenerative diseases (Yu et al., 2003). In addition, degenerated mitochondria were also detected within neurons in the cerebellum, shown by the presence of onion-ring structures associated with mitochondria (Fig. 5.17 E & E′).

We also identified findings of mitochondrial degeneration within the skeletal muscle in *uba5* mutants. In the skeletal muscle, mitochondria are typically aligned in rows between the myofibrils and have tightly packed cristae (Fig. 5.18 A & B). In *uba5* mutants, mitochondria exhibit altered cristae conformation, presenting swollen cristae and condensed matrix, and are mostly associated with autophagic vacuoles (Fig. 5.18 C & D). Increased numbers of abnormally enlarged mitochondria were additionally evident along muscle fibres (Fig. 5.18 E), and severely disrupted mitochondria were identified by the presence of multiple vacuolated mitochondria (Fig. 5.18 F). In contrast, the myofibrils pattern in *uba5* mutants was indistinguishable from those of control embryos demonstrating that the muscle structure is still intact.

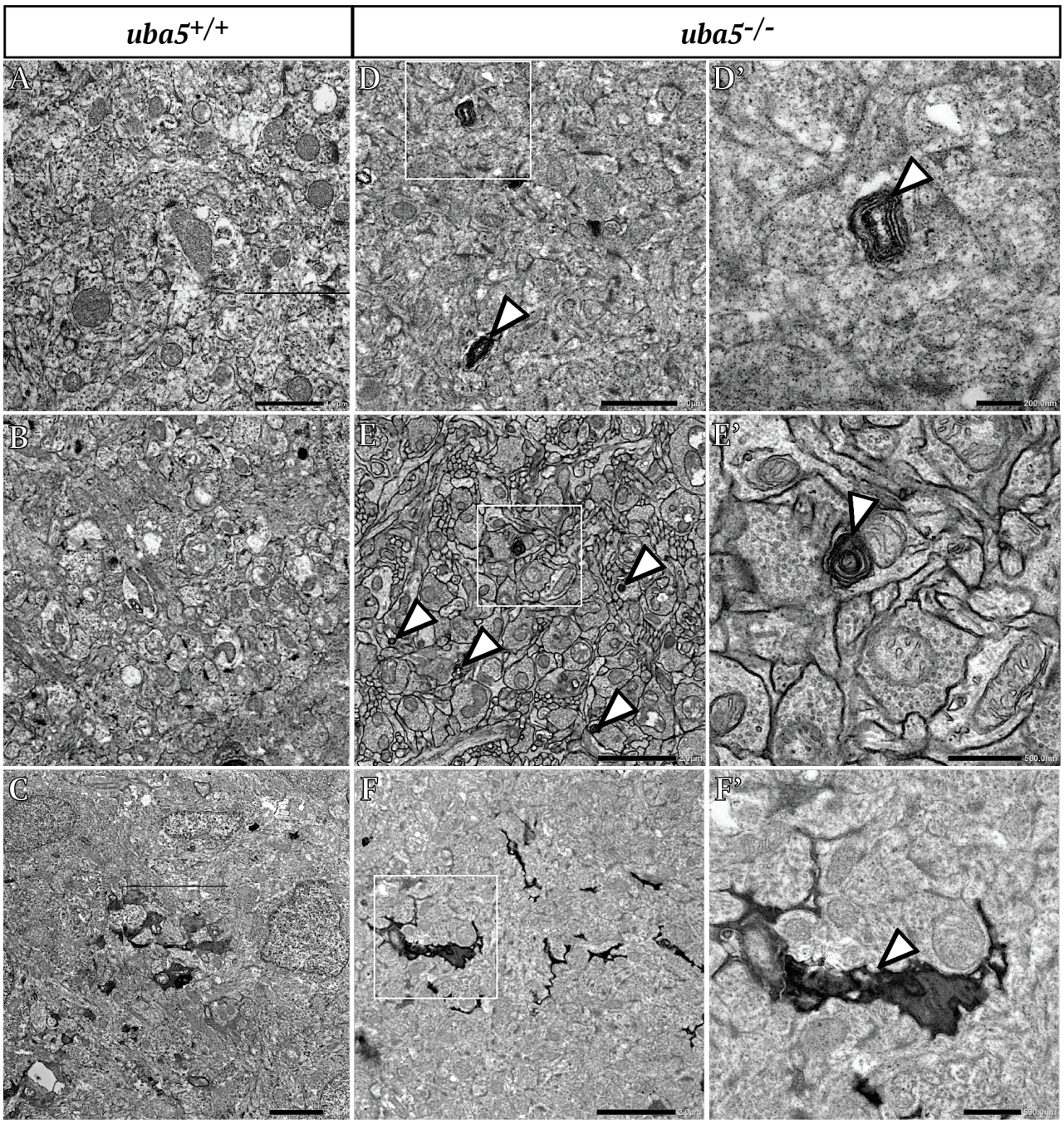

Figure 5.17. Ultrastructural characterization of the cerebellum in wild type and *uba5* mutant embryos. (A, B & C) EM sections of the cerebellum in *uba5*$^{+/+}$ zebrafish showing normal patterning of neurons and mitochondria. (D - F & D' - F') EM sections of the cerebellum in *uba5*$^{-/-}$ zebrafish showing abnormal findings. (D) Axonal degeneration and resulting myelin swirls (arrowheads). (D') Higher magnification view of the boxed area in (D). (E) Membrane whorls inside neurons, representing mitochondrial degeneration (arrowheads). (E') Higher magnification view of the boxed area in (E). (F) Cytoplasmic condensation with abnormal mitochondria. (F') Higher magnification view of the boxed area in (F). Scale bars are 1 µm in (A & D), 2 µm in (C, F & E), 200 nm in (D') and 500 nm in (E' & F').

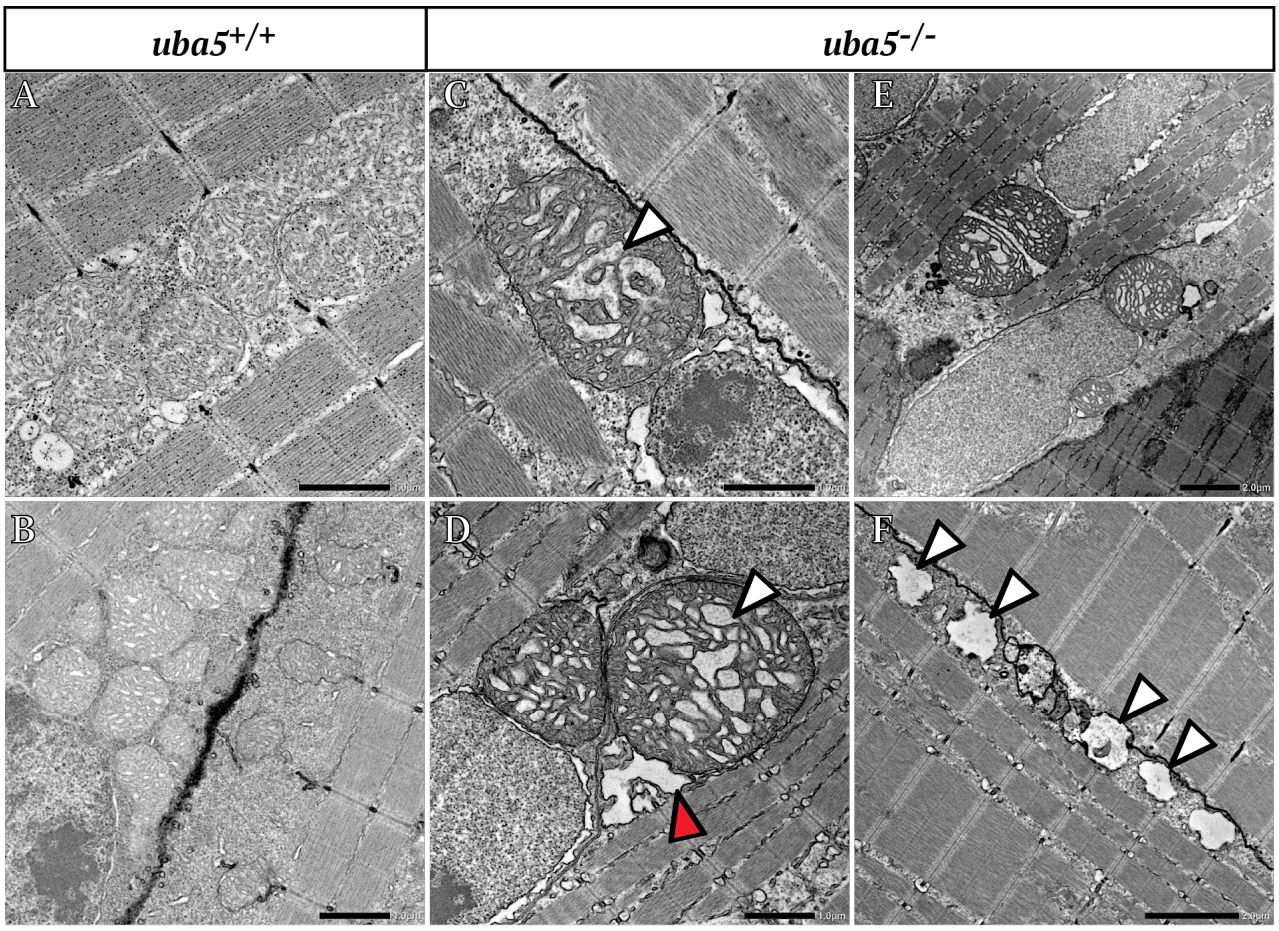

Figure 5.18. Electron microscopy images of muscle from wild type and *uba5* mutant zebrafish. (A & B) EM sections of the skeletal muscle in *uba5*$^{+/+}$ zebrafish showing normal patterning of muscle fibres and mitochondria. (C – F) EM sections of the skeletal muscle in *uba5*$^{-/-}$ zebrafish showing abnormal mitochondria. (C & D) Mitochondria with swollen cristae (white arrowheads) and vacuoles (red arrowheads). (E) Large mitochondria and (F) vacuolated mitochondria (white arrowheads). Scale bars are 1 µm in (A – D) and 2 µm in (E & F).

Taken together, our data shows that a neuropathy associated with delayed growth is developed after loss of Uba5 in zebrafish. This shows that the zebrafish is a useful model for assessing the direct role of Uba5 in the nervous system.

5.9. The Ufm1 pathway is disrupted in *uba5* mutants

Previous work demonstrated that UFM1-conjugate protein levels are significantly reduced in tissue samples derived from *UBA5* patients, being associated with impaired UBA5 activity (Muona et al., 2016). We carried out western blot analysis for Ufm1 and detected reduced levels of Ufm1 and Ufm1-conjugates in *uba5* mutant fish. Ufm1 protein levels were reduced to 10% in *uba5*$^{ex1s/ex1s}$ embryos, and 10% in *uba5*$^{ex3d/ex3d}$ embryos. In addition, Ufm1-conjugates levels were reduced to 50% in *uba5*$^{ex1s/ex1s}$, and 30% in *uba5*$^{ex3d/ex3d}$ mutants, compared to wild type (Fig. 5.19 A & B). These data indicate that the Ufm1 pathway is compromised in *uba5* mutant fish.

Due to the lack of a suitable antibody for Uba5, we were not able to confirm whether Uba5 protein is still made in *uba5*$^{ex1s/ex1s}$ mutants. It is possible that a downstream start site can possibly be utilised in the mutants, making a truncated protein. However, the analysis of Ufm1 protein indicates that the Ufm1 pathway is compromised. Therefore, although a truncated protein might still be made it is not sufficient to carry its normal function.

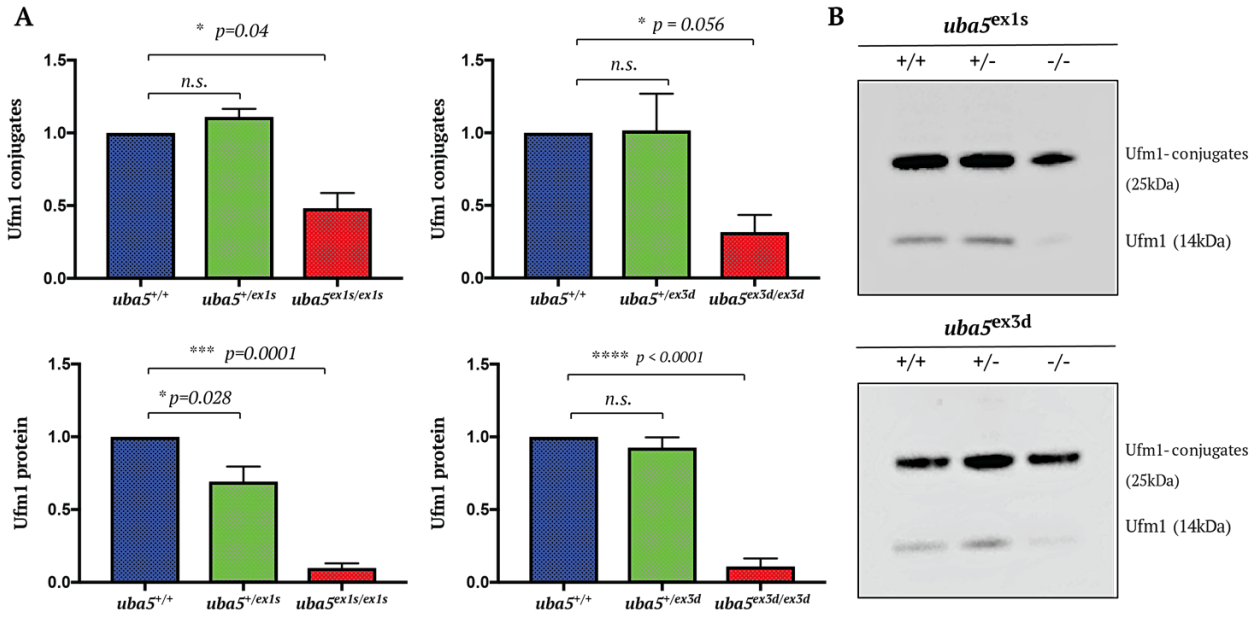

Figure 5.19. Western blot analysis showing Ufm1 protein and Ufm1-conjugates relative levels are reduced in *uba5* mutants at 6 dpf. (A) Graphical representation shows the relative abundances of Ufm1 and Ufm1-conjugates after normalization with total protein and subsequent normalization with wild type embryos. Data are presented as mean ± SEM for three independent experiments. (B) Representative western blots for Ufm1 and Ufm1 conjugates in *uba5*$^{ex1s/ex1s}$ and *uba5*$^{ex3d/ex3d}$ embryos.

The neural cell adhesion molecule, NCAM, was reported as one of the targets of the UFM1 post-translational modification system. The UFM1 pathway is involved in the endocytosis of NCAM in neurons (Homrich et al., 2014), which is then recycled to the plasma membrane or degraded by lysosomes (Chen and Tang, 2010). To examine whether NCAM levels are altered in *uba5* mutant fish, we carried out western blot at 6 dpf. We observed a 3.7-fold increase (*p=0.021*) in NCAM protein levels in *uba5* mutants (Fig. 5.20), suggesting that *uba5* mutants potentially have a lower rate of NCAM protein turnover.

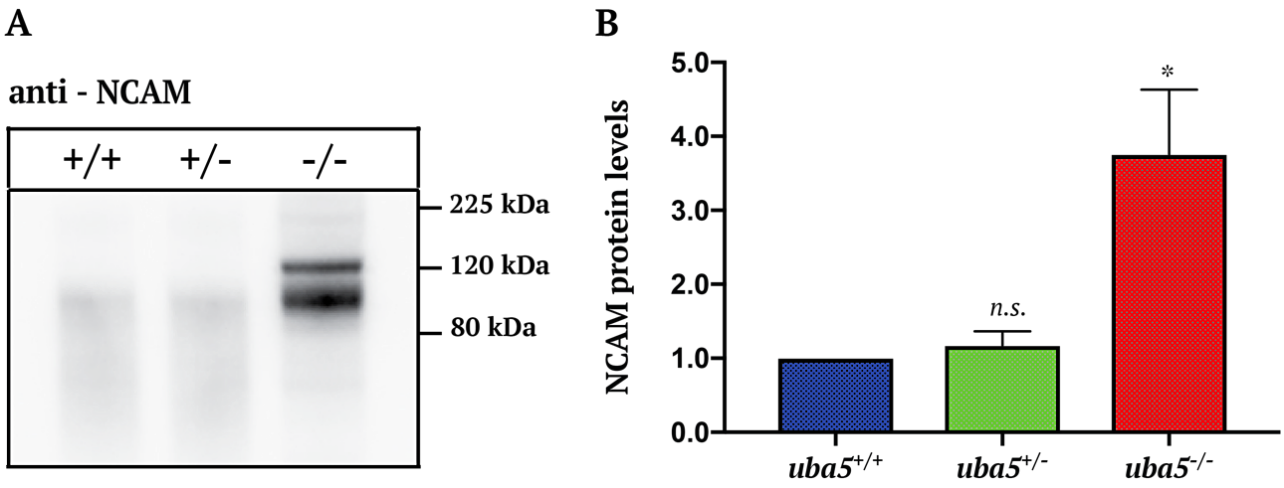

Figure 5.20. Expression of Neural Cell Adhesion Molecule (NCAM) based on western blot analysis in 6 dpf whole embryo tissue homogenates. (A) Representative western blot for NCAM. (B) Statistical analysis of western blot results. All values were normalized to total protein, and then normalized to wild type values. Data are represented as mean ± SEM for 3 biological replicates. Statistical significance was assessed using one-way ANOVA with Tukey's multiple comparison test; *P=0.02; *n.s.* non-significant.

5.10. *uba5* mutants show evidence of astrocyte dysfunction

Neuronal damage in the CNS induces a reactive response termed astrogliosis. Astrogliosis involves activation of astrocytes, resulting in astrocytes swelling and overexpressing glial fibrillary acidic protein (GFAP) (Devinsky et al., 2013). To investigate whether *uba5* mutants demonstrate astrogliosis, we examined the levels of GFAP at 6 dpf. We detected a significant (*p=0.0002*) increase in GFAP protein levels in *uba5* mutants. Notably, *uba5* mutants presented a distinct expression pattern of GFAP isoforms compared to wild type fish. A GFAP isoform with higher molecular weight (50kDa) was predominantly expressed in *uba5* mutants, while it was expressed at low levels in wild type and heterozygotes. Similarly, GFAP isoforms of lower molecular weight (30-40 kDa), predominantly expressed in the controls, were expressed at low levels in *uba5* mutant fish (Fig. 5.21).

Differential expression of GFAP isoforms has been associated with disruption of the astrocytes interfilament network and astrocytes dysfunction (Moeton et al., 2014; Moeton et al., 2016). Therefore, our data suggests that astrocytes are compromised.

Due to the evidence of potential astrocyte dysfunction, we next hypothesized that the level of glutamine synthetase (GS), which in the brain is mainly expressed in astrocytes, could be impaired. GS metabolises ammonia and glutamate, resulting in the synthesis of glutamine. Using western blot analysis, we detected a significant (*p=0.024*) increase in GS protein levels in *uba5* mutant fish compared to wild types (Fig. 5.21). This result suggests that the glutamate-glutamine cycle is possibly dysregulated.

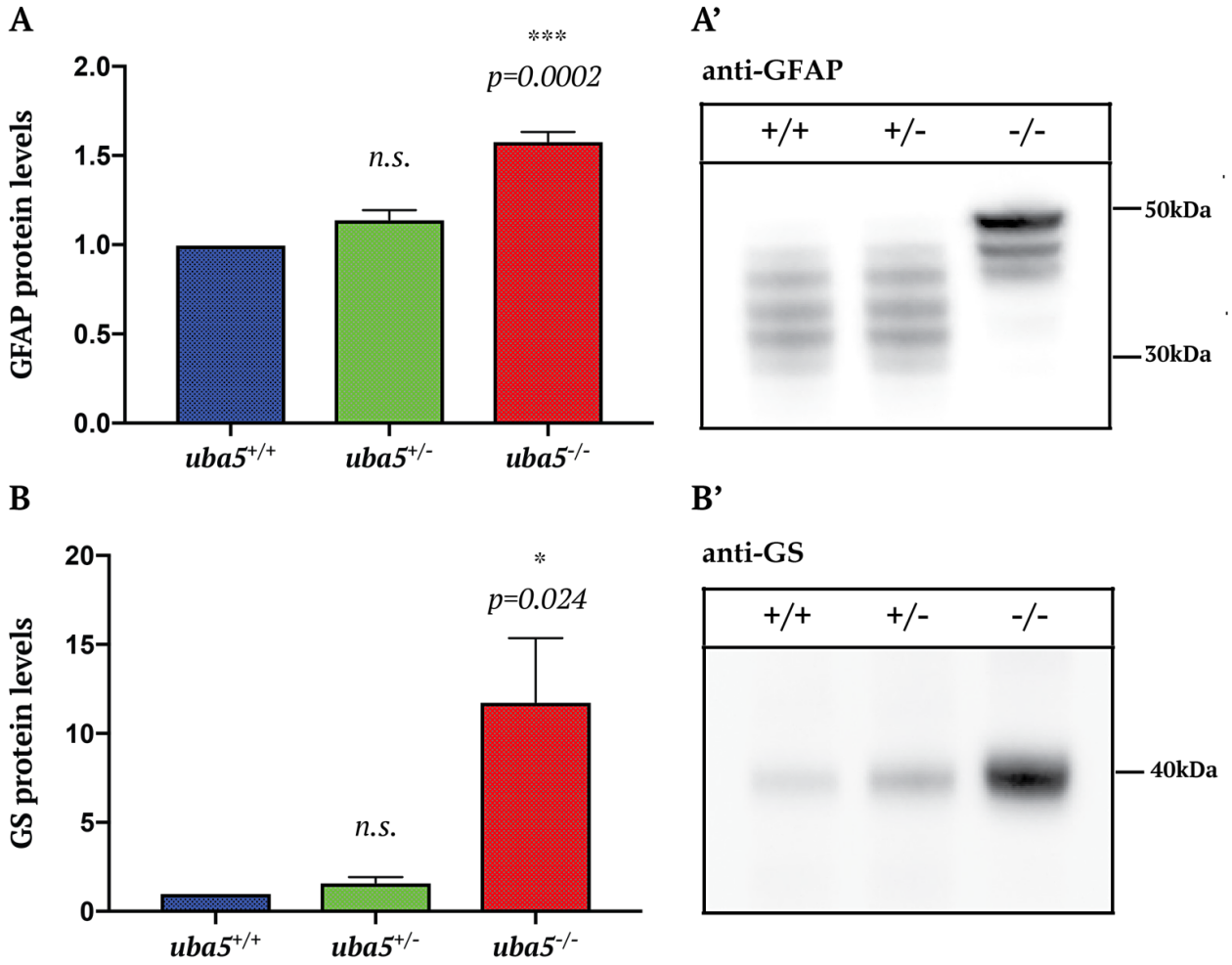

Figure 5.21. Expression of glial fibrillary acidic protein (GFAP) and glutamine synthetase (GS) based on western blot analysis in 6 dpf whole embryo tissue homogenates. (A) Representative western blots for GFAP and GS. (B) Statistical analysis of western blot results. GFAP and GS western blot analysis represent 3 biological replicates. All values were normalized to total protein, and subsequently normalized to wild type values. Data are represented as mean ± SEM. Statistical significance was assessed using one-way ANOVA with Tukey's multiple comparison test *P<0.05; ***P<0.001; *n.s.* non-significant.

5.11. Comparative profiling reveals alteration of glutamine levels in *uba5* mutants

Based on the increased levels of GS protein, we hypothesized that the glutamate levels could be increased, or glutamine levels reduced, in *uba5* mutant fish. To elucidate the consequences of *uba5* loss of function on the glutamate-glutamine cycle, the levels of glutamate and glutamine were analysed using Liquid Chromatography and Mass Spectrometry (LC-MS/MS). The concentration of each amino acid was determined by ratio-metric comparison of the peak area of the unlabelled amino acid to the labelled amino acid (e.g. Conc. (Glutamate) = Conc. (labelled-Glutamate) x Peak Area(Glutamate)/Peak Area(labelled-Glutamate), based on the concentrations of the reference standard for the corresponding counterpart. The molar amount of each amino acid was then determined using the volume of extraction solvent, and each replicate was normalized to the mass of the pellet. A 16% reduction (*p=0.003*) in glutamine levels was observed in *uba5* mutant fish compared with the control group, suggesting an elevated intracellular utilization, or deprivation, of this amino acid. In contrast, no significant difference was detected in glutamate levels in *uba5* mutants compared with the wild type group (Figure 5.22).

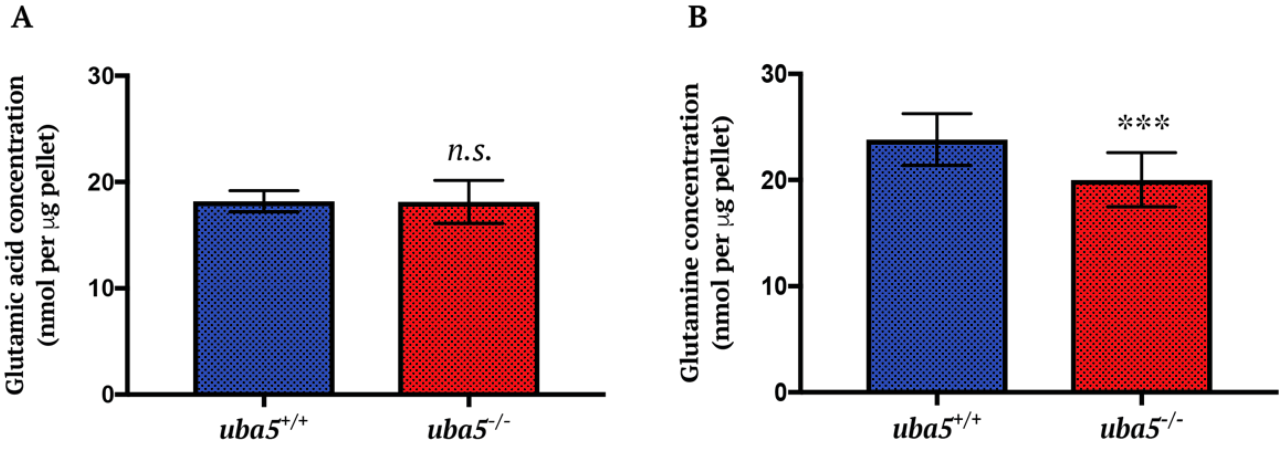

Figure 5.22. Concentration of glutamic acid and glutamine based on LC-MS/MS analysis in 6 dpf whole embryo tissue homogenates. Glutamate (A) and glutamine (B) concentration is expressed nmol per μg of pellet. Data are represented as mean ± SEM for 5 biological replicates. Statistical significance was assessed using a paired t-test. ***P<0.005; *n.s.* non-significant.

Discussion

There are multiple genes in which mutations cause early-onset epileptic encephalopathy and cerebellar ataxia. Biallelic variants in *UBA5* cause acquired microcephaly, movement disorder, developmental delay/arrest and cerebellar atrophy (Arnadottir et al., 2017; Colin et al., 2016; Daida et al., 2018; Duan et al., 2016; Low et al., 2018; Mignon-Ravix et al., 2018; Muona et al., 2016).

The role of UBA5 in the nervous system, and the molecular events resulting from UBA5 dysfunction that causes the associated clinical phenotype has not yet been fully investigated, and is relevant to understand the phenotype of the patients. The literature to date has shown that loss of *UBA5* is embryonic lethal in mice and results in impaired erythroid and megakaryocyte differentiation (Tatsumi et al., 2011). Studies in *Drosophila* have further demonstrated that Uba5 is essential for locomotor activity and homeostasis of the neuromuscular junctions (Duan et al., 2016). In addition, *uba5* knockdown in *C. elegans* has suggested that dysfunction of acetylcholine signalling may contribute to the epileptic phenotype observed in patients (Colin et al., 2016).

In this study, we show that loss of *uba5* in zebrafish results in progressive locomotor impairment associated with developmental delay, cerebellar degeneration and reduced lifespan, phenotypes characteristic of *UBA5* patients. Characterization of *uba5* mutants did not detect structural abnormalities within the muscle, motor neurons, or neuromuscular junctions, but there is evidence of cellular degradation and mitochondria degeneration in the nerves innervating the skeletal muscle at the onset of the motor impairment. Additional investigation of the phenotype revealed that there is a drastic decrease in locomotor function at later stages of development, accompanied by axonal degeneration and mitochondria death in the cerebellum, and increased number of vacuolated mitochondria in the skeletal muscle. These findings indicate that the motility defects observed in zebrafish *uba5* mutants are primarily due to defects in the nervous system, which is line with previous work on *Drosophila uba5* knockdown models that showed *uba5*–related pathology is specific to the nervous system (Duan et al., 2016). Specifically, Duan et al (2016) demonstrated that *uba5* knockdown in neurons recapitulates the locomotor deficits in flies deficient for *uba5*, while *uba5* knockdown in muscle does not cause phenotypic alterations. Importantly, our results provide the first evidence that the PNS is compromised at early stages of the motility defect, indicating that there may be an early sub-clinical phenotype in the PNS that could contribute to the overall pathology observed in *UBA5* patients. Moreover, our data suggests that mitochondrial degeneration may represent an early event associated with the onset of disease.

Epileptic encephalopathy and cerebellar ataxia are disorders predominantly associated with the CNS. However, signs of PNS impairment have been previously reported in CNS disorders, constituting sub-clinical or major components of the phenotype. In particular, sensory and motor

peripheral neuropathies were reported in cases of epileptic encephalopathy and cerebellar ataxia (Kobayashi et al., 2011; Ohtahara and Neurophysiology, 2003; Storey, 2014). Although dysfunction of the PNS in *UBA5* patients has not been fully investigated, there is evidence of impairment of the PNS associated with mutations in *UBA5*. Duan et al (2016) reported the case of a patient with biallelic variants in *UBA5* showing partial peripheral nerve impairment with a demyelinating sensory-motor peripheral neuropathy. Assessing the involvement of the PNS in the patients could, therefore, help expand the clinical spectrum of the disease and contribute to our understanding of the function of UBA5 in the nervous system and disease.

While it is currently unknown how Uba5 loss of function causes a severe neurological phenotype and mitochondrial degeneration in both the PNS and CNS in zebrafish, it is interesting to note that mitochondrial morphological changes and mitochondrial dysfunction have been implicated in motor disorders. For example, reduced mitochondrial respiratory chain complex I activity (Keeney et al., 2006; Mortiboys et al., 2008), increased mitochondrial branching (Mortiboys et al., 2008), and swollen mitochondria (Moore et al., 2005) were associated with Parkinson's disease, whereas impaired mitochondrial trafficking (Chang et al., 2006) and fragmented mitochondria (Zheng and Diamond, 2012) were associated with Huntington's disease. Moreover, degeneration of mitochondria in motor neurons has been reported to occur at the onset of motor dysfunction in ALS (Xu et al., 2004). Considering that alterations in mitochondria occur in *uba5* mutant fish at an early stage of motor dysfunction, and mitochondria are the major source of ATP through oxidative phosphorylation, dysregulation of mitochondrial function may contribute to motor deficiency. In addition, as ATP and regulation of calcium intracellular levels is required for neuronal excitability and survival, mitochondrial malfunction has also been implicated in epilepsy (Khurana et al., 2013).

While epilepsy is a common clinical finding observed in *UBA5* patients (Arnadottir et al., 2017; Colin et al., 2016; Daida et al., 2018; Duan et al., 2016; Low et al., 2018; Mignon-Ravix et al., 2018; Muona et al., 2016), whether *uba5* mutant fish exhibit seizure-like behaviour remains to be answered. This could be addressed in future experiments through stimulation of seizures with epileptic drugs, such as pentylenetetrazol (PTZ), and assessment of whether *uba5* mutant fish have a lower threshold of seizure-induction compared to wild type fish, a method previously used to evaluate epileptic behaviour in zebrafish (Gupta et al., 2014; Mei et al., 2013).

Our work provides the first evidence that the glutamate-glutamine cycle is likely impaired at the onset of the motor dysfunction. We detected reduced concentration of glutamine, and increased glutamine synthetase levels, in *uba5* mutant fish that were not observed in wild type controls. Glutamine synthetase is the key enzyme in the conversion of glutamate and ammonia into glutamine, known as the glutamate-glutamine cycle (Hertz, 2013). The glutamate-glutamine cycle is required to avoid accumulation of ammonia that can disturb the brain metabolism, and excessive

stimulation of neurons via glutamate (Albrecht et al., 2010; Hertz, 2013). Since glutamate is the precursor for the synthesis of GABA, the glutamate-glutamine cycle is additionally needed to maintain the balance between excitatory (glutamate-dependent) and inhibitory (GABA-dependent) synaptic transmission (Albrecht et al., 2010; Hertz, 2013).

As our experiments were performed on whole larvae, we cannot exclusively associate the reduced glutamine levels with the nervous system. To evaluate the levels of glutamate and glutamine solely in the brain, metabolomics analysis should be conducted on isolated heads. However, due to the small size of the fish at 6 days (at the onset of motor dysfunction), hindered growth of *uba5* mutant fish at later stages of development, and large number of embryos required for metabolic analysis this was not feasible. Glutamine synthetase is ubiquitously expressed, so it is possible that reduction of glutamine concentration affects other systems. However, even if reduced glutamine levels are causing global metabolic deficiencies, it will likely affect predominantly the brain, as the brain does not possess an alternative mechanism for ammonia removal. It is known, for example, that deletion of glutamine synthetase in the mouse liver, which impairs the synthesis of glutamine, results in hyperammonia, and oxidative stress in the brain, leading to motor deficits (Qvartskhava et al., 2015). Furthermore, mutations in the gene encoding glutamine synthetase (*GLUL*) were identified in patients with neonatal onset severe epileptic encephalopathy, associated with low glutamine levels, brain malformation, white matter lesions, developmental delay, drug-resistant seizures, and infant death (Häberle et al., 2005; Häberle et al., 2006; Spodenkiewicz et al., 2016). These findings indicate that overall dysregulation of glutamine levels compromises the nervous system, and results in a phenotype highly reminiscent of the phenotype observed in *UBA5* patients.

We hypothesize that dietary supplementation of glutamine is a promising strategy to treat *UBA5* patients. Glutamine supplementation is currently approved by the US Food and Drug Administration board for clinical use. It is widely used for treating sickle cell anaemia and short bowel syndrome, and several clinical trials have pointed out that causes no adverse effects (Jiang et al., 1993; Lacey et al., 1996; Mercier, 2003; Ziegler et al., 2016). Glutamine supplementation was previously tested in a GS-deficient patient with severe neurological abnormalities, and shown to increase glutamine concentration in the brain, while improving the patient's alertness and electroencephalographic activity (Häberle et al., 2012). Additionally, the patient showed no exacerbation of glutamate or ammonia levels, suggesting that glutamine supplementation is a safe therapeutic approach in epileptic encephalopathy due to glutamine deficiency (Häberle et al., 2012). Future studies could therefore evaluate the impact of glutamine supplementation on survival, locomotor activity and growth in *uba5* mutant fish.

Chapter 6. Final discussion

Epileptic encephalopathy and cerebellar ataxia are two debilitating nervous system disorders. There are currently no effective therapies for these disorders, therefore determining new pathways or targets for therapy is important. As epileptic encephalopathies and cerebellar ataxias are caused by mutations in different genes, it may not be feasible to develop a single therapy that will improve or impede the progression of symptoms observed in all subtypes. However, it is essential to understand the role of the genes associated with the disorders. By understanding the molecular pathways regulated by each gene and the consequences of its dysfunction, we can provide clinicians, patients, and families with a better comprehension of the biology of the disease, and identify targetable pathways for potential therapies for these debilitating disorders.

This study focused on investigating the consequences of *plxnb3* and *tmem33* loss of function, two candidate genes for cerebellar ataxia, and *uba5* loss of function, known to cause both epileptic encephalopathy and cerebellar ataxia. *Plxnb3* was excluded as a candidate gene for cerebellar ataxia. In addition, my evidence didn't support variants in *tmem33* as causal of cerebellar ataxia. On the other hand, I have demonstrated that *uba5* mutant fish recapitulate most of the symptoms observed in *UBA5* patients, including motor dysfunction, delayed growth, cerebellar neuronal degeneration, and early death. These fish provide a new tool for characterizing the function of UBA5 in the neuromuscular system and determining the role of UBA5 and the UFM1 pathway in causing nervous system disorders. Notably, I discovered that degenerating or abnormal mitochondria are present in the nervous system, astrocytes are compromised, and glutamine levels are reduced, in *uba5* mutant fish at early stages of the motor dysfunction and before the onset of delayed growth (Fig. 6.1).

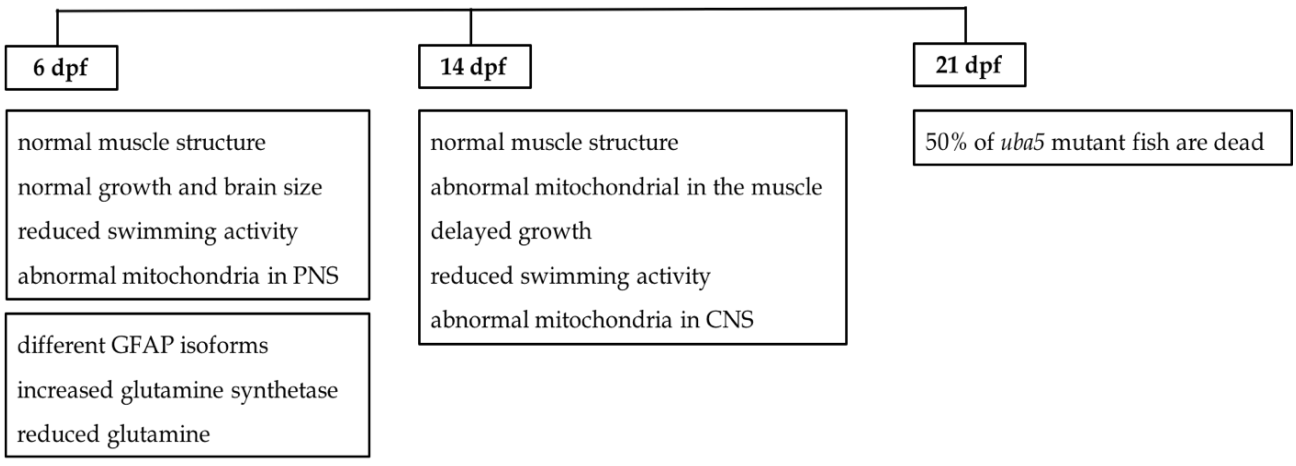

Figure 6.1. Progression of *uba5* mutant fish phenotype. The peripheral nerves are affected at the onset of motor dysfunction, but no signs of growth impairment are observed. The severity of the phenotype

rapidly progresses, accompanied with mitochondrial abnormalities in both skeletal muscle and brain, and the majority of *uba5* mutant fish die within 21 dpf.

What is the role of glutamine?

Glutamine is involved in the formation of important metabolites (Fig. 6.2). It is involved in the biosynthesis of nucleotides by transferring its amide group as nitrogen source. Deamination of glutamine is further required for production of glutamate via glutaminase (GLS). The resulting glutamate, derived from glutamine, is used for synthesis of glutathione, an antioxidant that protects the cells against damage induced by reactive oxygen species (ROS), or is converted in α-ketoglutarate, contributing to the mitochondrial tricarboxylic acid (TCA) cycle. The mitochondrial TCA cycle generates metabolic products that are essential for generation of ATP, and amino acids, fatty acids and cholesterol biosynthesis (Cruzat et al., 2018; Soeters and Grecu, 2012). Glutamine is thus a fundamental metabolite, and changes in its concentration may result in detrimental effects, including lower ATP ratio and mitochondrial dysfunction (Ahmad et al., 2001). This can possibly explain the mitochondrial abnormalities observed in *uba5* mutant fish.

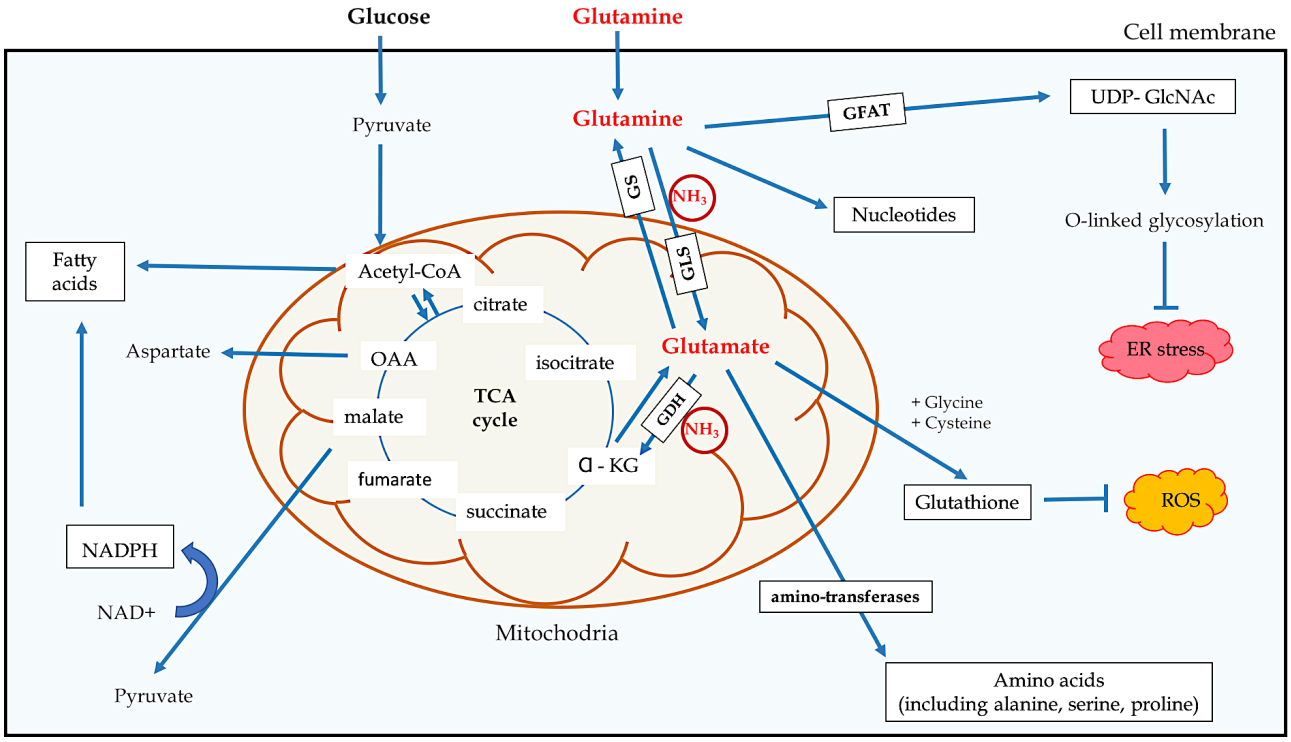

Figure 6.2. Synthesis and metabolism of glutamine. (A) Several enzymes are involved in glutamine homeostasis, but two enzymes play crucial roles: glutamine synthetase (GS) and glutaminase (GLS). GLS catalyses the deamination of glutamine into glutamate and ammonium, and GS converts glutamate and ammonium in glutamine. Abbreviations: α-KG – α-ketoglutarate; GFAT – glutamine: fructose-6-phosphate amidotransferase; UDP – GlcNAc – uridine diphosphate-N-acetylglucosamine.

Previous work has also demonstrated that glutamine is essential to mediate mTORC1 signalling, which is known to regulate cell growth, protein translation and autophagy (Bernfeld et al., 2018; Nicklin et al., 2009; Zhu et al., 2014). Glutamine has been shown to activate mTORC1 signalling and inhibit autophagy, whereas glutamine depletion results in inactivation of mTORC1 signalling and increased autophagy (Bernfeld et al., 2018; Nicklin et al., 2009; Zhu et al., 2014). Particularly, Zhu et al. (2014) demonstrated that glutamine deficiency results in reduced cell growth, accumulation of autophagosomes, and disruption of overall amino acid metabolism, while glutamine availability induces mTORC1 signalling, leading to increased cell growth and reduced number of autophagosomes. Glutamine deficiency is therefore likely to result in delayed cell growth and cell death, possibly explaining the growth impairment and neurodegeneration in *UBA5* patients.

The functionality of the nervous system is greatly supported by synthesis and breakdown of glutamine. The glutamine intracellular pool is maintained by *de novo* synthesis due to the activity of glutamine synthetase (GS). In the brain, glutamine synthetase is mainly expressed in astrocytes and its activity is essential to prevent the intracellular accumulation of ammonia and balance the extracellular concentration of glutamate, which can result in neurotoxicity (Albrecht et al., 2010b; Brusilow et al., 2010; Dąbrowska et al., 2017; He et al., 2010). Specifically, astrocytes are required to remove glutamate from the synaptic cleft, preventing the excessive activation of neurons, and convert glutamate and ammonium in glutamine using glutamine synthetase. Glutamine is then transported back to neurons and used to generate glutamate, which serves as a precursor for the production of GABA. In this way, glutamine is involved in the regulation of excitatory and inhibitory signal neurotransmission (Albrecht et al., 2010a; Hertz, 2013; Newsholme et al., 2003).

Previous studies have suggested that glutamine has, in fact, a neuroprotective role. Chen and Herrup (2012) demonstrated that glutamine supplementation results in reduced levels of phosphorylated tau and increased density of synaptic proteins, such as SNARE and synaptophysin, in mouse models of Alzheimer's disease (Chen and Herrup, 2012). Moreover, glutamine supplementation has been shown to significantly improve the synaptic activity of a mouse model of ataxia-telangiectasia (Chen et al., 2016). Given the increase in glutamine synthetase levels and decrease of glutamine concentration (Fig. 6.3), and the increase in GFAP protein levels, it is likely that astrocytes are compromised in *uba5* mutant fish. Astrocyte dysfunction may likely impair synaptic activity, and explain the epileptic behaviour and motor dysfunction in *UBA5* patients.

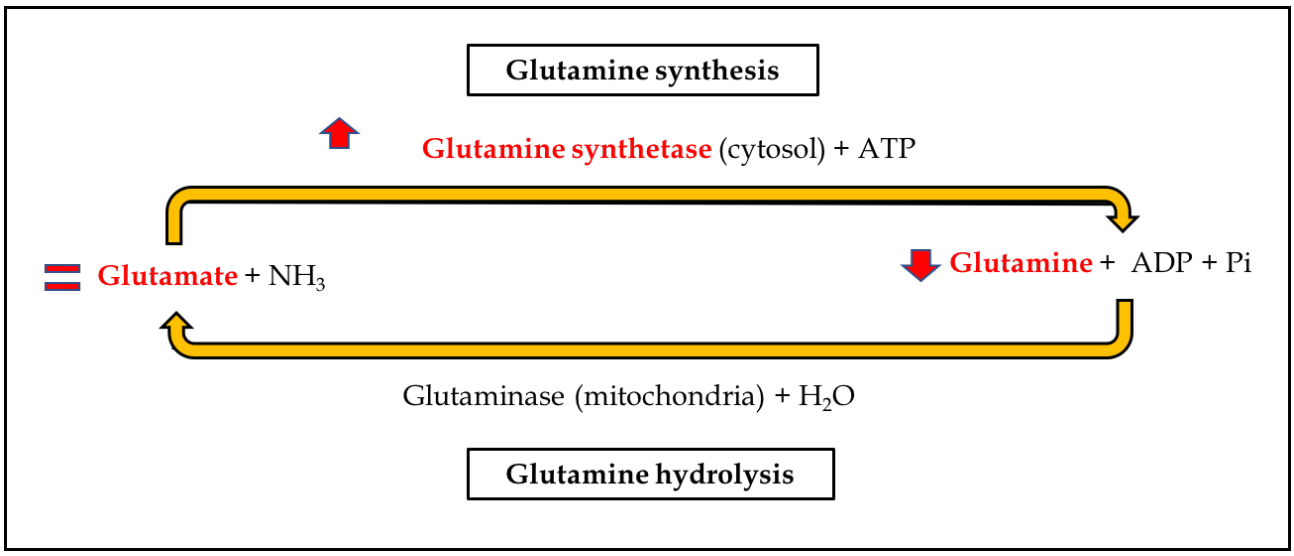

Figure 6.3. Glutamate-glutamine cycle. In our study, we detected increased levels of glutamine synthetase, accompanied with decreased glutamine and normal glutamate concentrations (in red).

How does *UBA5* dysfunction leads to glutamine depletion?

UBA5 is the activating-enzyme of the UFM1 pathway, so the next question is how UBA5 and ufmylation are involved in the maintenance of glutamine levels. Since UFM1 is a ubiquitin-like protein (Daniel and Liebau, 2014), ufmylation may be required for the correct localization, degradation, or function, of a target protein involved in the synthesis or metabolism of glutamine. The decrease in glutamine levels could in turn result from a decreased rate of glutamine synthesis, or an increased rate of glutamine consumption by de-repressing the activity of enzymes that use glutamine as substrate.

One possible scenario is that ufmylation could directly mediate the activity of glutamine synthetase (GS), and consequently regulating the synthesis of glutamine. Deficient glutamine synthetase has been previously shown to cause a severe early-onset epileptic encephalopathy, associated with seizures, psychomotor retardation, mild to moderate brain atrophy, and hypomyelination or hyperintensities in the brain (Häberle et al., 2005; Häberle et al., 2012). The striking similarity between the phenotypes of *GS*-deficient and *UBA5* patients suggests that glutamine synthetase and UBA5 may at least be partially involved in the same pathway. Similar to *uba5* mutant fish, GS mutant patients exhibit a decrease in glutamine concentration, an increase in glutamine synthetase levels, and glutamate concentration within normal range (Häberle et al., 2005; Häberle et al., 2012). The increased level of glutamine synthetase observed in GS mutant patients is hypothesized to be a compensatory mechanism associated with the loss of glutamine synthetase activity (Häberle et al., 2005). In agreement, other studies have demonstrated that the activity of glutamine synthetase is

regulated via an inhibitory feedback mechanism that responds to intracellular glutamine concentration (Chen and Herrup, 2012; Feng et al., 1990; Hu et al., 2015; Huang et al., 2007). Upregulation of GS may therefore occur in *uba5* mutant fish due to reduced glutamine concentration. However, upregulation of GS is unable to compensate for the glutamine decrease.

Alternatively, ufmylation could be required to modulate the function of a regulatory protein that controls the activity of glutamine synthetase. Recently, Huyghe et al. (2019) revealed that phosphorylation of glutamine synthetase by cAMP-dependent protein kinase (PKA) regulates the enzyme's activity, resulting in decreased glutamine synthesis. Based on the STRING database (Szklarczyk et al., 2019), one of the UBA5-interacting partners is Praja2, a protein that functions as an E3-ligase and targets other proteins for proteasomal degradation (Yu et al., 2002). Particularly, Praja2 has been reported to co-localize with PKA and mediate its stability by promoting the degradation of PKA regulatory subunits. Praja2 is therefore required to control the rate and duration of PKA signalling (Lignitto et al., 2011). Dysfunction of the UFM1 pathway could lead to deficient Praja2 activity, resulting in excessive phosphorylation of glutamine synthetase and impaired glutamine production.

A second scenario is that ufmylation could be required to mediate the activity of a regulatory protein in the downstream pathway of glutamine metabolism. As an example, it is possible that dysfunction of the Ufm1 pathway could lead to over-activation of a regulatory protein (e.g. 56K1) of the mTORC1 pathway, known to stimulate glutamine metabolism via glutamate dehydrogenase (Csibi et al., 2013). In this scenario, glutamine metabolism could occur at a higher rate and the concentration of glutamine would decrease, but the concentration of glutamate would likely decrease at the same rate. Given the increase in glutamine synthetase levels and no change in glutamate concentration detected in *uba5* mutant fish (Fig. 6.2 B), this scenario is unlikely as more glutamine would be expected to be made from glutamate. The scenario in which the synthesis of glutamine is impeded is consequently more plausible.

The reason behind the normal concentration of glutamate in *uba5* mutant fish remains to be answered, but I speculate that glutamate is not significantly altered because glutamine is not the only source of glutamate (Mckena et al., 2007; Shokati et al., 2005; Waagepetersen et al., 2005). There are data reporting that glucose can produce glutamate, depending on glutamine availability (Son et al., 2013; Cheng et al., 2011; Shokati et al., 2005). Glucose can contribute to the synthesis of glutamate via pyruvate carboxylase and production of α-ketoglutarate (Son et al., 2013; Cheng et al., 2011; Shokati et al., 2005). Glucose may therefore act as a complementary pathway that maintain the concentration of glutamate in *uba5* mutant fish.

Further studies could determine the targets of ufmylation that are critical for glutamine synthesis,

and the phosphorylation level of glutamine synthetase in *uba5* mutant fish. These additional studies will increase our knowledge about the pathophysiologic mechanism of the disease, and how *uba5* loss of function results in decreased glutamine concentration.

Glutamine deficiency causes accumulation of ammonia?

It is interesting to note that glutamine deficiency due to impaired glutamine synthetase activity has been associated with chronic hyperammonia (Häberle et al., 2005; Häberle et al., 2006; He et al., 2010; Rangroo Thrane et al., 2013). Hyperammonia results from insufficient incorporation of ammonium into glutamine, leading to accumulation of intracellular ammonia. In turn, hyperammonia has been implicated in the development of seizures (Cagnon and Braissant, 2007; Rangroo Thrane et al., 2013), oxidative stress (Cagnon and Braissant, 2007), cognitive impairment (Aguilar et al., 2000; Qvartskhava et al., 2015), and astrocytes dysfunction (Rangroo Thrane et al., 2013). Increased intracellular ammonia may consequently also contribute to the phenotype in *UBA5* patients.

Concluding remarks

My work identified mitochondrial abnormalities, astrocytes dysfunction, and depletion of glutamine concentration as hallmarks associated with *uba5* loss of function. These findings may provide a basis for identification of therapeutic targets for treatment of epileptic encephalopathy and cerebellar ataxia associated with *UBA5* mutation. Furthermore, the detection of glutamine depletion, identifies that UBA5 dysfunction leads to metabolic alterations. This might help the future recognition of undiagnosed patients with a similar clinical phenotype.

References

Aguilar, M.A., Minarro, J., and Felipo, V. (2000). Chronic moderate hyperammonemia impairs active and passive avoidance behavior and conditional discrimination learning in rats. Experimental neurology *161*, 704-713.

Ahmad, S., White, C.W., Chang, L.Y., Schneider, B.K., and Allen, C.B. (2001). Glutamine protects mitochondrial structure and function in oxygen toxicity. American journal of physiology Lung cellular and molecular physiology *280*, L779-791.

Akizu, N., Cantagrel, V., Zaki, M.S., Al-Gazali, L., Wang, X., Rosti, R.O., Dikoglu, E., Gelot, A.B., Rosti, B., Vaux, K.K., *et al.* (2015). Biallelic mutations in SNX14 cause a syndromic form of cerebellar atrophy and lysosome-autophagosome dysfunction. Nat Genet *47*, 528-534

Albrecht, J., Sidoryk-Węgrzynowicz, M., Zielińska, M., and Aschner, M. (2010a). Roles of glutamine in neurotransmission. Neuron Glia Biology *6*, 263-276.

Albrecht, J., Zielińska, M., and Norenberg, M.D. (2010b). Glutamine As A Mediator Of Ammonia Neurotoxicity: A Critical Appraisal. Biochemical Pharmacology *80*, 1303-1308.

Allen, N.M., Mannion, M., Conroy, J., Lynch, S.A., Shahwan, A., Lynch, B., and King, M.D. (2014). The variable phenotypes of KCNQ-related epilepsy. Epilepsia *55*, e99-105.

Alsbeih, G. (2011). MRE11A Gene Mutations Responsible for the Rare Ataxia Telangiectasia-Like Disorder, Human Genetic Diseases, Dr. Dijana Plaseska-Karanfilska (Ed.), ISBN: 978-953-307-936-3, InTech.

Al Tassan, N., Khalil, D., Shinwari, J., Al Sharif, L., Bavi, P., Abduljaleel, Z., Abu Dhaim, N., Magrashi, A., Bobis, S., Ahmed, H., *et al.* (2012). A missense mutation in PIK3R5 gene in a family with ataxia and oculomotor apraxia. Hum Mutat *33*, 351-354.

Alto, L.T., and Terman, J.R. (2017). Semaphorins and their Signaling Mechanisms. Methods in molecular biology (Clifton, NJ) *1493*, 1-25.

André, V.M., Cepeda, C., and Levine, M.S. (2010). Dopamine and Glutamate in Huntington Disease: A Balancing Act. CNS Neuroscience & Therapeutics *16*, 163-178.

Anheim, M., Tranchant, C., and Koenig, M. (2012). The Autosomal Recessive Cerebellar Ataxias. New England Journal of Medicine *366*, 636-646.

Arnadottir, G.A., Jensson, B.O., Marelsson, S.E., Sulem, G., Oddsson, A., Kristjansson, R.P., Benonisdottir, S., Gudjonsson, S.A., Masson, G., Thorisson, G.A., *et al.* (2017). Compound heterozygous mutations in UBA5 causing early-onset epileptic encephalopathy in two sisters. Bmc Medical Genetics *18*.

Artigiani, S., Conrotto, P., Fazzari, P., Gilestro, G.F., Barberis, D., Giordano, S., Comoglio, P.M., and Tamagnone, L. (2004). Plexin-B3 is a functional receptor for semaphorin 5A. EMBO reports *5*, 710-714.

Arzimanoglou, A., French, J., Blume, W.T., Cross, J.H., Ernst, J.P., Feucht, M., Genton, P., Guerrini, R., Kluger, G., Pellock, J.M., *et al.* (2009). Lennox-Gastaut syndrome: a consensus approach on diagnosis, assessment, management, and trial methodology. The Lancet Neurology *8*, 82-93.

Aspatwar, A., Tolvanen, M.E., Jokitalo, E., Parikka, M., Ortutay, C., Harjula, S.K., Ramet, M., Vihinen, M., and Parkkila, S. (2013). Abnormal cerebellar development and ataxia in CARP VIII morphant zebrafish. Hum Mol Genet *22*, 417-432.

Auluck, P.K., Chan, H.Y.E., Trojanowski, J.Q., Lee, V.M.-Y., and Bonini, N.M. (2002). Chaperone Suppression of α-Synuclein Toxicity in a Drosophila Model for Parkinson's Disease. Science *295*, 865-868.

Auvin, S., Cilio, M.R., and Vezzani, A. (2016). Current understanding and neurobiology of epileptic encephalopathies. Neurobiol Dis *92*, 72-89.

Azfer, A., Niu, J., Rogers, L.M., Adamski, F.M., and Kolattukudy, P.E. (2006). Activation of endoplasmic reticulum stress response during the development of ischemic heart disease. American journal of physiology Heart and circulatory physiology *291*, H1411-1420.

Bae, Y.-K., Kani, S., Shimizu, T., Tanabe, K., Nojima, H., Kimura, Y., Higashijima, S.-i., and Hibi, M. (2009). Anatomy of zebrafish cerebellum and screen for mutations affecting its development. Developmental Biology *330*, 406-426.

Baraban, S.C., Dinday, M.T., and Hortopan, G.A. (2013). Drug screening in Scn1a zebrafish mutant identifies clemizole as a potential Dravet syndrome treatment. Nat Commun *4*, 2410.

Barnea-Goraly, N., Lotspeich, L.J., and Reiss, A.L. (2010). Similar white matter aberrations in children with autism and their unaffected siblings: a diffusion tensor imaging study using tract-based spatial statistics. Archives of general psychiatry *67*, 1052-1060.

Beal, J.C., Cherian, K., and Moshe, S.L. (2012). Early-Onset Epileptic Encephalopathies: Ohtahara Syndrome and Early Myoclonic Encephalopathy. Pediatric Neurology *47*, 317-323.

Ben-Zvi, A., Manor, O., Schachner, M., Yaron, A., Tessier-Lavigne, M., and Behar, O. (2008). The Semaphorin Receptor PlexinA3 Mediates Neuronal Apoptosis during Dorsal Root Ganglia Development. Journal of Neuroscience *28*, 12427-12432.

Berg, A.T., Berkovic, S.F., Brodie, M.J., Buchhalter, J., Cross, J.H., Boas, W.v.E., Engel, J., French, J., Glauser, T.A., Mathern, G.W., *et al.* (2010). Revised terminology and concepts for organization of

seizures and epilepsies: Report of the ILAE Commission on Classification and Terminology, 2005-2009. Epilepsia *51*, 676-685.

Bernfeld, E., Menon, D., Vaghela, V., Zerin, I., Faruque, P., Frias, M.A., and Foster, D.A. (2018). Phospholipase D-Dependent mTORC1 Activation by Glutamine. Journal of Biological Chemistry.

Boglev, Y., Badrock, A.P., Trotter, A.J., Du, Q., Richardson, E.J., Parslow, A.C., Markmiller, S.J., Hall, N.E., de Jong-Curtain, T.A., Ng, A.Y., *et al.* (2013). Autophagy induction is a Tor- and Tp53-independent cell survival response in a zebrafish model of disrupted ribosome biogenesis. PLoS genetics *9*, e1003279.

Brusilow, S.W., Koehler, R.C., Traystman, R.J., and Cooper, A.J.L. (2010). Astrocyte Glutamine Synthetase: Importance in Hyperammonemic Syndromes and Potential Target for Therapy. Neurotherapeutics *7*, 452-470.

Burnashev, N., and Szepetowski, P. (2015). NMDA receptor subunit mutations in neurodevelopmental disorders. Curr Opin Pharmacol. *20, 73-82*.

Burns, R., Majczenko, K., Xu, J., Peng, W., Yapici, Z., Dowling, J.J., Li, J.Z., and Burmeister, M. (2014). Homozygous splice mutation in CWF19L1 in a Turkish family with recessive ataxia syndrome. Neurology *83*, 2175-2182.

Burridge, K., and Wennerberg, K. (2004). Rho and Rac take center stage. Cell *116*, 167-179.

Buzatu, M., Bulteau, C., Altuzarra, C., Dulac, O., and Van Bogaert, P. (2009). Corticosteroids as treatment of epileptic syndromes with continuous spike-waves during slow-wave sleep. Epilepsia *50 Suppl 7*, 68-72.

Cabral-Miranda, F., and Hetz, C. (2018). ER Stress and Neurodegenerative Disease: A Cause or Effect Relationship? Current topics in microbiology and immunology *414*, 131-157.

Cai, Y., Pi, W., Sivaprakasam, S., Zhu, X., Zhang, M., Chen, J., Makala, L., Lu, C., Wu, J., Teng, Y., *et al.* (2015). UFBP1, a Key Component of the Ufm1 Conjugation System, Is Essential for Ufmylation-Mediated Regulation of Erythroid Development. PLoS genetics *11*, e1005643.

Cagnon, L., and Braissant, O. (2007). Hyperammonemia-induced toxicity for the developing central nervous system. Brain Res Rev *56*, 183-197.

Cappadocia, L., and Lima, C.D. (2018). Ubiquitin-like Protein Conjugation: Structures, Chemistry, and Mechanism. Chemical reviews *118*, 889-918.

Cariboni, A., Davidson, K., Rakic, S., Maggi, R., Parnavelas, J.G., and Ruhrberg, C. (2011). Defective gonadotropin-releasing hormone neuron migration in mice lacking SEMA3A signalling through

NRP1 and NRP2: implications for the aetiology of hypogonadotropic hypogonadism. Hum Mol Genet *20*, 336-344.

Carlson, K.M., Andresen, J.M., and Orr, H.T. (2009). Emerging pathogenic pathways in the spinocerebellar ataxias. Curr Opin Genet Dev *19*, 247-253.

Carson, J.A., and Turner, A.J. (2002). β-Amyloid catabolism: roles for neprilysin (NEP) and other metallopeptidases? Journal of Neurochemistry *81*, 1-8.

Chang, D.T.W., Rintoul, G.L., Pandipati, S., and Reynolds, I.J. (2006). Mutant huntingtin aggregates impair mitochondrial movement and trafficking in cortical neurons. Neurobiology of disease *22*, 388-400.

Chapman, D.C., Stocki, P., and Williams, D.B. (2015). Cyclophilin C Participates in the US2-Mediated Degradation of Major Histocompatibility Complex Class I Molecules. PloS one *10*, e0145458.

Chen, J., Chen, Y., Vail, G., Chow, H., Zhang, Y., Louie, L., Li, J., Hart, R.P., Plummer, M.R., and Herrup, K. (2016). The impact of glutamine supplementation on the symptoms of ataxia-telangiectasia: a preclinical assessment. Mol Neurodegener *11*, 60-60.

Chen, J., and Herrup, K. (2012). Glutamine acts as a neuroprotectant against DNA damage, beta-amyloid and H2O2-induced stress. PloS one *7*, e33177-e33177.

Chen, Y., and Tang, B.L. (2010). Unique Intracellular Trafficking Processes Associated With Neural Cell Adhesion Molecule and Its Intracellular Signaling. Cell Communication and Adhesion *17*, 69-74.

Christodoulou, A., Santarella-Mellwig, R., Santama, N., and Mattaj, I.W. (2016). Transmembrane protein TMEM170A is a newly discovered regulator of ER and nuclear envelope morphogenesis in human cells. Journal of Cell Science *129*, 1552-1565.

Colin, E., Daniel, J., Ziegler, A., Wakim, J., Scrivo, A., Haack, T.B., Khiati, S., Denomme, A.-S., Amati-Bonneau, P., Charif, M.*, et al.* (2016). Biallelic Variants in UBAS Reveal that Disruption of the UFM1 Cascade Can Result in Early-Onset Encephalopathy. The American Journal of Human Genetics *99*, 695-703.

Coppola, G. (2013). Malignant migrating partial seizures in infancy. Handbook of clinical neurology *111*, 605-609.

Cruchaga, C., Graff, C., Chiang, H.H., Wang, J., Hinrichs, A.L., Spiegel, N., Bertelsen, S., Mayo, K., Norton, J.B., Morris, J.C., *et al.* (2011). Association of TMEM106B gene polymorphism with age at onset in granulin mutation carriers and plasma granulin protein levels. Arch Neurol *68*, 581-586.

Cruzat, V., Macedo Rogero, M., Noel Keane, K., Curi, R., and Newsholme, P. (2018). Glutamine: Metabolism and Immune Function, Supplementation and Clinical Translation. Nutrients *10*, E1564.

Csibi, A., Fendt, S.-M., Li, C., Poulogiannis, G., Choo, A.Y., Chapski, D.J., Jeong, S.M., Dempsey, J.M., Parkhitko, A., Morrison, T., *et al.* (2013). The mTORC1 Pathway Stimulates Glutamine Metabolism and Cell Proliferation by Repressing SIRT4. Cell *153*, 840-854.

Dąbrowska, K., Skowrońska, K., Popek, M., Obara-Michlewska, M., Albrecht, J., and Zielińska, M. (2017). Roles of Glutamate and Glutamine Transport in Ammonia Neurotoxicity: State of the Art and Question Marks. Endocr Metab Immune Disord Drug Targets *18, 306-315.*

D'Alonzo, R., Rigante, D., Mencaroni, E., and Esposito, S. (2018). West Syndrome: A Review and Guide for Paediatricians. Clinical drug investigation *38*, 113-124.

D'Adamo, M.C., Hasan, S., Guglielmi, L., Servettini, I., Cenciarini, M., Catacuzzeno, L., and Franciolini, F. (2015). New insights into the pathogenesis and therapeutics of episodic ataxia type 1. Frontiers in Cellular Neuroscience *9*, 317.

Daida, A., Hamano, S.-i., Ikemoto, S., Matsuura, R., Nakashima, M., Matsumoto, N., and Kato, M. (2018). Biallelic loss-of-function UBA5 mutations in a patient with intractable West syndrome and profound failure to thrive. Epileptic Disorders *20*, 313-318.

Daniel, J., and Liebau, E. (2014). The Ufm1 Cascade. Cells *3*, 627-638.

Danysz, W., and Parsons, C.G. (2012). Alzheimer's disease, β-amyloid, glutamate, NMDA receptors and memantine – searching for the connections. British Journal of Pharmacology *167*, 324-352.

Dawson, T.M., and Dawson, V.L. (2010). The role of parkin in familial and sporadic Parkinson's disease. Movement disorders : official journal of the Movement Disorder Society *25 Suppl 1*, S32-39.

Delloye-Bourgeois, C., Jacquier, A., Charoy, C., Reynaud, F., Nawabi, H., Thoinet, K., Kindbeiter, K., Yoshida, Y., Zagar, Y., Kong, Y., *et al.* (2015). PlexinA1 is a new Slit receptor and mediates axon guidance function of Slit C-terminal fragments. Nature Neuroscience *18*, 36-45.

Delplanque, J., Devos, D., Huin, V., Genet, A., Sand, O., Moreau, C., Goizet, C., Charles, P., Anheim, M., Monin, M.L., *et al.* (2014). TMEM240 mutations cause spinocerebellar ataxia 21 with mental retardation and severe cognitive impairment. Brain *137*, 2657-2663.

Deng, S., Hirschberg, A., Worzfeld, T., Penachioni, J.Y., Korostylev, A., Swiercz, J.M., Vodrazka, P., Mauti, O., Stoeckli, E.T., Tamagnone, L., *et al.* (2007). Plexin-B2, But Not Plexin-B1, Critically Modulates Neuronal Migration and Patterning of the Developing Nervous System In Vivo. Journal of Neuroscience *27*, 6333-6347.

Deng, H.X., Shi, Y., Yang, Y., Ahmeti, K.B., Miller, N., Huang, C., Cheng, L., Zhai, H., Deng, S., Nuytemans, K., *et al.* (2016). Identification of TMEM230 mutations in familial Parkinson's disease. Nat Genet *48*, 733-739.

Depienne, C., Bouteiller, D., Keren, B., Cheuret, E., Poirier, K., Trouillard, O., Benyahia, B., Quelin, C., Carpentier, W., Julia, S., *et al.* (2009a). Sporadic infantile epileptic encephalopathy caused by mutations in PCDH19 resembles Dravet syndrome but mainly affects females. PLoS Genet *5*, e1000381.

Depienne, C., Trouillard, O., Saint-Martin, C., Gourfinkel-An, I., Bouteiller, D., Carpentier, W., Keren, B., Abert, B., Gautier, A., Baulac, S., *et al.* (2009b). Spectrum of SCN1A gene mutations associated with Dravet syndrome: analysis of 333 patients. J Med Genet *46*, 183-191.

Devinsky, O., Vezzani, A., Najjar, S., De Lanerolle, N.C., and Rogawski, M.A. (2013). Glia and epilepsy: excitability and inflammation. Trends in Neurosciences *36*, 174-184.

Dhindsa, R.S., Bradrick, S.S., Yao, X., Heinzen, E.L., Petrovski, S., Krueger, B.J., Johnson, M.R., Frankel, W.N., Petrou, S., Boumil, R.M., *et al.* (2015). Epileptic encephalopathy-causing mutations in DNM1 impair synaptic vesicle endocytosis. Neurology Genetics *1*, e4.

Di Bella, D., Lazzaro, F., Brusco, A., Plumari, M., Battaglia, G., Pastore, A., Finardi, A., Cagnoli, C., Tempia, F., Frontali, M., *et al.* (2010). Mutations in the mitochondrial protease gene AFG3L2 cause dominant hereditary ataxia SCA28. Nat Genet *42*, 313-321.

Doege, C., May, T.W., Siniatchkin, M., von Spiczak, S., Stephani, U., and Boor, R. (2013). Myoclonic astatic epilepsy (Doose syndrome) - a lamotrigine responsive epilepsy? European journal of paediatric neurology : EJPN : official journal of the European Paediatric Neurology Society *17*, 29-35.

Doi, H., Yoshida, K., Yasuda, T., Fukuda, M., Fukuda, Y., Morita, H., Ikeda, S.-i., Kato, R., Tsurusaki, Y., Miyake, N., *et al.* (2011). Exome Sequencing Reveals a Homozygous SYT14 Mutation in Adult-Onset, Autosomal-Recessive Spinocerebellar Ataxia with Psychomotor Retardation. The American Journal of Human Genetics *89*, 320-327.

Duan, R., Shi, Y., Yu, L., Zhang, G., Li, J., Lin, Y., Guo, J., Wang, J., Shen, L., Jiang, H., *et al.* (2016). UBA5 Mutations Cause a New Form of Autosomal Recessive Cerebellar Ataxia. PloS one *11*, e0149039.

Duan, Y., Wang, S.-H., Song, J., Mironova, Y., Ming, G.-l., Kolodkin, A.L., and Giger, R.J. (2014). Semaphorin 5A inhibits synaptogenesis in early postnatal- and adult-born hippocampal dentate granule cells. eLife *3*, 33.

Duenas, A.M., Goold, R., Brain, P.G. (2006). Molecular pathogenesis of spinocerebellar ataxias. Brain *129, 1357-1370.*

Edvardson, S., Shaag, A., Zenvirt, S., Erlich, Y., Hannon, G.J., Shanske, A.L., Gomori, J.M., Ekstein, J., and Elpeleg, O. (2010). Joubert syndrome 2 (JBTS2) in Ashkenazi Jews is associated with a TMEM216 mutation. American journal of human genetics *86*, 93-97.

El-Brolosy, M., Rossi, A., Kontarakis, Z., Kuenne, C., Guenther, S., Fukuda, N., Takacs, C., Lai, S.-L., Fukuda, R., Gerri, C., *et al.* (2018). Genetic compensation is triggered by mutant mRNA degradation. bioRxiv, 328153.

Eltze, C.M., Chong, W.K., Cox, T., Whitney, A., Cortina-Borja, M., Chin, R.F., Scott, R.C., and Cross, J.H. (2013). A population-based study of newly diagnosed epilepsy in infants. Epilepsia *54*, 437-445.

Erhardt, A., Czibere, L., Roeske, D., Lucae, S., Unschuld, P.G., Ripke, S., Specht, M., Kohli, M.A., Kloiber, S., Ising, M., *et al.* (2010). TMEM132D, a new candidate for anxiety phenotypes: evidence from human and mouse studies. Molecular Psychiatry *16*, 647-663.

Feigin, V.L., Abajobir, A.A., Abate, K.H., Abd-Allah, F., Abdulle, A.M., Abera, S.F., Abyu, G.Y., Ahmed, M.B., Aichour, A.N., Aichour, I., *et al.* (2017). Global, regional, and national burden of neurological disorders: a systematic analysis for the Global Burden of Disease Study 2015. The Lancet Neurology *16*, 877-897.

Feng, B., Shiber, S.K., and Max, S.R. (1990). Glutamine regulates glutamine synthetase expression in skeletal muscle cells in culture. Journal of Cellular Physiology *145*, 376-380.

Fiore, R., Rahim, B., Christoffels, V.M., Moorman, A.F.M., and Püschel, A.W. (2005). Inactivation of the Sema5a gene results in embryonic lethality and defective remodeling of the cranial vascular system. Molecular and cellular biology *25*, 2310-2319.

Fogel, B.L., and Perlman, S. (2007). Clinical features and molecular genetics of autosomal recessive cerebellar ataxias. The Lancet Neurology *6*, 245-257.

Frumin, M., Golland, P., Kikinis, R., Hirayasu, Y., Salisbury, D.F., Hennen, J., Dickey, C.C., Anderson, M., Jolesz, F.A., Grimson, W.E., *et al.* (2002). Shape differences in the corpus callosum in first-episode schizophrenia and first-episode psychotic affective disorder. The American journal of psychiatry *159*, 866-868.

Gagnon, J.A., Valen, E., Thyme, S.B., Huang, P., Ahkmetova, L., Pauli, A., Montague, T.G., Zimmerman, S., Richter, C., and Schier, A.F. (2014). Efficient Mutagenesis by Cas9 Protein-Mediated Oligonucleotide Insertion and Large-Scale Assessment of Single-Guide RNAs. PloS one *9*, e98186.

Gannavaram, S., Connelly, P.S., Daniels, M.P., Duncan, R., Salotra, P., and Nakhasi, H.L. (2012). Deletion of mitochondrial associated ubiquitin fold modifier protein Ufm1 in Leishmania donovani results in loss of ss-oxidation of fatty acids and blocks cell division in the amastigote stage. Molecular Microbiology *86*, 187-198.

Gannavaram, S., Sharma, P., Duncan, R.C., Salotra, P., and Nakhasi, H.L. (2011). Mitochondrial associated ubiquitin fold modifier-1 mediated protein conjugation in Leishmania donovani. PloS one *6*, e16156.

Glauser, T., Kluger, G., Sachdeo, R., Krauss, G., Perdomo, C., and Arroyo, S. (2008). Rufinamide for generalized seizures associated with Lennox-Gastaut syndrome. Neurology *70*, 1950-1958.

Goldberg, J.L., Vargas, M.E., Wang, J.T., Mandemakers, W., Oster, S.F., Sretavan, D.W., and Barres, B.A. (2004). An oligodendrocyte lineage-specific semaphorin, sema5A, inhibits axon growth by retinal ganglion cells. Journal of Neuroscience *24*, 4989-4999.

Good, P.F., Alapat, D., Hsu, A., Chu, C., Perl, D., Wen, X., Burstein, D.E., and Kohtz, D.S. (2004). A role for semaphorin 3A signaling in the degeneration of hippocampal neurons during Alzheimer's disease. J Neurochem *91*, 716-736.

Gregersen, N.O., Buttenschon, H.N., Hedemand, A., Dahl, H.A., Kristensen, A.S., Clementsen, B., Woldbye, D.P., Koefoed, P., Erhardt, A., Kruse, T.A., *et al.* (2014). Are TMEM genes potential candidate genes for panic disorder? Psychiatric genetics *24*, 37-41.

Grone, B.P., Marchese, M., Hamling, K.R., Kumar, M.G., Krasniak, C.S., Sicca, F., Santorelli, F.M., Patel, M., and Baraban, S.C. (2016). Epilepsy, Behavioral Abnormalities, and Physiological Comorbidities in Syntaxin-Binding Protein 1 (STXBP1) Mutant Zebrafish. PLoS One *11*, e0151148.

Grone, B.P., Qu, T., and Baraban, S.C. (2017). Behavioral Comorbidities and Drug Treatments in a Zebrafish scn1lab Model of Dravet Syndrome. eNeuro *4*, ENEURO.0066-0017.2017.

Gupta, P., Khobragade, S.B., and Shingatgeri, V.M. (2014). Effect of Various Antiepileptic Drugs in Zebrafish PTZ-Seizure Model. Indian Journal of Pharmaceutical Sciences *76*, 157-163.

Gursoy, S., and Ercal, D. (2016). Diagnostic Approach to Genetic Causes of Early-Onset Epileptic Encephalopathy. J Child Neurol *31*, 523-532.

Gusarova, G.A., Wang, I.C., Major, M.L., Kalinichenko, V.V., Ackerson, T., Petrovic, V., and Costa, R.H. (2007). A cell-penetrating ARF peptide inhibitor of FoxM1 in mouse hepatocellular carcinoma treatment. The Journal of Clinical Investigation *117*, 99-111.

Häberle, J., Görg, B., Rutsch, F., Schmidt, E., Toutain, A., Benoist, J.-F., Gelot, A., Suc, A.-L., Höhne, W., Schliess, F., *et al.* (2005). Congenital glutamine deficiency with glutamine synthetase mutations. The New England journal of medicine *353*, 1926-1933.

Häberle, J., Görg, B., Toutain, A., Rutsch, F., Benoist, J.-F., Gelot, A., Suc, A.-L., Koch, H.G., Schliess, F., and Häussinger, D. (2006). Inborn error of amino acid synthesis: human glutamine synthetase deficiency. Journal of inherited metabolic disease *29*, 352-358.

Häberle, J., Shahbeck, N., Ibrahim, K., Schmitt, B., Scheer, I., O'Gorman, R., Chaudhry, F.A., and Ben-Omran, T. (2012). Glutamine supplementation in a child with inherited GS deficiency improves the clinical status and partially corrects the peripheral and central amino acid imbalance. Orphanet journal of rare diseases *7*, 48.

Hamdan, F.F., Myers, C.T., Cossette, P., Lemay, P., Spiegelman, D., Laporte, A.D., Nassif, C., Diallo, O., Monlong, J., Cadieux-Dion, M., *et al.* (2017). High Rate of Recurrent De Novo Mutations in Developmental and Epileptic Encephalopathies. American journal of human genetics *101*, 664-685.

Hamilton, E.M.C., Bertini, E., Kalaydjieva, L., Morar, B., Dojčáková, D., Liu, J., Vanderver, A., Curiel, J., Persoon, C.M., Diodato, D., *et al.* (2017). UFM1 founder mutation in the Roma population causes recessive variant of H-ABC. Neurology *89*, 1821-1828.

Han, S., Tai, C., Westenbroek, R.E., Yu, F.H., Cheah, C.S., Potter, G.B., Rubenstein, J.L., Scheuer, T., de la Iglesia, H.O., and Catterall, W.A. (2012). Autistic-like behaviour in Scn1a+/- mice and rescue by enhanced GABA-mediated neurotransmission. Nature *489*, 385-390.

Hanchate, N.K., Giacobini, P., Lhuillier, P., Parkash, J., Espy, C., Fouveaut, C., Leroy, C., Baron, S., Campagne, C., Vanacker, C., *et al.* (2012). SEMA3A, a gene involved in axonal pathfinding, is mutated in patients with Kallmann syndrome. PLoS Genet *8*, e1002896.

He, Y., Hakvoort, T.B., Vermeulen, J.L., Labruyere, W.T., De Waart, D.R., Van Der Hel, W.S., Ruijter, J.M., Uylings, H.B., and Lamers, W.H. (2010). Glutamine synthetase deficiency in murine astrocytes results in neonatal death. Glia *58*, 741-754.

Helbig, I., and Tayoun, A.N.A. (2016). Understanding Genotypes and Phenotypes in Epileptic Encephalopathies. Molecular Syndromology *7*, 172-181.

Helbig, I., von Deimling, M., and Marsh, E.D. (2017). Epileptic Encephalopathies as Neurodegenerative Disorders. Advances in neurobiology *15*, 295-315.

Hertz, L. (2013). The Glutamate-Glutamine (GABA) Cycle: Importance of Late Postnatal Development and Potential Reciprocal Interactions between Biosynthesis and Degradation. Front Endocrinol (Lausanne) *4*, 59.

Hochstrasser, M. (1996). Ubiquitin-dependent protein degradation. Annual review of genetics *30*, 405-439.

Holland, K.D., and Hallinan, B.E. (2010). What causes epileptic encephalopathy in infancy?: the answer may lie in our genes. Neurology *75*, 1132-1133.

Holmes, S.E., O'Hearn, E., and Margolis, R.L. (2003). Why is SCA12 different from other SCAs? Cytogenetic and Genome Research *100*, 189-197.

Homrich, M., Wobst, H., Laurini, C., Sabrowski, J., Schmitz, B., and Diestel, S. (2014). Cytoplasmic domain of NCAM140 interacts with ubiquitin-fold modifier-conjugating enzyme-1 (Ufc1). Experimental cell research *324*, 192-199.

Hoxha, E., Balbo, I., Miniaci, M.C., and Tempia, F. (2018). Purkinje Cell Signaling Deficits in Animal Models of Ataxia. Frontiers in Synaptic Neuroscience *10*, 6.

Hu, L., Ibrahim, K., Stucki, M., Frapolli, M., Shahbeck, N., Chaudhry, F.A., Görg, B., Häussinger, D., Penberthy, W.T., Ben-Omran, T., *et al.* (2015). Secondary NAD+ deficiency in the inherited defect of glutamine synthetase. Journal of inherited metabolic disease *38*, 1075-1083.

Hua, Y., Sahashi, K., Hung, G., Rigo, F., Passini, M.A., Bennett, C.F., and Krainer, A.R. (2010). Antisense correction of SMN2 splicing in the CNS rescues necrosis in a type III SMA mouse model. Genes & development *24*, 1634-1644.

Huang, L., Szymanska, K., Jensen, V.L., Janecke, A.R., Innes, A.M., Davis, E.E., Frosk, P., Li, C., Willer, J.R., Chodirker, B.N., *et al.* (2011). TMEM237 is mutated in individuals with a Joubert syndrome related disorder and expands the role of the TMEM family at the ciliary transition zone. American journal of human genetics *89*, 713-730.

Huang, Y.F., Wang, Y., and Watford, M. (2007). Glutamine directly downregulates glutamine synthetase protein levels in mouse C2C12 skeletal muscle myotubes. J Nutr *137, 1357-1362.*

Hughes, J.R. (2011). A review of the relationships between Landau–Kleffner syndrome, electrical status epilepticus during sleep, and continuous spike–waves during sleep. Epilepsy & Behavior *20*, 247-253.

Hussman, J.P., Chung, R.H., Griswold, A.J., Jaworski, J.M., Salyakina, D., Ma, D., Konidari, I., Whitehead, P.L., Vance, J.M., Martin, E.R., *et al.* (2011). A noise-reduction GWAS analysis implicates altered regulation of neurite outgrowth and guidance in autism. Molecular autism *2*, 1.

Huyghe, D., Denninger, A.R., Voss, C.M., Frank, P., Gao, N., Brandon, N., Waagepetersen, H.S., Ferguson, A.D., Pangalos, M., Doig, P., *et al.* (2019). Phosphorylation Of Glutamine Synthetase On Threonine 301 Contributes To Its Inactivation During Epilepsy. Frontiers in Molecular Neuroscience *12*, 120.

Huynh, J.M., Galindo, M., and Laukaitis, C.M. (2018). Missense variants in TMEM67 in a patient with Joubert syndrome. Clinical case reports *6*, 2189-2192.

Ito, Y., Hartley, T., Baird, S., Venkateswaran, S., Simons, C., Wolf, N., M. Boycott, K., A. Dyment, D., and Kernohan, K. (2018). Lysosomal dysfunction in TMEM106B hypomyelinating leukodystrophy. Neurol Genet *4, e228.*

Jain, P., Sharma, S., and Tripathi, M. (2013). Diagnosis and Management of Epileptic Encephalopathies in Children. Epilepsy Res Treat *2013, 501981*.

Jayadev, S., and Bird, T.D. (2013). Hereditary ataxias: overview. Genet Med *15*, 673-683.

Jiang, Y.-h., and L Beaudet, A. (2004). Human disorders of ubiquitination and proteasomal degradation. Curr Opin Pediatr *16, 419-426*.

Jiang, Z.M., Wang, L.J., Qi, Y., Liu, T.H., Qiu, M.R., Yang, N.F., and Wilmore, D.W. (1993). Comparison of Parenteral Nutrition Supplemented With L-Glutamine or Glutamine Dipeptides. Journal of Parenteral and Enteral Nutrition *17*, 134-141.

Jun, G., Asai, H., Zeldich, E., Drapeau, E., Chen, C., Chung, J., Park, J.H., Kim, S., Haroutunian, V., Foroud, T., *et al.* (2014). PLXNA4 is associated with Alzheimer disease and modulates tau phosphorylation. Ann Neurol *76*, 379-392.

Kalueff, A.V., Stewart, A.M., and Gerlai, R. (2014). Zebrafish as an emerging model for studying complex brain disorders. Trends in pharmacological sciences *35*, 63-75.

Kansakoski, J., Fagerholm, R., Laitinen, E.M., Vaaralahti, K., Hackman, P., Pitteloud, N., Raivio, T., and Tommiska, J. (2014). Mutation screening of SEMA3A and SEMA7A in patients with congenital hypogonadotropic hypogonadism. Pediatr Res *75*, 641-644.

Kase, D., and Imoto, K. (2012). The Role of HCN Channels on Membrane Excitability in the Nervous System. Journal of signal transduction *2012*, 619747.

Kato, M., Saitoh, S., Kamei, A., Shiraishi, H., Ueda, Y., Akasaka, M., Tohyama, J., Akasaka, N., and Hayasaka, K. (2007). A longer polyalanine expansion mutation in the ARX gene causes early infantile epileptic encephalopathy with suppression-burst pattern (Ohtahara syndrome). American journal of human genetics *81*, 361-366.

Keeney, P.M., Xie, J., Capaldi, R.A., and Bennett, J.P. (2006). Parkinson's Disease Brain Mitochondrial Complex I Has Oxidatively Damaged Subunits and Is Functionally Impaired and Misassembled. Journal of Neuroscience *26*, 5256-5264.

Khurana, D.S., Valencia, I., Goldenthal, M.J., and Legido, A. (2013). Mitochondrial Dysfunction in Epilepsy. Seminars in pediatric neurology *20*, 176-187.

Kim, J.-M., Kim, J.S., Ki, C. S., and Jeon, B. S. (2006). Episodic Ataxia Type 2 due to a Deletion Mutation in the CACNA1A Gene in a Korean Family. J Clin Neurol *2*, 268-271.

Klockgether, T. (2008). The clinical diagnosis of autosomal dominant spinocerebellar ataxias. Cerebellum (London, England) *7*, 101-105.

Kobayashi, H., Abe, K., Matsuura, T., Ikeda, Y., Hitomi, T., Akechi, Y., Habu, T., Liu, W., Okuda, H., and Koizumi, A. (2011). Expansion of Intronic GGCCTG Hexanucleotide Repeat in NOP56 Causes SCA36, a Type of Spinocerebellar Ataxia Accompanied by Motor Neuron Involvement. The American Journal of Human Genetics *89*, 121-130.

Komander, D., and Rape, M. (2012). The Ubiquitin Code. Annual Review of Biochemistry *81*, 203-229.

Komatsu, M., Chiba, T., Tatsumi, K., Iemura, S., Tanida, I., Okazaki, N., Ueno, T., Kominami, E., Natsume, T., and Tanaka, K. (2004). A novel protein-conjugating system for Ufm1, a ubiquitin-fold modifier. Embo Journal *23*, 1977-1986.

Kong, Y., Janssen, B.J.C., Malinauskas, T., Vangoor, V.R., Coles, C.H., Kaufmann, R., Ni, T., Gilbert, R.J.C., Padilla-Parra, S., Pasterkamp, R.J., *et al.* (2016). Structural Basis for Plexin Activation and Regulation. Neuron *91*, 548-560.

Korner, S., Boselt, S., Wichmann, K., Thau-Habermann, N., Zapf, A., Knippenberg, S., Dengler, R., and Petri, S. (2016). The Axon Guidance Protein Semaphorin 3A Is Increased in the Motor Cortex of Patients With Amyotrophic Lateral Sclerosis. Journal of neuropathology and experimental neurology, nlw003.

Lacey, J.M., Crouch, J.B., Benfell, K., Ringer, S.A., Wilmore, C.K., Maguire, D., and Wilmore, D.W. (1996). The Effects of Glutamine-Supplemented Parenteral Nutrition in Premature Infants. Journal of Parenteral and Enteral Nutrition *20*, 74-80.

Lagier-Tourenne, C., Tazir, M., Lopez, L.C., Quinzii, C.M., Assoum, M., Drouot, N., Busso, C., Makri, S., Ali-Pacha, L., Benhassine, T., *et al.* (2008). ADCK3, an ancestral kinase, is mutated in a form of recessive ataxia associated with coenzyme Q10 deficiency. Am J Hum Genet *82*, 661-672.

Laht, P., Tammaru, E., Otsus, M., Rohtla, J., Tiismus, L., and Veske, A. (2015). Plexin-B3 suppresses excitatory and promotes inhibitory synapse formation in rat hippocampal neurons. Experimental cell research *335*, 269-278

Lee, J.H., Silhavy, J.L., Lee, J.E., Al-Gazali, L., Thomas, S., Davis, E.E., Bielas, S.L., Hill, K.J., Iannicelli, M., Brancati, F., *et al.* (2012). Evolutionarily assembled cis-regulatory module at a human ciliopathy locus. Science (New York, NY) *335*, 966-969.

Lemaire, K., Moura, R.F., Granvik, M., Igoillo-Esteve, M., Hohmeier, H.E., Hendrickx, N., Newgard, C.B., Waelkens, E., Cnop, M., and Schuit, F. (2011). Ubiquitin Fold Modifier 1 (UFM1) and Its Target UFBP1 Protect Pancreatic Beta Cells from ER Stress-Induced Apoptosis. PloS one *6*, e18517.

Lemmon, M.E., and Kossoff, E.H. (2013). New treatment options for lennox-gastaut syndrome. Current treatment options in neurology *15*, 519-528.

Lesca, G., Rudolf, G., Bruneau, N., Lozovaya, N., Labalme, A., Boutry-Kryza, N., Salmi, M., Tsintsadze, T., et al. (2013). GRIN2A mutations in acquired epileptic aphasia and related childhood focal epilepsies and encephalopathies with speech and language dysfunction. Natu Genet. *45, 1061-1066*.

Li, D., Yuan, H., Ortiz-Gonzalez, X. R., Marsh, E. D., Tian, L., McCormick, E. M., Kosobucki, G. J., Chen, W., *et al.* (2016). *GRIN2D* Recurrent De Novo Dominant Mutation Causes a Severe Epileptic Encephalopathy Treatable with NMDA Receptor Channel Blockers. Am J Hum Genet. *99, 802-816*.

Li, H., Lu, Y., Smith, H.K., and Richardson, W.D. (2007). Olig1 and Sox10 Interact Synergistically to Drive Myelin Basic Protein Transcription in Oligodendrocytes. Journal of Neuroscience *27*, 14375-14382.

Lignitto, L., Carlucci, A., Sepe, M., Stefan, E., Cuomo, O., Nistico, R., Scorziello, A., Savoia, C., Garbi, C., Annunziato, L., *et al.* (2011). Control of PKA stability and signalling by the RING ligase praja2. Nature cell biology *13*, 412-422.

Lin, P.-H., Duann, P., Komazaki, S., Park, K.H., Li, H., Sun, M., Sermersheim, M., Gumpper, K., Parrington, J., Galione, A., *et al.* (2015). Lysosomal two-pore channel subtype 2 (TPC2) regulates skeletal muscle autophagic signaling. Journal of Biological Chemistry *290*, 3377-3389.

Lin-Moshier, Y., Keebler, M.V., Hooper, R., Boulware, M.J., Liu, X., Churamani, D., Abood, M.E., Walseth, T.F., Brailoiu, E., Patel, S., *et al.* (2014). The Two-pore channel (TPC) interactome unmasks isoform-specific roles for TPCs in endolysosomal morphology and cell pigmentation. Proceedings of the National Academy of Sciences of the United States of America *111*, 13087-13092.

Lotte, J., Haberlandt, E., Neubauer, B., Staudt, M., and Kluger, G.J. (2012). Bromide in patients with SCN1A-mutations manifesting as Dravet syndrome. Neuropediatrics *43*, 17-21.

Low, K.J., Baptista, J., Babiker, M., Caswell, R., King, C., Ellard, S., and Scurr, I. (2018). Hemizygous UBA5 missense mutation unmasks recessive disorder in a patient with infantile-onset encephalopathy, acquired microcephaly, small cerebellum, movement disorder and severe neurodevelopmental delay. European journal of medical genetics *62*, 97-102.

Lyon, G.J., and Wang, K. (2012). Identifying disease mutations in genomic medicine settings: current challenges and how to accelerate progress. Genome Medicine *4*, 58.

Mackay, M.T., Weiss, S.K., Adams-Webber, T., Ashwal, S., Stephens, D., Ballaban-Gill, K., Baram, T.Z., Duchowny, M., Hirtz, D., Pellock, J.M., *et al.* (2004). Practice parameter: medical treatment of infantile spasms: report of the American Academy of Neurology and the Child Neurology Society. Neurology *62*, 1668-1681.

Mah, S., Nelson, M.R., Delisi, L.E., Reneland, R.H., Markward, N., James, M.R., Nyholt, D.R., Hayward, N., Handoko, H., Mowry, B., *et al.* (2006). Identification of the semaphorin receptor PLXNA2 as a candidate for susceptibility to schizophrenia. Mol Psychiatry *11*, 471-478.

Mahmood, F., Mozere, M., Zdebik, A.A., Stanescu, H.C., Tobin, J., Beales, P.L., Kleta, R., Bockenhauer, D., and Russell, C. (2013). Generation and validation of a zebrafish model of EAST (epilepsy, ataxia, sensorineural deafness and tubulopathy) syndrome. Dis Model Mech *6*, 652-660.

Mann, F., Chauvet, S., and Rougon, G. (2007). Semaphorins in development and adult brain: Implication for neurological diseases. Progress in neurobiology *82*, 57-79.

Manto, M.U. (2005). The wide spectrum of spinocerebellar ataxias (SCAs). Cerebellum (London, England) *4*, 2-6.

Marchler-Bauer, A., Anderson, J.B., Derbyshire, M.K., DeWeese-Scott, C., Gonzales, N.R., Gwadz, M., Hao, L., He, S., Hurwitz, D.I., Jackson, J.D., *et al.* (2007). CDD: a conserved domain database for interactive domain family analysis. Nucleic acids research *35*, 237-240.

Margolin, D.H., Kousi, M., Chan, Y.M., Lim, E.T., Schmahmann, J.D., Hadjivassiliou, M., Hall, J.E., Adam, I., Dwyer, A., Plummer, L., *et al.* (2013). Ataxia, dementia, and hypogonadotropism caused by disordered ubiquitination. N Engl J Med *368*, 1992-2003.

Martin, D.D.O., Ladha, S., Ehrnhoefer, D.E., and Hayden, M.R. (2015). Autophagy in Huntington disease and huntingtin in autophagy. Trends in Neurosciences *38*, 26-35.

Mastrangelo, M. (2015). Novel Genes of Early-Onset Epileptic Encephalopathies: From Genotype to Phenotypes. Pediatr Neurol *53*, 119-129.

Mastrangelo, M. (2017). Lennox-Gastaut Syndrome: A State of the Art Review. Neuropediatrics *48*, 143-151.

Matsuoka, R.L., Chivatakarn, O., Badea, T.C., Samuels, I.S., Cahill, H., Katayama, K.-I., Kumar, S.R., Suto, F., Chedotal, A., Peachey, N.S., *et al.* (2011). Class 5 transmembrane semaphorins control selective Mammalian retinal lamination and function. Neuron *71*, 460-473.

Matsuura, T., Yamagata, T., Burgess, D.L., Rasmussen, A., Grewal, R.P., Watase, K., Khajavi, M., McCall, A.E., Davis, C.F., Zu, L., *et al.* (2000). Large expansion of the ATTCT pentanucleotide repeat in spinocerebellar ataxia type 10. Nat Genet *26*, 191-194.

McCammon, J.M., and Sive, H. (2015). Challenges in understanding psychiatric disorders and developing therapeutics: a role for zebrafish. Dis Model Mech *8*, 647-656.

Mei, X., Wu, S., Bassuk, A.G., and Slusarski, D.C. (2013). Mechanisms of prickle1a function in zebrafish epilepsy and retinal neurogenesis. Dis Model Mech *6*, 679-688.

Melin, M., Carlsson, B., Anckarsater, H., Rastam, M., Betancur, C., Isaksson, A., Gillberg, C., and Dahl, N. (2006). Constitutional downregulation of SEMA5A expression in autism. Neuropsychobiology *54*, 64-69.

Mercier, A. (2003). Effect of enteral supplementation with glutamine on mesenteric blood flow in premature neonates. Clinical Nutrition *22*, 133-137.

Meyers, J. R. (2018). Zebrafish: Development of a vertebrate model organism. Current Protocols 16, e19.

Mignon-Ravix, C., Milh, M., Kaiser, C.S., Daniel, J., Riccardi, F., Cacciagli, P., Nagara, M., Busa, T., Liebau, E., and Villard, L. (2018). Abnormal function of the UBA5 protein in a case of early developmental and epileptic encephalopathy with suppression-burst. Human Mutation *39*, 934-938.

Mills, P.B., Camuzeaux, S.S.M., Footitt, E.J., Mills, K.A., Gissen, P., Fisher, L., Das, K.B., Varadkar, S.M., Zuberi, S., McWilliam, R.*, et al.* (2014). Epilepsy due to PNPO mutations: genotype, environment and treatment affect presentation and outcome. Brain : a journal of neurology *137*, 1350-1360.

Mizuno, T., Kashimada, A., Nomura, T., Moriyama, K., Yokoyama, H., Hasegawa, S., Takagi, M., and Mizutani, S. (2019). Infantile-onset spinocerebellar ataxia type 5 associated with a novel SPTBN2 mutation: A case report. Brain & development.

Moeton, M., Kanski, R., Stassen, O.M.J.A., Sluijs, J.A., Geerts, D., van Tijn, P., Wiche, G., van Strien, M.E., and Hol, E.M. (2014). Silencing GFAP isoforms in astrocytoma cells disturbs laminin-dependent motility and cell adhesion. The FASEB Journal *28*, 2942-2954.

Moeton, M., Stassen, O.M.J.A., Sluijs, J.A., van der Meer, V.W.N., Kluivers, L.J., van Hoorn, H., Schmidt, T., Reits, E.A.J., van Strien, M.E., and Hol, E.M. (2016). GFAP isoforms control intermediate filament network dynamics, cell morphology, and focal adhesions. Cellular and molecular life sciences : CMLS *73*, 4101-4120.

Molinari, F., Kaminska, A., Fiermonte, G., Boddaert, N., Rothschild, A.R., Plouin, P., Palmieri, L., Brunelle, F., Palmieri, F., Dulac, O.*, et al.* (2009). Mutations in the mitochondrial glutamate carrier SLC25A22 in neonatal epileptic encephalopathy with suppression bursts. Clinical genetics *76*, 188-194.

Montague, T.G., Cruz, J.M., Gagnon, J.A., Church, G.M., and Valen, E. (2014). CHOPCHOP: a CRISPR/Cas9 and TALEN web tool for genome editing. Nucleic Acids Res *42*, W401-407.

Moreira, M.C., Barbot, C., Tachi, N., Kozuka, N., Uchida, E., Gibson, T., Mendonca, P., Costa, M., Barros, J., Yanagisawa, T.*, et al.* (2001). The gene mutated in ataxia-ocular apraxia 1 encodes the new HIT/Zn-finger protein aprataxin. Nat Genet *29*, 189-193.

Moore, D.J., West, A.B., Dawson, V.L., and Dawson, T.M. (2005). Molecular pathophysiology of Parkinson's disease. Annu Rev Neurosci *28*, 57-87.

Mortiboys, H., Thomas, K.J., Koopman, W.J.H., Klaffke, S., Sleiman, P.A., Olpin, S., Wood, N.W., Willems, P.H.G.M., Smeitink, J.A.M., Cookson, M.R., *et al.* (2008). Mitochondrial function and morphology are impaired in parkin-mutant fibroblasts. Annals of Neurology *64*, 555-565.

Mueller, T., and Wullimann, M.F. (2003). Anatomy of neurogenesis in the early zebrafish brain. Brain research Developmental brain research *140*, 137-155.

Mukhopadhyay, D., and Riezman, H. (2007). Proteasome-independent functions of ubiquitin in endocytosis and signaling. Science *315*, 201-205.

Muona, M., Ishimura, R., Laari, A., Ichimura, Y., Linnankivi, T., Keski-Filppula, R., Herva, R., Rantala, H., Paetau, A., Poyhonen, M., *et al.* (2016). Biallelic Variants in UBA5 Link Dysfunctional UFM1 Ubiquitin-like Modifier Pathway to Severe Infantile-Onset Encephalopathy. The American Journal of Human Genetics *99*, 683-694.

Murakami, Y., Suto, F., Shimizu, M., Shinoda, T., Kameyama, T., and Fujisawa, H. (2001). Differential expression of plexin-a subfamily members in the mouse nervous system. Developmental Dynamics *220*, 246-258.

Muratani, M., and Tansey, W.P. (2003). How the ubiquitin-proteasome system controls transcription. Nature reviews Molecular cell biology *4*, 192-201.

Nabbout, R., Chemaly, N., Chipaux, M., Barcia, G., Bouis, C., Dubouch, C., Leunen, D., Jambaqué, I., Dulac, O., Dellatolas, G., *et al.* (2013). Encephalopathy in children with Dravet syndrome is not a pure consequence of epilepsy. Orphanet journal of rare diseases *8*, 176.

Nakadai, T., Kishimoto, T., Kokura, K., Ohkawa, N., Makino, Y., Muramatsu, M., and Tamura, T.-a. (1998). Cloning of a Novel Rat Gene, DB83, That Encodes a Putative Membrane Protein. DNA Research *5*, 315-317.

Nakamura, K., Kato, M., Osaka, H., Yamashita, S., Nakagawa, E., Haginoya, K., Tohyama, J., Okuda, M., Wada, T., Shimakawa, S., *et al.* (2013). Clinical spectrum of SCN2A mutations expanding to Ohtahara syndrome. Neurology *81*, 992-998.

Nakashima, M., Kouga, T., Lourenço, C.M., Shiina, M., Goto, T., Tsurusaki, Y., Miyatake, S., Miyake, N., Saitsu, H., Ogata, K., *et al.* (2016). De novo DNM1 mutations in two cases of epileptic encephalopathy. Epilepsia *57*, e18-e23.

Nahorski, M.S., Maddirevula, S., Ishimura, R., Alsahli, S., Brady, A.F., Begemann, A., Mizushima, T., Guzmán-Vega, F.J., Obata, M., Ichimura, Y., *et al.* (2018). Biallelic UFM1 and UFC1 mutations expand the essential role of ufmylation in brain development. Brain *141*, 1934-1945.

Namikawa, K., Dorigo, A., Zagrebelsky, M., Russo, G., Kirmann, T., Fahr, W., Dübel, S., Korte, M., and Köster, R.W. (2019). Modeling neurodegenerative Spinocerebellar Ataxia type 13 in zebrafish using a Purkinje neuron specific tunable co-expression system. Journal of Neuroscience 39, 3948-3969.

Nariai, H., Duberstein, S., and Shinnar, S. (2018). Treatment of Epileptic Encephalopathies: Current State of the Art. J Child Neurol *33*, 41-54.

Nava, C., Dalle, C., Rastetter, A., Striano, P., de Kovel, C.G., Nabbout, R., Cances, C., Ville, D., Brilstra, E.H., Gobbi, G., *et al.* (2014). De novo mutations in HCN1 cause early infantile epileptic encephalopathy. Nat Genet *46*, 640-645.

Negishi, M., Oinuma, I., and Katoh, H. (2005). Plexins: axon guidance and signal transduction. Cellular and molecular life sciences : CMLS *62*, 1363-1371.

Newsholme, P., Procopio, J., Lima, M.M.R., Pithon-Curi, T.C., and Curi, R. (2003). Glutamine and glutamate--their central role in cell metabolism and function. Cell biochemistry and function *21*, 1-9.

Nicklin, P., Bergman, P., Zhang, B., Triantafellow, E., Wang, H., Nyfeler, B., Yang, H., Hild, M., Kung, C., Wilson, C., *et al.* (2009). Bidirectional Transport of Amino Acids Regulates mTOR and Autophagy. Cell *136*, 521-534.

Nieh, S.E., and Sherr, E.H. (2014). Epileptic encephalopathies: new genes and new pathways. Neurotherapeutics *11*, 796-806.

Ogiwara, I., Miyamoto, H., Morita, N., Atapour, N., Mazaki, E., Inoue, I., Takeuchi, T., Itohara, S., Yanagawa, Y., Obata, K., *et al.* (2007). Nav1.1 localizes to axons of parvalbumin-positive inhibitory interneurons: a circuit basis for epileptic seizures in mice carrying an Scn1a gene mutation. The Journal of neuroscience : the official journal of the Society for Neuroscience *27*, 5903-5914.

Okada, A., Tominaga, M., Horiuchi, M., and Tomooka, Y. (2007). Plexin-A4 is expressed in oligodendrocyte precursor cells and acts as a mediator of semaphorin signals. Biochemical and biophysical research communications *352*, 158-163.

Okada, A., and Tomooka, Y. (2012). Possible roles of Plexin-A4 in positioning of oligodendrocyte precursor cells in developing cerebral cortex. Neuroscience letters *516*, 259-264.

Ohba, C., Shiina, M., Tohyama, J., Haginoya, K., Lerman-Sagie, T., Okamoto, N., Blumkin, L., Lev, D., Mukaida, S., *et al.* (2015). GRIN1 mutations cause encephalopathy with infantile-onset epilepsy, and hyperkinetic and stereotyped movement disorders. Epilepsia *56, 841-848*.

Ohtahara, S., and Neurophysiology, Y.Y.J.o.C. (2003). Epileptic encephalopathies in early infancy with suppression-burst. J Clin Neurophysiol *20, 398-407*.

Organization, W.H. (2006). Neurological disorders: public health challenges.

Oweis, W., Padala, P., Hassouna, F., Cohen-Kfir, E., Gibbs, D.R., Todd, E.A., Berndsen, C.E., and Wiener, R. (2016). Trans-Binding Mechanism of Ubiquitin-like Protein Activation Revealed by a UBA5-UFM1 Complex. Cell Rep *16*, 3113-3120.

Park, H.C., Kim, C.H., Bae, Y.K., Yee, S.Y., Kim, S.H., Hong, S.K., Shin, J., Yoo, K.W., Hibi, M., Hirano, T., *et al.* (2000). Analysis of upstream elements in the HuC promoter leads to the establishment of transgenic zebrafish with fluorescent neurons. Developmental Biology *227*, 279-293.

Pasterkamp, R.J., and Giger, R.J. (2009). Semaphorin function in neural plasticity and disease. Current opinion in neurobiology *19*, 263-274.

Pasterkamp, R.J., and Kolodkin, A.L. (2003). Semaphorin junction: making tracks toward neural connectivity. Current opinion in neurobiology *13*, 79-89.

Paulson, H.L. (2009). The spinocerebellar ataxias. Journal of neuro-ophthalmology : the official journal of the North American Neuro-Ophthalmology Society *29*, 227-237.

Pellock, J.M., Hrachovy, R., Shinnar, S., Baram, T.Z., Bettis, D., Dlugos, D.J., Gaillard, W.D., Gibson, P.A., Holmes, G.L., Nordl, D.R., *et al.* (2010). Infantile spasms: a U.S. consensus report. Epilepsia *51*, 2175-2189.

Perälä, N., Peitsaro, N., Sundvik, M., Koivula, H., Sainio, K., Sariola, H., Panula, P., and Immonen, T. (2010). Conservation, expression, and knockdown of zebrafish plxnb2a and plxnb2b. Developmental Dynamics *239*, 2722-2734.

Perlman, S.L. (2000). Cerebellar Ataxia. Current treatment options in neurology *2*, 215-224.

Peters, H.C., Hu, H., Pongs, O., Storm, J.F., and Isbrandt, D. (2005). Conditional transgenic suppression of M channels in mouse brain reveals functions in neuronal excitability, resonance and behavior. Nat Neurosci *8*, 51-60.

Philips, T., Bento-Abreu, A., Nonneman, A., Haeck, W., Staats, K., Geelen, V., Hersmus, N., Kusters, B., Van Den Bosch, L., Van Damme, P., *et al.* (2013). Oligodendrocyte dysfunction in the pathogenesis of amyotrophic lateral sclerosis. Brain *136*, 471-482.

Piaton, G., Aigrot, M.-S., Williams, A., Moyon, S., Tepavcevic, V., Moutkine, I., Gras, J., Matho, K.S., Schmitt, A., Soellner, H., *et al.* (2011). Class 3 semaphorins influence oligodendrocyte precursor recruitment and remyelination in adult central nervous system. Brain *134*, 1156-1167.

Prasad, A.N., and Hoffmann, G.F. (2010). Early onset epilepsy and inherited metabolic disorders: diagnosis and management. The Canadian journal of neurological sciences Le journal canadien des sciences neurologiques *37*, 350-358.

Qureshi, M., Hatem, M., Alroughani, R., Jacob, S.P., and Al-Temaimi, R.A. (2017). PLXNA3 Variant rs5945430 is Associated with Severe Clinical Course in Male Multiple Sclerosis Patients. Neuromolecular medicine *19*, 286-292.

Qvartskhava, N., Lang, P.A., Görg, B., Pozdeev, V.I., Ortiz, M.P., Lang, K.S., Bidmon, H.J., Lang, E., Leibrock, C.B., Herebian, D., *et al.* (2015). Hyperammonemia in gene-targeted mice lacking functional hepatic glutamine synthetase. Proceedings of the National Academy of Sciences of the United States of America *112*, 5521-5526.

Rangroo Thrane, V., Thrane, A.S., Wang, F., Cotrina, M.L., Smith, N.A., Chen, M., Xu, Q., Kang, N., Fujita, T., Nagelhus, E.A., *et al.* (2013). Ammonia triggers neuronal disinhibition and seizures by impairing astrocyte potassium buffering. Nat Med *19*, 1643-1648.

Robertson, E.E., Hall, D.A., McAsey, A.R., and O'Keefe, J.A. (2016). Fragile X-associated tremor/ataxia syndrome: phenotypic comparisons with other movement disorders. The Clinical Neuropsychologist *30*, 849-900.

Rossi, A., Kontarakis, Z., Gerri, C., Nolte, H., Hölper, S., Krüger, M., and Stainier, D.Y.R. (2015). Genetic compensation induced by deleterious mutations but not gene knockdowns. Nature *524*, 230-233.

Rubio, M.D., Wood, K., Haroutunian, V., and Meador-Woodruff, J.H. (2013). Dysfunction of the ubiquitin proteasome and ubiquitin-like systems in schizophrenia. Neuropsychopharmacology : official publication of the American College of Neuropsychopharmacology *38*, 1910-1920.

Rujescu, D., Meisenzahl, E.M., Krejcova, S., Giegling, I., Zetzsche, T., Reiser, M., Born, C.M., Möller, H.-J., Veske, A., Gal, A., *et al.* (2007). Plexin B3 is genetically associated with verbal performance and white matter volume in human brain. Molecular Psychiatry *12*, 190-194.

Rutherford, N.J., Carrasquillo, M.M., Li, M., Bisceglio, G., Menke, J., Josephs, K.A., Parisi, J.E., Petersen, R.C., Graff-Radford, N.R., Younkin, S.G., *et al.* (2012). TMEM106B risk variant is implicated in the pathologic presentation of Alzheimer disease. Neurology *79*, 717-718.

Sandford, E., and Burmeister, M. (2014). Genes and genetic testing in hereditary ataxias. Genes *5*, 586-603.

Sakabe, I., Hu, R., Jin, L., Clarke, R., and Kasid, U.N. (2015). TMEM33: a new stress-inducible endoplasmic reticulum transmembrane protein and modulator of the unfolded protein response signaling. Breast Cancer Res Treat *153*, 285-297.

Sarva, H., and Shanker, V.L. (2014). Treatment Options in Degenerative Cerebellar Ataxia: A Systematic Review. Mov Disord Clin Pract *1*, 291-298.

Sato, N., Amino, T., Kobayashi, K., Asakawa, S., Ishiguro, T., Tsunemi, T., Takahashi, M., Matsuura, T., Flanigan, K.M., Iwasaki, S., *et al.* (2009). Spinocerebellar ataxia type 31 is associated with "inserted" penta-nucleotide repeats containing (TGGAA)n. American journal of human genetics *85*, 544-557.

Satoh, J.-I., Kino, Y., Kawana, N., Yamamoto, Y., Ishida, T., Saito, Y., and Arima, K. (2014). TMEM106B expression is reduced in Alzheimer's disease brains. Alzheimers Res Ther *6*, 17-17.

Savage, A.M., Kurusamy, S., Chen, Y., Jiang, Z., Chhabria, K., MacDonald, R.B., Kim, H.R., Wilson, H.L., van Eeden, F.J.M., Armesilla, A.L., *et al.* (2019). tmem33 is essential for VEGF-mediated endothelial calcium oscillations and angiogenesis. Nature Communications *10*, 732.

Scharfman, H.E. (2007). The neurobiology of epilepsy. Current neurology and neuroscience reports *7*, 348-354.

Scheffer, I.E., Berkovic, S., Capovilla, G., Connolly, M.B., French, J., Guilhoto, L., Hirsch, E., Jain, S., Mathern, G.W., Moshe, S.L., *et al.* (2017). ILAE classification of the epilepsies: Position paper of the ILAE Commission for Classification and Terminology. Epilepsia *58*, 512-521.

Senderek, J., Krieger, M., Stendel, C., Bergmann, C., Moser, M., Breitbach-Faller, N., Rudnik-Schöneborn, S., Blaschek, A., Wolf, N., Harting, I., *et al.* (2006). Mutations in SIL1 cause Marinesco-Sjogren syndrome, a cerebellar ataxia with cataract and myopathy. Nat Genet *37, 1312-1314*.

Shao, J., and Diamond, M.I. (2007). Polyglutamine diseases: emerging concepts in pathogenesis and therapy. Hum Mol Genet *16 Spec No. 2*, R115-123.

Shim, S.-O., Cafferty, W.B.J., Schmidt, E.C., Kim, B.G., Fujisawa, H., and Strittmatter, S.M. (2012). PlexinA2 limits recovery from corticospinal axotomy by mediating oligodendrocyte-derived Sema6A growth inhibition. Mol Cell Neurosci *50*, 193-200.

Siekierska, A., Stamberger, H., Deconinck, T., Oprescu, S.N., Partoens, M., Zhang, Y., Sourbron, J., Adriaenssens, E., Mullen, P., Wiencek, P., *et al.* (2019). Biallelic VARS variants cause developmental encephalopathy with microcephaly that is recapitulated in vars knockout zebrafish. Nat Commun *10*, 708.

Simmons, A.D., Püschel, A.W., McPherson, J.D., Overhauser, J., and Lovett, M. (1998). Molecular cloning and mapping of human semaphorin F from the Cri-du-chat candidate interval. Biochemical and biophysical research communications *242*, 685-691.

Simons, C., Dyment, D., Bent, S.J., Crawford, J., D'Hooghe, M., Kohlschutter, A., Venkateswaran, S., Helman, G., Poll-The, B.T., Makowski, C.C., *et al.* (2017). A recurrent de novo mutation in TMEM106B causes hypomyelinating leukodystrophy. Brain *140*, 3105-3111.

Singhal, N.S., and Sullivan, J.E. (2014). Continuous Spike-Wave during Slow Wave Sleep and Related Conditions. ISRN Neurol *2014*, 619079-619079.

Sklar, P., Smoller, J.W., Fan, J., Ferreira, M.A.R., Perlis, R.H., Chambert, K., Nimgaonkar, V.L., McQueen, M.B., Faraone, S.V., Kirby, A., *et al.* (2008). Whole-genome association study of bipolar disorder. Molecular psychiatry *13*, 558-569.

Smigiel, R., Landsberg, G., Schilling, M., Rydzanicz, M., Pollak, A., Walczak, A., Stodolak, A., Stawinski, P., Mierzewska, H., Sasiadek, M.M., *et al.* (2018). Developmental epileptic encephalopathy with hypomyelination and brain atrophy associated with PTPN23 variants affecting the assembly of UsnRNPs. European Journal of Human Genetics *26*, 1502-1511.

Soeters, P.B., and Grecu, I. (2012). Have we enough glutamine and how does it work? A clinician's view. Annals of nutrition & metabolism *60*, 17-26.

Soto, C. (2003). Unfolding the role of protein misfolding in neurodegenerative diseases. Nature reviews Neuroscience *4*, 49-60.

Spodenkiewicz, M., Diez-Fernandez, C., Rüfenacht, V., Gemperle-Britschgi, C., and Häberle, J. (2016). Minireview on Glutamine Synthetase Deficiency, an Ultra-Rare Inborn Error of Amino Acid Biosynthesis. Biology *5*, 40.

Srour, M., Hamdan, F.F., Schwartzentruber, J.A., Patry, L., Ospina, L.H., Shevell, M.I., Désilets, V., Dobrzeniecka, S., Mathonnet, G., Lemyre, E., *et al.* (2012). Mutations in TMEM231 cause Joubert syndrome in French Canadians. Journal of Medical Genetics *49*, 636-641.

Storey, E. (2014). Genetic Cerebellar Ataxias. Seminars in Neurology *34*, 280-292.

Su, C.-Y., Kemp, H.A., and Moens, C.B. (2014). Cerebellar development in the absence of Gbx function in zebrafish. Developmental Biology *386*, 181-190.

Suda, S., Iwata, K., Shimmura, C., Kameno, Y., Anitha, A., Thanseem, I., Nakamura, K., Matsuzaki, H., Tsuchiya, K.J., Sugihara, G., *et al.* (2011). Decreased expression of axon-guidance receptors in the anterior cingulate cortex in autism. Molecular autism *2*, 14.

Sullivan, R., Yau, W.Y., O'Connor, E., and Houlden, H. (2019). Spinocerebellar ataxia: an update. Journal of neurology *266*, 533-544.

Suls, A., Jaehn, J.A., Kecskes, A., Weber, Y., Weckhuysen, S., Craiu, D.C., Siekierska, A., Djemie, T., Afrikanova, T., Gormley, P., *et al.* (2013). De novo loss-of-function mutations in CHD2 cause a fever-

sensitive myoclonic epileptic encephalopathy sharing features with Dravet syndrome. Am J Hum Genet *93*, 967-975.

Suls, A., Mullen, S.A., Weber, Y.G., Verhaert, K., Ceulemans, B., Guerrini, R., Wuttke, T.V., Salvo-Vargas, A., Deprez, L., Claes, L.R., *et al.* (2009). Early-onset absence epilepsy caused by mutations in the glucose transporter GLUT1. Ann Neurol *66*, 415-419.

Suto, F., Ito, K., Uemura, M., Shimizu, M., Shinkawa, Y., Sanbo, M., Shinoda, T., Tsuboi, M., Takashima, S., Yagi, T., *et al.* (2005). Plexin-A4 Mediates Axon-Repulsive Activities of Both Secreted and Transmembrane Semaphorins and Plays Roles in Nerve Fiber Guidance. The Journal of Neuroscience *25*, 3628.

Szklarczyk, D., Gable, A.L., Lyon, D., Junge, A., Wyder, S., Huerta-Cepas, J., Simonovic, M., Doncheva, N.T., Morris, J.H., Bork, P., *et al.* (2019). STRING v11: protein-protein association networks with increased coverage, supporting functional discovery in genome-wide experimental datasets. Nucleic Acids Res *47*, 607-613.

Sztal, T.E., McKaige, E.A., Williams, C., Ruparelia, A.A., and Bryson-Richardson, R.J. (2018). Genetic compensation triggered by actin mutation prevents the muscle damage caused by loss of actin protein. PLOS Genetics *14*, e1007212.

Sztal, T.E., Ruparelia, A.A., Williams, C., and Bryson-Richardson, R.J. (2016). Using Touch-evoked Response and Locomotion Assays to Assess Muscle Performance and Function in Zebrafish. Journal of Visualized Experiments : JoVE.

Ta-Shma, A., Khan, T.N., Vivante, A., Willer, J.R., Matak, P., Jalas, C., Pode-Shakked, B., Salem, Y., Anikster, Y., Hildebrandt, F., *et al.* (2017). Mutations in TMEM260 Cause a Pediatric Neurodevelopmental, Cardiac, and Renal Syndrome. American journal of human genetics *100*, 666-675.

Tamagnone, L., Artigiani, S., Chen, H., He, Z., Ming, G.-l., Song, H.-j., Chedotal, A., Winberg, M.L., Goodman, C.S., Poo, M.-m., *et al.* (1999). Plexins Are a Large Family of Receptors for Transmembrane, Secreted, and GPI-Anchored Semaphorins in Vertebrates. Cell *99*, 71-80.

Tamura, K., Stecher, G., Peterson, D., Filipski, A., and Kumar, S. (2013). MEGA6: Molecular Evolutionary Genetics Analysis version 6.0. Molecular biology and evolution *30*, 2725-2729.

Taniguchi, M., Nagao, H., Takahashi, Y.K., Yamaguchi, M., Mitsui, S., Yagi, T., Mori, K., and Shimizu, T. (2003). Distorted Odor Maps in the Olfactory Bulb of Semaphorin 3A-Deficient Mice. The Journal of Neuroscience *23*, 1390-1397.

Tara, E., Vitenzon, A., Hess, E., and Khodakhah, K. (2018). Aberrant cerebellar Purkinje cell activity as the cause of motor attacks in a mouse model of episodic ataxia type 2. Disease Models & Mechanisms *11*, dmm034181.

Tatsumi, K., Sou, Y.S., Tada, N., Nakamura, E., Iemura, S., Natsume, T., Kang, S.H., Chung, C.H., Kasahara, M., Kominami, E., *et al.* (2010). A novel type of E3 ligase for the Ufm1 conjugation system. The Journal of biological chemistry *285*, 5417-5427.

Tatsumi, K., Yamamoto-Mukai, H., Shimizu, R., Waguri, S., Sou, Y.-S., Sakamoto, A., Taya, C., Shitara, H., Hara, T., Chung, C.H., *et al.* (2011). The Ufm1-activating enzyme Uba5 is indispensable for erythroid differentiation in mice. Nature Communications *2*, 181.

Thisse, C., and Thisse, B. (2008). High-resolution in situ hybridization to whole-mount zebrafish embryos. Nature protocols *3*, 59-69.

Todd, P.K., Oh, S.Y., Krans, A., He, F., Sellier, C., Frazer, M., Renoux, A.J., Chen, K.C., Scaglione, K.M., Basrur, V., *et al.* (2013). CGG repeat-associated translation mediates neurodegeneration in fragile X tremor ataxia syndrome. Neuron *78*, 440-455.

Trivisano, M., Specchio, N., Cappelletti, S., Di Ciommo, V., Claps, D., Specchio, L.M., Vigevano, F., and Fusco, L. (2011). Myoclonic astatic epilepsy: an age-dependent epileptic syndrome with favorable seizure outcome but variable cognitive evolution. Epilepsy research *97*, 133-141.

Urade, T., Yamamoto, Y., Zhang, X., Ku, Y., and Sakisaka, T. (2014). Identification and characterization of TMEM33 as a reticulon-binding protein. The Kobe journal of medical sciences *60*, E57-65.

Usuki, F., and Maruyama, K. (2000). Ataxia caused by mutations in the α-tocopherol transfer protein gene. Journal of Neurology, Neurosurgery & Psychiatry *69*, 254-256.

Van Deerlin, V.M., Sleiman, P.M., Martinez-Lage, M., Chen-Plotkin, A., Wang, L.S., Graff-Radford, N.R., Dickson, D.W., Rademakers, R., Boeve, B.F., Grossman, M., *et al.* (2010). Common variants at 7p21 are associated with frontotemporal lobar degeneration with TDP-43 inclusions. Nat Genet *42*, 234-239.

van der Zee, J., Van Langenhove, T., Kleinberger, G., Sleegers, K., Engelborghs, S., Vandenberghe, R., Santens, P., Van den Broeck, M., Joris, G., Brys, J., *et al.* (2011). TMEM106B is associated with frontotemporal lobar degeneration in a clinically diagnosed patient cohort. Brain *134*, 808-815.

Varade, J., Comabella, M., Ortiz, M.A., Arroyo, R., Fernandez, O., Pinto-Medel, M.J., Fedetz, M., Izquierdo, G., Lucas, M., Gomez, C.L., *et al.* (2012). Replication study of 10 genes showing evidence for association with multiple sclerosis: validation of TMEM39A, IL12B and CBLB [correction of CLBL] genes. Multiple sclerosis (Houndmills, Basingstoke, England) *18*, 959-965.

Vass, R., Ashbridge, E., Geser, F., Hu, W.T., Grossman, M., Clay-Falcone, D., Elman, L., McCluskey, L., Lee, V.M., Van Deerlin, V.M., *et al.* (2011). Risk genotypes at TMEM106B are associated with cognitive impairment in amyotrophic lateral sclerosis. Acta neuropathologica *121*, 373-380.

Velazquez, E.F., Yancovitz, M., Pavlick, A., Berman, R., Shapiro, R., Bogunovic, D., O'Neill, D., Yu, Y.-L., Spira, J., Christos, P.J., *et al.* (2007). Clinical relevance of Neutral Endopeptidase (NEP/CD10) in melanoma. Journal of Translational Medicine *5*, 2.

Venkateswaran, S., Myers, K.A., Smith, A.C., Beaulieu, C.L., Schwartzentruber, J.A., *et al.* (2014). Whole-exome sequencing in an individual with severe global developmental delay and intractable epilepsy identifies a novel, de novo GRIN2A mutation. Epilepsia *55, e75-79.*

Waimey, K.E., and Cheng, H.J. (2006). Axon pruning and synaptic development: how are they perplexin? The Neuroscientist : a review journal bringing neurobiology, neurology and psychiatry *12*, 398-409.

Wallin, E., and von Heijne, G. (1998). Genome-wide analysis of integral membrane proteins from eubacterial, archaean, and eukaryotic organisms. Protein science: a publication of the Protein Society *7*, 1029-1038.

Wang, H., Chen, X., Dudinsky, L., Patenia, C., Chen, Y., Li, Y., Wei, Y., Abboud, E.B., Al-Rajhi, A.A., Lewis, R.A., *et al.* (2011). Exome capture sequencing identifies a novel mutation in BBS4. Molecular Vision *17*, 3529-3540.

Watson, C.M., Crinnion, L.A., Gleghorn, L., Newman, W.G., Ramesar, R., Beighton, P., and Wallis, G.A. (2015). Identification of a mutation in the ubiquitin-fold modifier 1-specific peptidase 2 gene, UFSP2, in an extended South African family with Beukes hip dysplasia. S Afr Med J *105*, 558-563.

Weisz Hubshman, M., Broekman, S., van Wijk, E., Cremers, F., Abu-Diab, A., Khateb, S., Tzur, S., Lagovsky, I., Smirin-Yosef, P., Sharon, D., *et al.* (2018). Whole-exome sequencing reveals POC5 as a novel gene associated with autosomal recessive retinitis pigmentosa. Human Molecular Genetics *27*, 614-624.

Westrate, L.M., Lee, J.E., Prinz, W.A., and Voeltz, G.K. (2015). Form Follows Function: The Importance of Endoplasmic Reticulum Shape. dxdoiorg *84*, 791-811.

Williams, A., Piaton, G., Aigrot, M.S., Belhadi, A., Theaudin, M., Petermann, F., Thomas, J.L., Zalc, B., and Lubetzki, C. (2007). Semaphorin 3A and 3F: key players in myelin repair in multiple sclerosis? Brain *130*, 2554-2565.

Wilkinson, R.N., Elworthy, S., Ingham, P.W., and van Eeden, F.J.M. (2018). A method for high-throughput PCR-based genotyping of larval zebrafish tail biopsies. BioTechniques *55*, 314-316.

Wilson, R.B. (2006). Iron dysregulation in Friedreich ataxia. Semin Pediatr Neurol *13*, 166-175.

Wolff, M., Casse-Perrot, C., and Dravet, C. (2006). Severe myoclonic epilepsy of infants (Dravet syndrome): natural history and neuropsychological findings. Epilepsia *47 Suppl 2*, 45-48.

Worzfeld, T., and Offermanns, S. (2014). Semaphorins and plexins as therapeutic targets. Nature Reviews Drug Discovery *13*, 603-621.

Worzfeld, T., Püschel, A.W., Offermanns, S., and Kuner, R. (2004). Plexin-B family members demonstrate non-redundant expression patterns in the developing mouse nervous system: an anatomical basis for morphogenetic effects of Sema4D during development. European Journal of Neuroscience *19*, 2622-2632.

Worzfeld, T., Rauch, P., Karram, K., Trotter, J., Kuner, R., and Offermanns, S. (2009). Mice lacking Plexin-B3 display normal CNS morphology and behaviour. Molecular and Cellular Neuroscience *42*, 372-381.

Wu, J., Lei, G., Mei, M., Tang, Y., and Li, H. (2010). A Novel C53/LZAP-interacting Protein Regulates Stability of C53/LZAP and DDRGK Domain-containing Protein 1 (DDRGK1) and Modulates NF-κB Signaling. Journal of Biological Chemistry *285*, 15126-15136.

Xiang, X., Zhang, X., and Huang, Q.-L. (2012). Plexin A3 is involved in semaphorin 3F-mediated oligodendrocyte precursor cell migration. Neuroscience letters *530*, 127-132.

Xiao, G., and Fu, J. (2010). NF-κB and cancer: a paradigm of Yin-Yang. Am J Cancer Res *1*, 192-221.

Xu, Z., Jung, C., Higgins, C., Levine, J., and Kong, J. (2004). Mitochondrial degeneration in amyotrophic lateral sclerosis. J Bioenerg Biomembr *36*, 395-399.

Yamamoto, A., Lucas, J.J., and Hen, R. (2000). Reversal of neuropathology and motor dysfunction in a conditional model of Huntington's disease. Cell *101*, 57-66.

Yang, Y.S., Harel, N.Y., and Strittmatter, S.M. (2009). Reticulon-4A (Nogo-A) redistributes protein disulfide isomerase to protect mice from SOD1-dependent amyotrophic lateral sclerosis. Journal of Neuroscience *29*, 13850-13859.

Yanicostas, C., Barbieri, E., Hibi, M., Brice, A., Stevanin, G., and Soussi-Yanicostas, N. (2012). Requirement for zebrafish ataxin-7 in differentiation of photoreceptors and cerebellar neurons. PLoS One *7*, e50705.

Yaron, A., Huang, P.H., Cheng, H.J., and Tessier-Lavigne, M. (2005). Differential requirement for Plexin-A3 and -A4 in mediating responses of sensory and sympathetic neurons to distinct class 3 Semaphorins. Neuron *45*, 513-523.

Yazdani, U., and Terman, J.R. (2006). The semaphorins. Genome Biology *7*, 211.

Yeo, S.-Y., and Chitnis, A.B. (2007). Jagged-mediated Notch signaling maintains proliferating neural progenitors and regulates cell diversity in the ventral spinal cord. Proceedings of the National Academy of Sciences *104*, 5913-5918.

Yoo, Hee M., Kang, Sung H., Kim, Jae Y., Lee, Joo E., Seong, Min W., Lee, Seong W., Ka, Seung H., Sou, Y.-S., Komatsu, M., Tanaka, K., *et al.* (2014). Modification of ASC1 by UFM1 Is Crucial for ERα Transactivation and Breast Cancer Development. Molecular Cell *56*, 261-274.

Yu, F.H., Mantegazza, M., Westenbroek, R.E., Robbins, C.A., Kalume, F., Burton, K.A., Spain, W.J., McKnight, G.S., Scheuer, T., and Catterall, W.A. (2006). Reduced sodium current in GABAergic interneurons in a mouse model of severe myoclonic epilepsy in infancy. Nat Neurosci *9*, 1142-1149.

Yu, P., Chen, Y., Tagle, D.A., and Cai, T. (2002). PJA1, encoding a RING-H2 finger ubiquitin ligase, is a novel human X chromosome gene abundantly expressed in brain. Genomics *79*, 869-874.

Yu, Z.-X., Li, S.-H., Evans, J., Pillarisetti, A., Li, H., and Li, X.-J. (2003). Mutant Huntingtin Causes Context-Dependent Neurodegeneration in Mice with Huntington's Disease. Journal of Neuroscience *23*, 2193-2202.

Zhang, D., and Oliferenko, S. (2014). Tts1, the fission yeast homologue of the TMEM33 family, functions in NE remodeling during mitosis. Molecular biology of the cell *25*, 2970-2983.

Zhang, Y., Zhang, M., Wu, J., Lei, G., and Li, H. (2012). Transcriptional regulation of the Ufm1 conjugation system in response to disturbance of the endoplasmic reticulum homeostasis and inhibition of vesicle trafficking. PloS one *7*, e48587.

Zhou, Q., Choi, G., and Anderson, D.J. (2001). The bHLH Transcription Factor Olig2 Promotes Oligodendrocyte Differentiation in Collaboration with Nkx2.2. Neuron *31*, 791-807.

Zhu, Y., Lin, G., Dai, Z., Zhou, T., Li, T., Yuan, T., Wu, Z., Wu, G., and Wang, J. (2014). Glutamine deprivation induces autophagy and alters the mTOR and MAPK signaling pathways in porcine intestinal epithelial cells. Amino Acids *47*, 2185-2197.

Zupanc, M.L., Roell Werner, R., Schwabe, M.S., O'Connor, S.E., Marcuccilli, C.J., Hecox, K.E., Chico, M.S., and Eggener, K.A. (2010). Efficacy of felbamate in the treatment of intractable pediatric epilepsy. Pediatr Neurol *42*, 396-403.